

METHUEN'S MONOGRAPHS  
ON PHYSICAL SUBJECTS

---

# X-RAYS

B. L. WORSNOP  
AND  
F. C. CHALKLIN



# METHUEN'S MONOGRAPHS ON PHYSICAL SUBJECTS

*General Editor:* B. L. WORSNOP, B.Sc., Ph.D.

F'cap 8vo.

Illustrated.

---

THIS series is intended to supply readers of average scientific attainment with a compact statement of the modern position in each subject. The Honours student and the research worker in other branches of physics, those engaged on work in related sciences, and those who are no longer in contact with active scientific work, will find here a series of expositions by authors who are actively engaged in research on the subject of which they write.

*For list of series, see  
back of this jacket*

---

METHUEN & CO. LTD. LONDON  
CAT. No. 4038/U

£2.50



Digitized by the Internet Archive  
in 2022 with funding from  
Kahle/Austin Foundation



Methuen's Monographs on Physical Subjects

General Editor: B. L. WORSNOP, B.Sc., Ph.D.

## X-RAYS

# METHUEN'S MONOGRAPHS ON PHYSICAL SUBJECTS

*General Editor : B. L. WORSNOP, B.Sc., Ph.D.*

## 3s. net

THE CONDUCTION OF ELECTRICITY  
THROUGH GASES  
PHOTOCHEMISTRY  
ATMOSPHERIC ELECTRICITY  
MOLECULAR BEAMS  
COSMOLOGICAL THEORY

K. G. EMELÉUS  
D. W. G. STYLE  
B. F. J. SCHONLANE  
R. G. J. FRASER  
G. G. MCVITTIE

## 3s. 6d. net

THE KINETIC THEORY OF GASES  
LOW TEMPERATURE PHYSICS  
HIGH VOLTAGE PHYSICS  
FINE STRUCTURE IN LINE SPECTRA  
AND NUCLEAR SPIN  
INFRA-RED AND RAMAN SPECTRA  
THERMIONIC EMISSION  
ELECTRON DIFFRACTION  
MERCURY ARCS

MARTIN KNUDSEN  
L. C. JACKSON  
L. JACOB  
S. TOLANSKY  
G. B. B. M. SUTHERLAND  
T. J. JONES  
R. BEECHING  
F. J. TEAGO and J. F. GILL

## 4s. net

THE METHOD OF DIMENSIONS  
APPLICATIONS OF INTERFEROMETRY  
THE CYCLOTRON  
WIRELESS RECEIVERS  
THE SPECIAL THEORY OF RELATIVITY  
THE EARTH'S MAGNETISM  
ALTERNATING CURRENT MEASUREMENTS  
DIPOLE MOMENTS  
FLUORESCENCE AND PHOSPHORESCENCE  
X-RAY CRYSTALLOGRAPHY

A. W. PORTER  
W. E. WILLIAMS  
W. B. MANN  
C. W. OATLEY  
H. DINGLE  
S. CHAPMAN  
D. OWEN  
R. J. W. LE FÈVRE  
E. HIRSCHLAFF  
R. W. JAMES

## 4s. 6d. net

ELECTROMAGNETIC WAVES  
PHYSICAL CONSTANTS  
COLLISION PROCESSES IN GASES  
THE COMMUTATOR MOTOR  
THE GENERAL PRINCIPLES OF QUANTUM THEORY  
THERMIONIC VACUUM TUBES  
THERMODYNAMICS  
THE PHYSICAL PRINCIPLES OF WIRELESS  
RELATIVITY PHYSICS  
WAVE MECHANICS  
AN INTRODUCTION TO VECTOR ANALYSIS FOR PHYSICISTS AND ENGINEERS  
HEAVISIDE'S ELECTRIC CIRCUIT THEORY  
WAVE FILTERS  
WAVE GUIDES

F. W. G. WHITE  
W. H. J. CHILDS  
F. L. ARNOT  
F. J. TEAGO  
G. TEMPLE  
E. V. APPLETON  
A. W. PORTER  
J. A. RATCLIFFE  
W. H. McCREA  
H. T. FLINT  
B. HAGUE  
H. J. JOSEPHS  
L. C. JACKSON  
H. R. L. LAMONT

## 5s. net

ATOMIC SPECTRA  
MAGNETISM  
X-RAYS

R. C. JOHNSON  
E. C. STONER  
B. L. WORSNOP

## 6s. net

HIGH FREQUENCY TRANSMISSION LINES WILLIS JACKSON

# X-RAYS

by

B. L. WORSNOP

B.Sc., Ph.D.

AND

F. C. CHALKLIN

Ph.D., D.Sc.

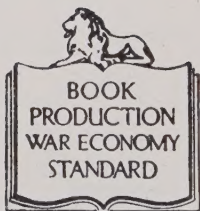
WITH 47 DIAGRAMS



METHUEN & CO. LTD., LONDON

36 Essex Street, Strand, W.C.2

*This second and revised edition  
first published in 1946*  
*The first edition (by B. L. Worsnop)  
was first published in 1930*



THIS BOOK IS PRODUCED IN  
COMPLETE CONFORMITY WITH THE  
AUTHORIZED ECONOMY STANDARDS

PRINTED IN GREAT BRITAIN

## PREFACE

THE need for a revised edition of the original monograph on X-rays came at a time when administrative work claimed so much of my time that it was clear that this could be done adequately only by the collaboration of one who was actively engaged on X-ray research, and I was pleased to have the co-operation of Dr. Chalklin in this work. However, dispersal under war conditions made real collaboration difficult, and as a result the main revision fell on his hands. I gladly acknowledge that the rearrangement and revision has been almost entirely carried out by him. Accounts of some of the earlier experimental work have been omitted and reference made to recent experiments of a more precise character, and it is hoped that the book will be found to be of more service in its new form. The main body of the monograph was completed in 1942, but the peculiar circumstances of the times have delayed its final publication.

Some of the new diagrams have been inspired by those in the various scientific journals, to which reference is made in the text. For the use of these, as well as those which first appeared in the former edition, I wish to express our grateful thanks.

B. L. W.



# CONTENTS

CHAP.		PAGE
I	INTRODUCTORY	I
	Gas (or ion) tubes. Hot filament tubes. Observation of X-rays. Absorption coefficients. Secondary radiations. Efficiency of X-ray production. Polarization. The diffraction of X-rays	
II	DETERMINATION OF WAVE-LENGTH AND X-RAY SPECTROSCOPY	21
	Reflection at crystals. The X-ray spectrometer. Crystal structure. Determination of $d$ and $\lambda$ . Spectrometers. The double crystal spectrometer. Bent crystal spectrometer. Powder method. Unit of wave-length	
III	X-RAY SPECTRA	40
	<i>Emission spectra.</i> Moseley's law. Bohr's theory and later modifications. X-ray satellites. Width of X-ray lines. Chemical and physical effects. The general X-ray spectrum. <i>Absorption</i>	
IV	THE SCATTERING OF X-RAYS	71
	Thomson's theory of scattering. Angular distribution of scattered X-rays. Scattering by gases. Scattering by liquids and amorphous solids. Intensity of scattering from crystals. The Compton effect	
V	OPTICAL PHENOMENA	90
	Refraction. Reflection. Interference. Diffraction. The use of ruled gratings	
VI	PHOTOELECTRONS AND IONIZATION	106
	Absorption and range. Experimental methods. Experimental results	
	BIBLIOGRAPHY	123
	INDEX	125



## CHAPTER I

### INTRODUCTORY

WHEN a sufficiently large potential difference is applied to two electrodes in an exhausted vessel, cathode rays are given off at right angles to the cathode. Inquiry into the nature of the cathode rays led to many experiments and much speculation towards the end of the last century.\* Crookes suggested a corpuscular nature for the 'rays', whereas the majority of the continental workers thought them to be a radiation. They are now known to be electrons (corpuscles of mass  $9.0 \times 10^{-28}$  gm. and negative charge  $4.8 \times 10^{-10}$  e.s.u.).

Röntgen, working on the problem in 1895, found that 'if the discharge from a fairly large induction coil be made to pass through a Crookes tube or a Hittorf tube which had been sufficiently exhausted', fluorescence was produced in crystals of barium platino-cyanide placed at distances of up to 2 metres away from the tube, which itself was entirely covered with black paper. This he traced to the effect of a radiation, quite distinct from the cathode rays, which had an origin at the place where the cathode rays were stopped. Referring to this, he says: 'for brevity's sake I shall use the expression "rays", and to distinguish them from others of this name I shall call them "X-rays":'

In addition to the property of producing fluorescence in crystals, X-rays were found to affect photographic plates and to ionize gases, i.e. to make them conductors of electricity. X-rays are, like light, electromagnetic waves. Satisfactory proof of their wave-nature was long delayed, but there is now abundance of it through the phenomena

\* See Emeléus, *Conduction of Electricity through Gases*.

of reflection, refraction, polarization, interference, and diffraction. Equally convincing is the evidence that they are electromagnetic.

Perhaps the most striking thing about X-rays is their penetrating power. As Röntgen's experiment shows, they pass not only through the glass wall of a Crookes tube but also through black paper. In fact, it was soon found that they penetrate a vast number of substances which are opaque to light, and that the opacity of substances to X-rays is dependent on their atomic weight and density. Thus lead cuts off more X-rays than an equal thickness of wood or paper, and bone is more absorbing than tissue. An early application of this was found in medicine, where shadow pictures of the bones of the hand, &c., indicated at least one use that X-rays might have. The penetrating power of X-rays depends on the way in which they are produced. The highly penetrating ones are called 'hard' X-rays, while those which are more easily absorbed are called 'soft'.

The many applications of X-rays have led to the construction of many types of X-ray tube to meet the requirements of the various experiments. Since X-rays are produced as the result of the stopping of cathode rays, the first requirement of an X-ray tube is that it shall provide a suitable source of these electrons. They are usually produced in one of two ways, and X-ray tubes thus fall into two distinct groups.

GAS (OR ION) TUBES. There is a large family of gas tubes, differing slightly in design, but all descended from Röntgen's tubes. For details the reader should consult the larger textbooks, as in this monograph we shall content ourselves with the basic principles involved.

Two electrodes, a cathode and an anticathode (an anode) are required (see Fig. 1). These are enclosed in an air-tight vessel which is exhausted to a pressure of nearly  $10^{-3}$  mm. Hg. When a potential of some tens of thou-

sands of volts is applied between cathode and anticathode, positive ions, produced in the resulting discharge, strike the cathode and cause the ejection of electrons (cathode rays) which are driven to the anticathode by the electric field. The low pressure and consequent sparse population of gas molecules permits most of the electrons to

The diagram illustrates the production of X-rays in a gas tube. At the top, a hatched rectangular area is labeled 'Cathode' with a minus sign (-). Below it, a vertical line labeled 'Window' passes through a central point where several dashed arrows labeled 'Electrons' are shown moving downwards. To the right of this central point is a vertical bar labeled 'Anticathode' with a plus sign (+). From the bottom of the Anticathode, two solid arrows point downwards towards a horizontal line labeled 'Water (cooling)'. Curved lines labeled 'X.Rays' (X-rays) are shown emanating from the central point between the Cathode and Anticathode.

FIG. I

Symbolic diagram of production of X-rays in gas tube

make an unimpeded journey. Just as a non-electrified missile such as a stone generates (non-electrical) sound waves when it strikes an object such as a sheet of iron, so the electrified particles known as electrons generate electromagnetic waves when they strike the anticathode. These waves are the X-rays. To an extent depending on

their hardness and on the nature of the wall of the tube, they pass out into the room, where they may be detected by the effects which we have already mentioned. Originally the tubes were made of glass: now they are commonly of metal construction. In this case a window is provided so that the X-rays, even if they are fairly soft, may pass out with little loss and be utilized. The window may conveniently be made of aluminium which can be obtained in the form of thin but strong foil, and which because of its low atomic weight is relatively transparent to X-radiations. The material of the anticathode is chosen for the particular problem under investigation, and in many cases it is highly important that it should not become contaminated during the operation of the tube by metal from the cathode. For this reason aluminium is particularly valuable as the cathode material, for it 'sputters' very little. The surface of the cathode is concave and spherical. The lines of electric force near it are therefore radial and it is possible to bring the cathode rays to a small focal spot on the anticathode. A point source of X-rays is obtained in this way. This early device permits sharp shadow pictures to be obtained in medical and industrial radiography, and, in X-ray spectroscopy and crystallography, increases the amount of radiation which can enter the slit of the apparatus. The latter is still further increased if the window of the tube is close to the anticathode, thus permitting the slit to be brought near.

The hardness of the radiation increases with increasing voltage across the X-ray tube. Since, however, at constant pressure the potential across a gas tube depends but little on the current through it, change in penetration requires change in pressure, a low pressure corresponding to a high voltage and high penetrating power. Conversely, any change in pressure occurring during the running of the tube entails a change in the voltage across it. In the case of constantly pumped tubes the required pres-

sure stabilization may be obtained by the use of an adjustable leak, whilst sealed-off tubes are often fitted with ingenious stabilizers. Gas tubes are particularly useful in X-ray crystallography, where the absence of anticathode contamination is of great advantage.

HOT FILAMENT TUBES (see Fig. 2). In this type of tube the vacuum is so good that the effect of gas molecules and ions is negligible. The source of electrons is an electrically heated tungsten filament situated in a metal shield, the two forming the cathode. Electrons, evaporated from the filament, are driven to the anticathode, being focused by the metal shield. In the commercial tube shown, the

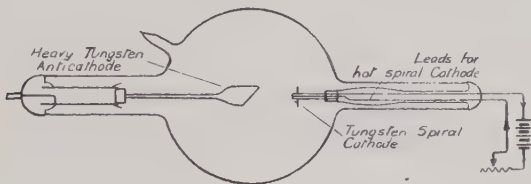


FIG. 2

filament is in the form of a flat spiral, but it is frequently convenient to have a line focus, and in this case the filament is in the form of a helix. For crystallographic and spectroscopic purposes the tubes are commonly of metal construction with suitable window and appropriately placed anticathode.

The current through the tube depends on the temperature of the filament, but depends very little on the applied voltage. Hence current and voltage may be varied independently of one another. This represents an important advantage over the gas tube. Hot filament tubes are, of course, self rectifying\*—a property which not all gas tubes possess.

\* Since the current of electrons can only flow in the direction from filament to anticathode.

The cathode rays, falling through the potential difference,  $V$ , between cathode and anticathode, arrive at the latter with kinetic energy  $\frac{1}{2}mv^2 = eV$ . Thus the energy consumed by the tube appears at the anticathode, and, as only a small proportion is converted into X-ray energy, almost all appears as heat. Anticathodes are therefore usually hollow and are cooled by flowing water. Even so there is a tendency for the surfaces to 'pit', and there is a definite limit to the current which can be passed safely, this limit depending on the thermal conductivity and the melting-point of the metal. The output of an X-ray tube is therefore restricted. If, however, the anticathode is in the form of a large disc with the focal spot near its edge, then, if the disc is spun about an axis through its centre, the heated portion is no longer a spot, but a ring of much greater area. This idea has been utilized in a number of tubes enabling very heavy currents to be used.\*

To obtain short wave-length X-rays and high penetrations, high voltages are required. For cancer treatment and for the radiography of metals, tubes to run at potentials ranging up to two million volts have been constructed.

OBSERVATION OF X-RAYS. A familiar way of detecting X-radiation is to allow it to fall on a barium platinocyanide screen, where visible fluorescence is excited. This procedure is not well suited to the precision requirements of the physical laboratory. Here the measurements usually depend upon one of two properties of the X-rays—the blackening of photographic plates and the ionization of gases.

The photographic plate or film is admirably suited for detecting X-ray beams and locating their position. Beams of small intensity can be detected by giving long exposure, and a photograph also allows a large number of beams to be observed *simultaneously*. The photographic method can also be used for comparing the intensities of X-ray

\* See, for example, Clay, *Phys. Soc. Proc.*, **46**, 703 (1934).

beams. Such comparisons are the more readily made since the laws governing the blackening of photographic emulsions are simpler for X-rays than for light (provided that the blackening is not too great). Most important is the fact that the reciprocity law holds. This means that a beam of intensity  $I$  acting on a plate for time  $t$  produces the same blackening as one of intensity  $I/2$  acting for time  $2t$ . Then again the density \* (blackening) is proportional to the intensity. (This law does not hold in the very soft X-ray region.)

Usually the ionization method is more suited for intensity measurements. When X-rays fall upon a gas, fast-moving electrons are ejected from the molecules, (leaving them as positively charged ions). Some of these are the result of direct photoelectric action, some the result of the Auger effect,<sup>†</sup> and some the result of Compton scattering (see Chapter VI). The electrons produce more ions, so many, in fact, that by comparison the number formed by direct X-ray action is negligible. The apparatus which employs this effect is known as the ionization chamber. It may conveniently consist of a metal cylinder,  $I$ , with an insulated metal rod,  $P$ , parallel to but displaced from the axis (see Fig. 3). The whole is enclosed in an airtight case (or the cylinder may constitute its own case), and the X-ray beam, rendered narrow by passing through apertures, enters through a thin window and passes down the cylinder without striking walls or rod. The gas enclosed should be heavy and the cylinder long to absorb as much as possible of the X-ray beam, and the radius should be so great that the photoelectrons should have yielded up their energy before reaching the walls. Methyl bromide, methyl iodide and argon are commonly used gases. The

\* Defined as  $\log_{10} \frac{i_0}{i}$ , where  $\frac{i}{i_0}$  is the fraction of the intensity of a beam of light of intensity  $i_0$  which will penetrate the developed plate.

<sup>†</sup> See page 118.

cylinder is maintained at a potential of one or two hundred volts and the rod is connected to an electrometer—initially earthed. The electric field drags the positive and negative ions to the negative and positive electrodes respectively, so quickly that they do not re-combine. Hence, when the electrometer (Fig. 3) is unearthened, it charges up at a rate proportional to the number of ions formed per second. This number is proportional to the intensity of the X-ray

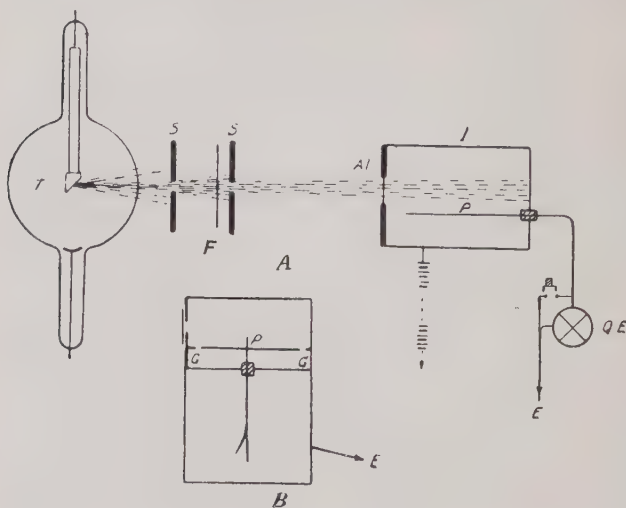


FIG. 3

beam, which is defined as the energy passing per second through unit area placed normally to it. Beams of the same wave-length, or beams of different wave-length, if suitable corrections are applied, may be compared in intensity by this method. The latter is made possible by the fact that the X-ray energy corresponding to the production of a pair of ions in the indirect manner indicated is independent of the X-ray wave-length. This point

seems pretty well established for air where the energy per pair amounts to about 33 electron-volts. It is about the same when  $\gamma$ -rays are used to produce the ionization. Again, since the ionization is supposed to be brought about by the electrons which the X-rays eject from the gas molecules, the same result should be obtained when the ionization is produced by fast-moving electrons. This appears to be true, but the energy per pair is higher for electrons of small velocity.

The observation and the measurement of intensity of X-rays may also be done by means of the 'counters' which have formed so important a tool in nuclear physics. The point counter is described as part of the Bothe-Geiger experiment (page 121), but of the tube counter, more frequently employed, we can only give a reference.\*

**ABSORPTION COEFFICIENTS.** If a sheet of aluminium is placed at  $F$  (Fig. 3), it is found that the intensity is reduced. When the beam is homogeneous † (not made up of a mixture of rays of different hardness), it is found that successive equal thicknesses of aluminium reduce the intensity by equal fractions.‡ In these ideal conditions we refer to the **linear absorption coefficient** of the homogeneous rays, as being the fractional reduction in the intensity of the beam per unit path in the absorbing substance.

An alternative expression for the absorption coefficient may be deduced. If the reduction in the intensity of the beam is  $-dI$  when it traverses a thickness  $dx$  of the absorber, we have from above  $-dI/I \propto dx$ , or  $-dI/I = \mu dx$ , where  $\mu$  is a constant (the absorption

\* It has been used, for example, by Neufeldt, *Zeits. f. Physik*, 68, 659 (1931).

† It will not be in the present case.

‡ e.g. if one thickness of absorber reduces the incident intensity,  $I$ , to  $9/10 I$ , and the transmitted beam falls on a second equal absorber, the intensity transmitted by this sheet is

$$9/10 (9/10 I) = 0.81 I,$$

and so on.

coefficient of the rays in the material of the absorber) and  $I$  is the initial intensity of the beam.

Integrating, we have  $\log I/I_0 = -\mu x$

or

$$I = I_0 e^{-\mu x} \dots \dots \dots \quad (1)$$

where  $I_0$  and  $I$  are the intensity before and after passing through a thickness,  $x$ , of the absorber.

In an experimental determination, the ratio of the ionization currents as measured by the quadrant electrometer replaces the ratio  $I/I_0$ , and so the value of  $\mu$  may be obtained by substitution in the following formula, where  $d_0$  and  $d$  are the rates of movement of the needle of the quadrant electrometer :

$$\mu = \frac{2.3 \times \log_{10} d_0/d}{x}$$

An alternative arrangement of apparatus for this determination is seen in Fig. 3, *B*. A gold-leaf electroscope is used : the plate  $P$  and the leaf are raised to a high potential and the case of the instrument is earthed. The measurement is made of the rate of discharge of the electroscope over a fixed part of the scale in the eyepiece of the observing low-power microscope to obtain the terms  $d$  and  $d_0$ .

The value of  $\mu$  obtained by such methods would be reliable only if the output of the X-ray tube were steady. A typical method of compensating for the fluctuation of the tube between the measurements of  $d_0$  and  $d$  is to use two ionization chambers and electrometers (or electroscopes). One chamber is placed directly in the path of a narrow beam from the tube and is used as a standard ; the other is used much in the way described above. The procedure is to find the number of divisions traversed on the electrometer or electroscope scale of the second chamber in the time that a certain definite number is traversed on the scale of the standard chamber. This is done for each thickness of absorber employed in the measurements.

In this way, even if the tube fluctuates, the measurements are always made for a fixed amount of energy from the tube. Other devices have been employed to enhance the accuracy and convenience of measurement, but the above shows the principles underlying the methods.

The absorption coefficient of a substance depends on its physical state. That of a gas is proportional to the pressure (temperature constant); and that of a solid is greater than that of the same substance in the gaseous state. This is because the absorption is governed by the number of atoms through which the radiation must pass rather than by the thickness of the absorber. For a beam of given cross-section, the number of atoms traversed is proportional to the density  $\rho$ . Consequently,  $\mu \left( = -\frac{dI}{Idx} \right)$  is proportional to  $\rho$ . Thus  $\mu/\rho$  is independent of the pressure in the case of a gas, and, provided that the absorption per atom is unchanged, is the same for a given substance in the solid and the gaseous states. This constancy of  $\mu/\rho$  for a given substance and radiation makes it of more importance than  $\mu$ . It is called the *mass absorption coefficient*. In the same way  $\mu$  divided by  $N$ , the number of atoms per cubic centimetre, is also constant for a given substance and independent of the physical state.  $\mu/N$  is called the *atomic absorption coefficient*.

In the early X-ray researches, the only test for homogeneity was by absorption. Thus, for homogeneous radiation there exists (equation (1)) a linear relation between  $\log I$  and  $x$ . It is clear that if the radiation is a mixture of rays of differing hardness, then, for small values of  $x$ , the softer components will be present, whilst if the thickness is doubled and then trebled, &c., the proportion of soft radiation will diminish with each increment of thickness. Hence, for a heterogeneous beam, the absorption coefficient, and therefore the slope of the  $\log I - x$  curve, must diminish with increase of  $x$ .

The radiation from an X-ray tube is far from homogeneous, but by passing it through an absorber and so removing the softer components, its homogeneity may be improved. This process is known as 'filtering' the beam. There are more refined ways of doing it, as, for example, that of the Ross differential filter.\*

**SECONDARY RADIATIONS.** When X-rays fall on matter, some of the beam passes through with reduced intensity, but, in addition, the matter becomes the source of the so-called secondary radiations. These were originally separated out by analysis of the absorption curves ( $\log I - x$ ) and are :

(1) **Scattered radiation**, which, in almost every particular, is identical with the incident beam, and may be compared with visible light scattered by tobacco smoke. It passes out of the scattering substance in all directions to a greater or less extent.

(2) **Electronic 'radiation'**, which consists of electrons ejected from matter by the incident beam and is therefore not a true radiation, but is like the photoelectric emission set up when ultra-violet light falls on substances.

(3) **Homogeneous radiations**, which are characteristic of the substance irradiated. They are always of a less penetrating nature than the incident beam (i.e. of longer wave-length). Barkla found from absorption measurements that the range of elements from calcium to silver gave out a single homogeneous or characteristic radiation, whilst elements of greater atomic weight gave out, in addition, a second and softer homogeneous radiation. These two radiations were named by Barkla the K and L radiations. He found that both K and L radiations increased in hardness with increasing atomic weight of the emitting substance. Nowadays we should say that the elements in question gave out two monochromatic radiations, the K of short wave-length and the L of longer

\* Ross, *Phys. Rev.*, 28, 425 (1926).

wave-length, and that the frequency of each type or series of radiation increased with increasing atomic number. The K series has now been traced and measured down to its theoretical limit at Li (atomic number  $Z = 3$ ) and the L series to its end at Na ( $Z = 11$ ). For the heavier elements, M, N and, in one case, O-radiations have been found (each succeeding letter representing in general a softer radiation). In no case has a more penetrating radiation of a J series been established, although there was evidence which pointed that way at one time, and in 1917 Barkla sought to explain a softening of the X-ray beam on scattering in terms of such a radiation.\*

The monochromatic K and L radiations of an element are produced not only as secondary radiations, but, provided that the voltage is sufficient, as part of the primary radiation when the element forms the anticathode of an X-ray tube. This is the usual way of producing them. In this case the excitation is produced by the fast-moving electrons or cathode rays instead of by another beam of X-rays.

The bulk of the X-ray output of a tube, however, is in the form of heterogeneous radiation, a continuous band of wave-lengths forming a spectrum not unlike that of the white light emitted by an incandescent solid. It has this difference, however, that the heterogeneous X-rays stop at a definite short-wave limit. This limit depends only on the voltage on the tube and not at all on the material of the anticathode. The limiting wave-length varies inversely as the applied voltage. The heterogeneous radiation is sometimes called the 'white' or more often the *general* or *continuous* X-radiation. The form of the energy distribution in the general X-ray spectrum is given by the curves of Fig. 22 (page 57).

EFFICIENCY OF X-RAY PRODUCTION. It has been found

\*A summary of work on J 'Radiation' and J phenomenon is given in Worsnop, *Science Progress*, Oct. 1928.

that the rate of production of X-ray energy in a tube is proportional to the square of the voltage,  $V$ , driving the bombarding electrons, and proportional to the atomic number,  $Z$ , of the material of the anticathode. It is proportional to the number of electrons striking the anticathode per second and therefore to the electron current,  $I$ . In short, the energy output is proportional to  $IZV^2$ . But the energy supplied per second is  $IV$ . Consequently the efficiency ( $\eta$ )—the ratio of output to input energy—is :

$$\eta = kZV, \text{ where } k \text{ is a constant.}$$

Considering the work of several investigators, Compton and Allison suggest that the true value of  $k$  is about  $1.1 \times 10^{-9}$ . Several effects would diminish this efficiency in an actual tube. First, an appreciable number of bombarding electrons are 'scattered' out of the anticathode, and, even if they return to it under the influence of the field, may strike it in a place (perhaps at the back) where they are useless. Secondly, the electrons mostly penetrate to appreciable depths before causing a radiation process to occur. Consequently these X-rays, starting below the surface, have to pass through a layer of anticathode material on their way to the observing apparatus and therefore suffer some absorption. Thirdly, there is absorption in the window of the X-ray tube.

There is evidence that at very low voltages (several thousands of volts) the output is no longer proportional to atomic number, but depends rather on the position of the radiating element in its group of the periodic table. There is also considerable doubt as to the validity of the  $V^2$  law in this low voltage region.

**POLARIZATION.** A somewhat picturesque way of regarding the genesis of general X-rays by the stoppage of a moving electron, may be had by considering the electron as a charge moving with its lines of force spreading out in all directions. When a sudden impact arrests its flight,

an equally sharp pulse is transmitted along the lines of force, constituting the X-ray. This simple picture was the basis of the early theories of Stokes and J. J. Thomson but finds little support in the modern theory. Nevertheless, it gives a mental picture which is still useful.

According to classical mechanics an electron radiates whenever its velocity is changed. If we consider a parent cathode ray stream  $OA$  striking an anticathode at  $A$ , Fig. 4, the velocity of the electrons is changed in the direction  $OA$  and therefore the electric vector of the radiation so produced is in a direction parallel to  $OA$ , and, in particular, the electric vibrations in those rays which proceed in the direction  $AB$  are in the plane of the paper ; no vibrations will occur in a direction at right angles to this plane. In other words, the X-rays are plane polarized. This may be visualized by using the line of force picture. Such complete polarization is not to be expected in practice, however, as the electron is not stopped at one impact, but has a further life in a deflected direction before it is finally brought to rest, giving rise to softer radiation with planes of vibration in different directions.

The theory was first put to the test by Barkla in 1906. He found the intensity of radiation scattered from a substance at  $B$  (Fig. 4) in two directions such as  $BD$ , in the plane of the diagram, and  $BC$  at right angles to this plane. His measurement showed that there was a maximum amount of ionization in an electroscope at  $C$  and a minimum at  $D$ . If we think of the electrons in the scattering substance as being set in motion by the electric vector in the incident beam, it is clear from the diagram that such an up and down movement of the electrons at  $B$  will result in radiation in the plane normal to the diagram and in particular along the direction  $BC$ , but a radiation of this sort is not to be expected in the direction  $BD$ . Barkla found the difference in the two directions to correspond to a partial polarization of some 10 to 20 per cent.

Subsequent researches have shown that the completeness of the polarization (*a*) increases if the radiation is filtered, (*b*) is increased by using a very thin film as anti-cathode, and (*c*) is reduced when the speed of the cathode rays is increased. The effect (*b*) indicates that the cathode rays penetrating the material of the anti-cathode are deflected as they pass among the atoms and lose their original definite direction. On this basis it is evident that the thinner the anti-cathode is made, the less will be the

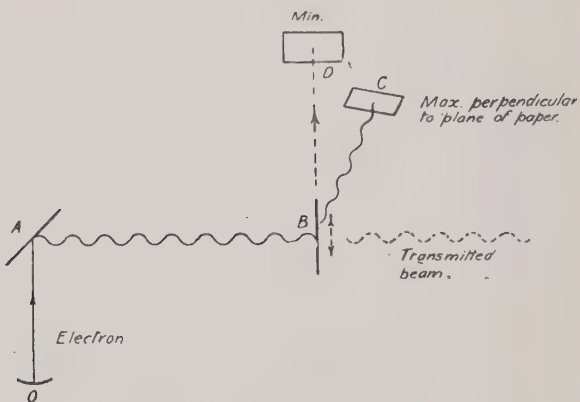


FIG. 4

diffusion of the cathode rays and the more complete the polarization. The effect (*a*) admits of the same explanation, for it may be taken that the electrons which have penetrated some distance into the anti-cathode and are diffused, will be slower and emit a softer radiation, more absorbable on the whole than that emitted near the surface of the anti-cathode. The result of filtering is therefore to a certain extent equivalent to using a thinner anti-cathode. The deflection theory will not explain why an increase in the velocity of the cathode rays in the

tube leads to reduced polarization, for faster electrons are presumably less deviated. This effect must, therefore, be ascribed to the fundamental process of general X-ray excitation. It is pretty certain that the effect of filtering is also, in part, fundamental. One may imagine the general radiation as being emitted by the electron in passing through the field of an atomic nucleus, and that the electron will emerge from the atom, not only with the magnitude, but with the direction of its velocity altered. Now the polarization will depend on the final as well as the original directions of motion, and consequently complete polarization of the beam cannot be expected. On the other hand, when the electron yields up all its energy in the collision with the atom, as it does for the shortest wave-lengths (or hardest radiation) emitted, the polarization should be complete. This is actually found in experiment.

THE DIFFRACTION OF X-RAYS. When announcing his discovery of X-rays Röntgen suggested that they might be longitudinal waves, but his endeavours to produce reflection, refraction and interference were unavailing.\*

Polarization and scattering experiments, however, led to the conclusion that X-rays were transverse waves. Haga and Wind, and later Walter and Pohl, endeavoured to measure the wave-length by diffraction at fine wedge-shaped slits. They estimated the order of the wave-length at not less than  $10^{-9}$  cm., but, due to the congested nature of their diffraction pattern, their results were not very convincing without further independent experiments.

Magnetic deflection experiments, described later, enabled a calculation of the velocity of the corpuscular radiation excited by X-rays to be made and, by an application of the quantum theory, the frequency of the X-rays used in their ejection was calculated.

From the above and other sources the probable order of

\* See, however, Chapter V.

the wave-length was  $10^{-8}$  to  $10^{-9}$  cm., i.e. of the same order as atomic dimensions. This led Laue in 1912 to make the most profitable suggestion that in the regular arrangement of atoms in a crystal there was a suitable means of producing diffraction of X-rays, in a way similar to that provided for visible radiation by a line grating.

The idea was that if a narrow pencil of X-rays were passed through a crystal, the individual atoms should set up secondary wavelets which, according to Laue, should reinforce in certain directions, in addition to the directly transmitted direction. At his suggestion Friedrich and

Knipping undertook experiments on these lines to test the theory. A narrow pencil of X-rays was limited in the usual way by lead stops and directed normally on to a thin slip of crystal and was received on a photographic plate placed some 15 cm. away on the side of emergence. The photographic plate showed a central spot surrounded by

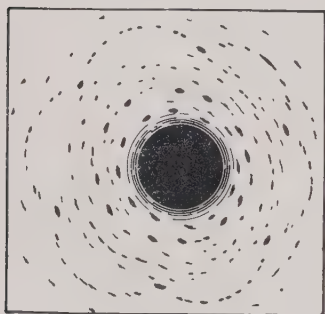


FIG. 5

a symmetrical system of spots, as seen in Fig. 5. When the plate was moved farther away the size of the spots remained the same, but the pattern spread out and was of the same form; rotation of the crystal resulted in a rotation of the pattern, which was therefore seen to be produced by the crystal and was the experimental realization of the results which Laue had anticipated by a mathematical analysis.

The accepted idea of the structure of crystals was some regular arrangement of atoms. This was the basis of the development referred to above. The constant form of

ocrystals had led to the belief that a crystal was made up by a repetition of a fundamental unit. For example, if we consider the simplest case of the cubic crystal, which, like common salt, is in the form of cubes no matter how small the crystal, the fundamental unit to assume is that of a cube. The unit may be considered to be made up of eight atoms set at the corners of this cube, in which case it is called a *simple cubic* system; or this may be modified by having an additional atom at the centre of each face, when it is said to be a *face centred* cubic system; or again, a modification is to be had if the unit has an



FIG. 6

additional atom at the centre of the cube, and is called a *body centred* cubic system (see Fig. 12).

Repetition of any of these units results in a regular spacing of atoms within the crystal which constitutes the *space lattice*.

On this supposition there will occur planes rich in atoms parallel to the faces of the crystal and equally spaced throughout. For example, in Fig. 6, which shows the crystal lattice in two dimensions only, it may be seen that vertical columns and horizontal rows satisfy this condition. W. L. Bragg suggested that there would occur other

planes less rich in atoms which would yet serve as *reflecting* planes for the X-rays (in Fig. 6 the planes, represented by thin lines, are examples of this kind of thing). It was shown that these planes would be symmetrical with respect to the incident beam, and that the spots of the Laue patterns could be accounted for in terms of 'reflection' at these planes throughout the crystal. This gives a much simpler way of regarding the Laue pattern than the complex analysis originally used.

W. H. and W. L. Bragg then tried, successfully, to bring about 'reflection' at the planes parallel to the cleavage surfaces of crystals. The success of these experiments, using an ionization method, led them to construct what is now known as the X-ray spectrometer, by means of which the determination of wave-length and an accurate knowledge of crystal structure have been deduced.

## CHAPTER II

### DETERMINATION OF WAVE-LENGTH AND X-RAY SPECTROSCOPY

REFLECTION AT CRYSTALS. If a beam of X-rays were to fall on to a single layer of atoms such as, say, one plane of a crystal containing a regularly spaced set of atoms, we should expect a *very* weak reflection for all angles of incidence and for all wave-lengths, and the problem of X-ray reflection would be analogous to the reflection of light at a polished surface.

In dealing with X-rays, however, the high polish of the surface does not bring about reflection as in the case of light. X-rays penetrate the very large number of atom layers contained in the thin surface sheath of the crystal, and each of the atoms irradiated sets up a new wave with an intensity which depends on the number of electrons within the atom. Therefore, in order to determine if there is any reflected ray corresponding to a ray incident at a given angle, we must find the integral effect of the secondary wavelets, as is done in the simpler case of Huyghens' construction in optics. The problem, in other words, is one of reflection at a very large number of parallel reflecting surfaces.

Suppose that in Fig. 7,  $L_1$ ,  $L_2$ ,  $L_3$  represent the layers of atoms in a crystal, separated by a distance  $d$ , called the *lattice constant*, which is of the order of  $10^{-8}$  cm. If the secondary wavelets from the adjacent layers are to reinforce each other in a given direction, they must be in *exactly* the same phase in that direction (i.e. the crests of the waves must fit together and not a crest and a trough together). The slightest departure from this condition

results in interference of the rays with a reduction in intensity to very minute values.

Let us consider a narrow beam of rays incident at a glancing angle  $\theta$ . In Fig. 7, five of the adjacent rays of this beam are shown. They are in phase at  $R, S, T, U, V$ . The ray  $R$  strikes an atom in the first layer at  $A$  and sends out a secondary wave: the ray  $S$  strikes an atom of the second layer at  $O$ , and so on, and in the direction  $QM$ , which is also inclined to the crystal at  $\theta^0$ , there is a contribution from all the secondary wavelets. Now ray 2 has a longer path than ray 1; ray 3 has an *equal excess path*

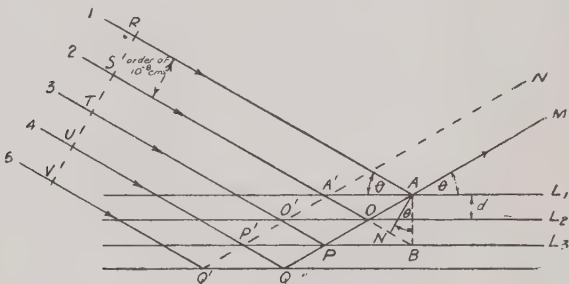


FIG. 7

over ray 2, and so on. To reach  $A$  the rays traverse the paths  $RA, SOA, TPA, \&c.$  Now  $SOA = SO + OA$ , and the geometry of the figure shows that  $OA = OB$ , also that  $RA$  is equal to  $SN$  where  $N$  is the foot of the perpendicular from  $A$  to  $SO$ , therefore the extra path traversed by ray 2 is equal to  $NB$ , which is clearly equal to  $2 \times d \sin \theta$ , which therefore represents the extra path traversed by successive neighbouring rays. If this extra path is equal to one whole wave-length of the radiation used ( $\lambda$ ), the rays will fit together crest to crest, or in other words, the rays will be in phase and they will reinforce each other: i.e. in the direction  $AM$  there will be reflection. This is said to be

reflection of the *first order*. Similarly, when for another angle  $\theta'$  the distance  $2d \sin \theta'$  is equal to  $2\lambda$ , there is again reinforcement and the reflection is said to be of the *second order*, and so on. Generally we have

$$2d \sin \theta = n\lambda \quad (\text{Bragg's Law}) \quad (1)$$

where  $n = 1$  for the first order,  $n = 2$  for second order, and so on. For the same conditions the rays scattered at  $A'$ ,  $O'$ ,  $P'$ ,  $Q'$  reinforce in this direction. It may also be seen that the reflection is for one wave-length only. Of course it may happen, if a heterogeneous beam be used, that the angle  $\theta$  is appropriate to the first order of one wave-length and the second order of a wave-length of about half the size; also, using a heterogeneous beam, it is apparent that each of the constituents is reflected when the appropriate angle of incidence, and the *same angle of reflection*, are used. For a given  $\lambda$ , the intensity of the beam is very small in a direction not quite coincident with  $AM$ , due to interference of the rays caused by the extra path difference introduced. In other words, the lines are sharp.

**THE X-RAY SPECTROMETER.** In the original Bragg spectrometer, a crystal of the kind considered in the preceding paragraph was mounted with its planes vertical on the prism table of a spectrometer, as at  $C$  in Fig. 8. An incident beam of X-rays was limited by two slits,  $A$  and  $B$ , and the telescope of the instrument was replaced by an ionization chamber  $I$ . The angle between the incident direction and the line from the crystal to the ionization chamber (as limited by the slit  $D$ ) was always maintained at twice the corresponding angle of glancing incidence at the crystal surface, in order to maintain the glancing angles of incidence and reflection the same.

The first experiments were made with rock salt, and the appearance of the curves showing the relation between the ionization and the glancing angle is seen in Fig. 9 ( $I$ ). As

may be seen, ionization was found for all angles of incidence (all wave-lengths), but there is a noticeable feature in the comparatively sharp rises at certain definite angles of incidence, as, for example, at  $A_1$ ,  $B_1$ ,  $C_1$ . The rises recur

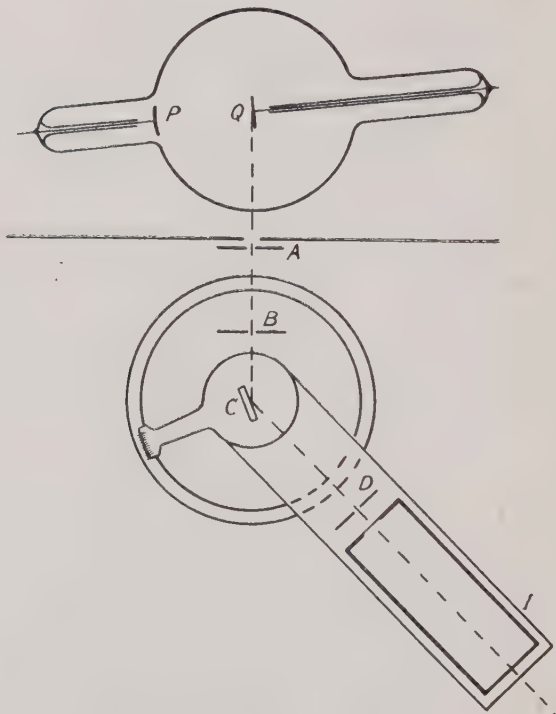


FIG. 8

in similar proportions, but separated by about twice the former amount at  $A_2$ ,  $B_2$ ,  $C_2$ , and there is further evidence of a third appearance of these peaks.

This showed that the radiation from the tube was not evenly distributed among the wave-lengths, but that,

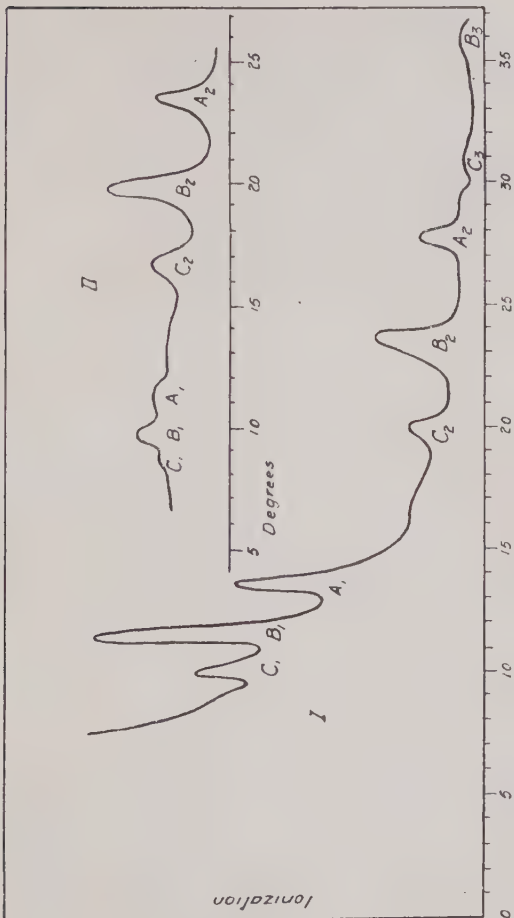


FIG. 9

corresponding to the angle  $\theta$  having the approximate values  $10^\circ$ ,  $11^\circ 30'$  and  $14^\circ$ , there was an excess of radiation. The repeated form,  $A_2 B_2 C_2$ , occurs at angles

whose sines are double the sines of the angles corresponding to  $A_1$ ,  $B_1$ ,  $C_1$ ; in other words, this radiation was reflected in the first and second orders and the relation between the sines verified expression (1) given above. When the crystal was turned so that a second cleavage face was employed, the form of the ionization curves was as shown in II of Fig. 9.

The conclusion that the peaks were due to the radiation was verified by using other crystals. The same form of ionization curves resulted, although the actual positions of the peaks were displaced to places which depended on the lattice constant of the new crystal used. Using X-ray tubes with different anticathodes and one crystal, the peaks were again of the same general form but in very different positions corresponding to other wave-lengths being emitted by the anticathodes. This showed that these elements gave out an excess of certain favoured wave-lengths. The suggestion arose that these might be the characteristic rays which had already been found by absorption measurements—a conclusion which was at once verified by simple absorption tests. The ‘peaks’ were, in fact, shown to be components of the K and L series, and may be called the emission lines of the material of the anticathode. Bragg investigated in this way the emission lines of Pt, Os, Ir, Pd and Rh.

In order to determine the wave-length corresponding to any angle of reflection, it is necessary to know  $d$ , the lattice constant of the crystal. To understand the method underlying the determination of this constant, it is advisable to have at least an elementary knowledge of the terminology and the simpler features involved in crystallography.

CRYSTAL STRUCTURE.\* If, as indicated at the end of the last chapter, we consider a crystal to be made up by a

\* For a fuller account of this, see *X-Ray Crystallography*, by R. W. James, in this series.

constant repetition of a fundamental unit, there is nothing in the crystallography of the case to decide the nature of the entities of which the unit is made ; they may be atoms, molecules or groups of molecules. X-ray analysis leaves no doubt about this. We may take it that we are dealing with *atoms*.

In Fig. 10 is shown a lattice unit (see page 19) whose sides (taken for simplicity at right angles) are  $p$ ,  $q$  and  $r$ . When

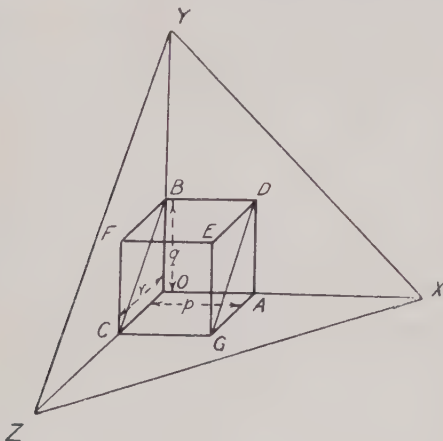


FIG. 10

this unit is repeated it is clear that there are planes of atoms in the crystal parallel to  $OBFC$  separated by a distance  $p$ , parallel to  $OAGC$  separated by a distance  $q$ , and parallel to  $OADB$  separated by a distance  $r$ , and in addition there are obviously atom planes such as  $ABC$ ,  $CBDG$ , &c., with other separations.

It is found convenient to refer to these planes in terms of the intercepts on three axes. In the case of the cubic crystals the axes are at right angles, and  $p = q = r$ . The axes chosen are parallel to the cube edges : the ratio

$p : q : r$  is called the *axial ratio*. If we take a plane  $XYZ$  passing through the atoms it is clear that

$$OX/p : OY/q : OZ/r = a : b : c,$$

where  $a$ ,  $b$ , and  $c$  are whole numbers. For the simple cubic crystal, when  $XYZ$  is parallel to  $ABC$  it is evident that  $a : b : c = 1 : 1 : 1$ .

The more usual ratio to take to define the plane is the reciprocal of the above, viz. :

$$p/OX : q/OY : r/OZ = bc : ca : ab = h : k : l,$$

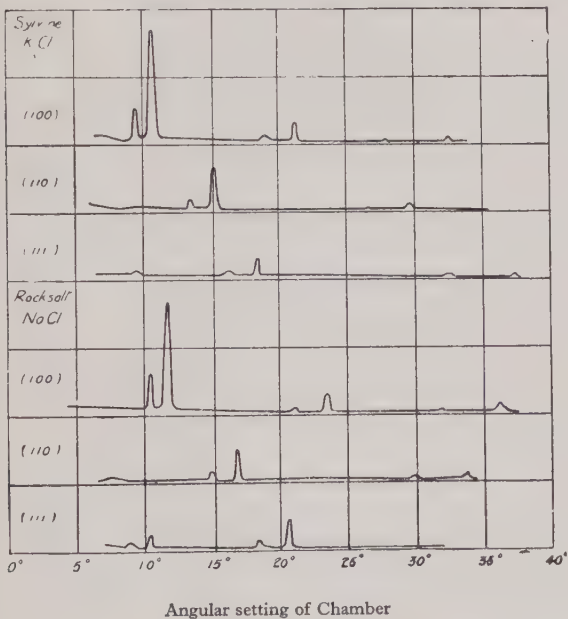
where  $h$ ,  $k$ , and  $l$  are again whole numbers and are usually written in brackets, viz. :  $(h, k, l)$ , and are called the *indices* of the plane in question. For example, a plane parallel to  $ABC$  is the  $(111)$  plane;  $ADEG$  is the  $(100)$  plane, as the intercepts on the  $y$  and  $z$  axes are infinite;  $BDGC$  is the  $(011)$  plane, and so on. When the crystal grows with faces such as  $(100)$ ,  $(010)$ , &c., it becomes a cube, and is said to be of the form  $\{100\}$ , &c.

DETERMINATION OF  $d$  AND  $\lambda$ . The problem of the determination of  $d$  and  $\lambda$  is one of finding two unknowns when only one relation, (1), is available.

Fortunately the palladium anticathode used in the experiments emitted a strong characteristic line, and it was by a close study of the distribution of intensity of this line in the different orders of reflection from the various planes of NaCl and KCl that the Braggs were able to make an estimate of the actual placing of the atoms, and hence the mass within a unit of the lattice. Direct calculation from a knowledge of the density gave a second estimate of this quantity, and so the value of  $d$  was obtained, as is seen in the following account.

The determination of  $d$  was first undertaken by Bragg for the cubic crystals rocksalt (NaCl) and sylvine (KCl). Cleavage faces were made parallel to three planes, and the ionization curves obtained by reflexion of the radiation from a tube with a palladium anticathode at these faces

are shown in Fig. 11. The first order reflection from the (100) plane of KCl is at  $2\theta = 10^\circ 43'$  and for NaCl at  $2\theta = 11^\circ 48'$ . Now equation (1) gives  $2d \sin \theta = \lambda$  for the first order, and therefore if these crystals are simple cubic in character with a lattice unit of side  $d_1$  and  $d_2$  respectively we have  $2d_1 \sin 5^\circ 21' = \lambda = 2d_2 \sin 5^\circ 54'$ , or



Angular setting of Chamber

FIG. 11

$d_1 = 5.48 \lambda$ ;  $d_2 = 4.85 \lambda$ , where  $\lambda$  is the wave-length of the prominent palladium line used.

Again, from general considerations it seems reasonable to suppose the molecular volumes of the crystals are in the ratio of the cube of the corresponding  $d$ , and if  $M$  and  $\rho$  are the molecular weight and density we have

mol. vol. KCl : mol. vol. NaCl =  $M_1/\rho_1$  :  $M_2/\rho_2 = d_1^3 : d_2^3$

$$\text{or } d^3 \rho_1/M_1 = d^3 \rho_2/M_2 = \text{a constant.}$$

For this type of crystal, therefore, one anticipates the constancy of  $d\sqrt[3]{\rho/M}$ . The results actually obtained in terms of  $\lambda$ , for three crystals, are :

$$d\sqrt[3]{\rho/M} = \text{KCl}, 1.63 \text{ } \lambda; \text{ NaCl}, 1.62 \text{ } \lambda; \text{ KBr}, 1.63 \text{ } \lambda,$$

which points to a similar structure in these cases.

In order to decide the exact form of the lattice unit we will next consider the spacing of atom layers for crystals made up of the units shown in Fig. 12, where (a) is a cube of side  $a$  with diffracting centres at the corners, (b) is a face centred cube of side  $2a$ , and (c) is a body centred unit of side  $2a$ . The reason for selecting  $a$  and  $2a$  in the different cases will appear later.

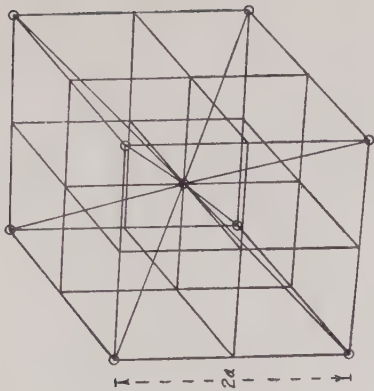
In these three cases the actual spacing of the planes is found by simple calculation to be :

	(100)	(110)	(111)
Simple cube lattice (a)	$a$	$a/\sqrt{2}$	$a/\sqrt{3}$
Face centred,, (b)	$a$	$a/\sqrt{2}$	$2a/\sqrt{3}$
Body centred,, (c)	$a$	$2a/\sqrt{2}$	$a/\sqrt{3}$

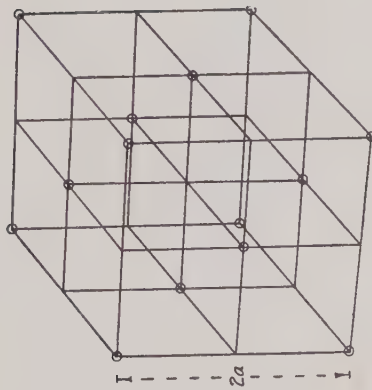
The next step, therefore, is fairly clear ; a ratio of the spacing of the various planes must be determined. For KCl, as shown in Fig. 11, the angle for the first order reflection at these faces has the values  $5^\circ 21'$ ,  $7^\circ 30'$ ,  $9^\circ 05'$ , i.e.

$$d_{(100)} : d_{(110)} : d_{(111)} = 1/\sin 5^\circ 21' : 1/\sin 7^\circ 30' : 1/\sin 9^\circ 05' \\ = 1 : 1/\sqrt{2} : 1/\sqrt{3},$$

which agrees with the simple cubic system. On the other hand, if we consider NaCl we find identical results only if we neglect the weak reflection at the (111) face at about

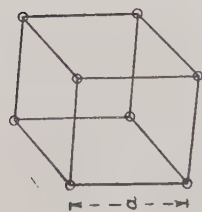


*c*



*b*

FIG. 12



*a*

$5^\circ$ . When we take this weak reflection into account we obtain

$$d_{(100)} : d_{(110)} : d_{(111)} = 1 : 1/\sqrt{2} : 2/\sqrt{3},$$

which corresponds to the face centred system.

The solution of the problem as given by Bragg is illustrated in Fig. 13, which represents either NaCl or KCl.

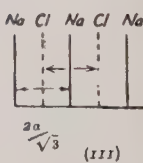
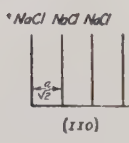
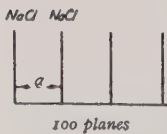
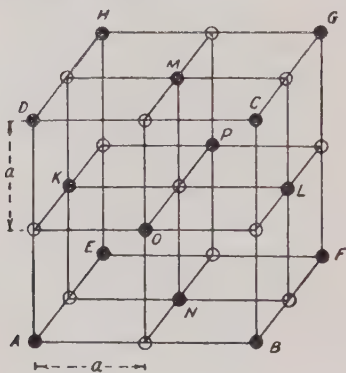


FIG. 13

The black dots show the positions of the Cl atoms, and the open circles either Na or K atoms. It will be seen that they form an interlocked face centred cube. In the case of KCl we are dealing with atoms of atomic number 19 (K) and 17 (Cl), which in combination have each 18 electrons, so that they each scatter to the same extent and from this point of view are indistinguishable: the

system of scattering centres therefore behaves as though made up of a simple cubic unit of side  $a$ .

In the case of NaCl we have atoms of atomic numbers 11 (Na) and 17 (Cl), which in combination have 10 and 18 electrons, respectively. As shown in the lower part of Fig. 13 the (100) and (110) planes are similar in composition, being made up of an equal number of Na and Cl atoms, but the alternate (111) planes are each made up entirely of Na or of Cl atoms. If we reflect at this face, the Cl atoms will act as a face centred cube of side  $2a$ , and if we could neglect the reflection from the Na atoms, the resulting reflection would be appropriate to a face centred cube. However, midway between the Cl planes are the Na planes which also give rise to a reflected beam. When the conditions are right for the first order reflection at the Cl planes the corresponding path difference for the reflection at adjacent planes, i.e. at alternate Na and Cl planes, is exactly that for destructive interference. If the intensity of reflection from the atom planes were the same, there would be no resulting intensity. But the Cl planes (18 electrons per atom) reflect more copiously than the Na, and the result is a reflection appropriate to the difference of the intensities, and a weak line is produced, as we have seen. The scheme of Fig. 13 therefore satisfies the observed results.

In order to find  $d$ , it must be realized that when the lattice unit is repeated throughout the crystal, the corner atoms are common to eight cubes, viz.  $A$ ,  $B$ ,  $C$ ,  $D$ , &c., are each common corner atoms to eight cubes, and since there are eight such corner atoms in each cube, only *one* is to be regarded as proper to each large cube. In the same way the face centering atoms are each common to two cubes, and there are six such atoms,  $K$ ,  $L$ ,  $M$ ,  $N$ ,  $O$ ,  $P$ , with a result that there is a contribution of three atoms from this source to the total content of the large cube unit, which has therefore a total of four atoms of

this kind. A similar reasoning shows that the other type of atom makes an equal contribution to the cube, with which we must consequently associate four *molecules*.

The X-ray data, therefore, show that each cube has four molecules and the mass of the cube is  $4\frac{M}{N}$ , where  $M$  is the mass of the molecule and  $N$  is the number of molecules per gram-molecule (Avogadro's number). But this mass, in a cube of side  $2d$  and density  $\rho$ , is  $(2d)^3\rho$ . Hence

$$8d^3\rho = 4\frac{M}{N}$$

$$d = \sqrt[3]{\frac{M}{2N\rho}}$$

For rock salt Bragg found the value of  $d$  to be  $2.81 \times 10^{-8}$  cm. and the wave-length of the palladium rays used,  $\lambda_{\text{Pd}} = 0.576 \times 10^{-8}$  cm. Having found the spacing for one crystal in this way, the wave-length of reflected X-rays can be calculated and the lattice constant of other crystals may be evaluated. In this manner the foundation of X-ray examination of crystal structure and of X-ray spectroscopy was laid.

**SPECTROMETERS.** The original Bragg spectrometer has already been described. In this instrument the X-rays were observed by means of an ionization chamber. In the Moseley experiments, the results of which are to be discussed later, a photographic method was used. A slightly diverging beam of X-rays was allowed to fall on the crystal, and the corresponding reflected rays formed images on the photographic plate appropriate to the small range of glancing angles determined by the divergence of the incident beam. In this way the photographic plate was useful for a limited range of wave-lengths, and the whole spectrum was mapped out in small stages by successive small rotations of the crystal,

The spectrometer employed by the Braggs in later experiments was automatically adjusted by a clockwork mechanism which moved the ionization chamber through twice the angle of the crystal, so that, as the crystal turned and hence reflected the various wave-lengths of the spectrum, the ionization chamber was always in the right place to receive the radiation. They also introduced a focusing device in which the slit of the ionization chamber was placed at the same distance from the crystal as the slit nearest to the source of X-rays. This enabled wider slits to be used and reduced the exposure time.

M. de Broglie introduced a photographic method whereby the whole spectrum was recorded on a photographic plate by clockwork rotation of the crystal and focusing was achieved by having plate and slit equidistant from the axis of rotation of the crystal.

A very large number of the precision determinations of X-ray wave-lengths has come from the laboratory of Siegbahn, and a detailed account of the spectrometers developed by him and by other workers is given in his book.\*

When wave-lengths appreciably above  $1\text{\AA}$  are to be measured, the absorption of the radiation in the wall of the X-ray tube and even in air becomes appreciable. Hence, for work in this region, the spectrometers are necessarily housed in vacuum chambers, the X-ray tube being sealed to the chamber and the radiation passing from it to the spectrograph through only a thin foil window—usually mounted on the slit. For wave-lengths greater than  $10\text{\AA}$  the foil is dispensed with, but the troublesome diffusion of vapours from the spectrograph to the X-ray tube † is restricted by the narrowness of the slit.

THE DOUBLE CRYSTAL SPECTROMETER. For the examination of the width, shape or fine structure of X-ray spectral lines, an instrument of high resolution is required. For

\* *Spectroskopie der Rontgenstrahlen* (Springer).

† The hot-filament type is used.

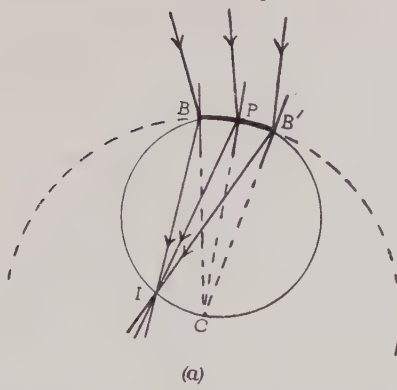
this purpose the double crystal spectrometer is specially suited. In this instrument the first crystal acts as a collimator. The incident beam, still fairly diverging after passing through two relatively wide slits, falls on this crystal, which is set in such a position as to reflect the wave-lengths in the small region of the spectrum under examination. For any given wave-length, this crystal will only reflect at a definite angle (that prescribed by Bragg's law) relative to the reflecting planes. Hence, the crystal, picking out the radiation of this wave-length coming through the slits at the correct angle, reflects it, as a parallel beam, to the second (analysing) crystal. Other slightly different wave-lengths are also reflected to the second crystal as parallel beams, but in slightly different directions. Since the incident radiation is parallel, the second crystal will only reflect a given wave-length when it is in one definite position. The spectrum is therefore obtained by rotating the crystal, noting its position, and observing the current in an ionization chamber, the wide slits providing adequate intensity. The system is clearly similar to that of a single crystal with an incident beam collimated by infinitely narrow slits—but avoids the total loss of intensity which such slits would entail.

BENT CRYSTAL SPECTROMETER. For the observation and measurement of weak emission spectra and of secondary spectra, a sacrifice in resolution might be justified in the attempt to attain higher intensity. It is, however, possible to obtain satisfactorily sharp spectra, and greatly enhanced intensity by the use of bent crystalline sheets. The method adopted by Mlle Cauchois \* has proved very successful. A sheet of mica, of the order of 1 cm. across, bent so as to form a cylindrical surface of radius 20–100 cm., is arranged with its reflecting planes † parallel to the

\* Cauchois, *J. de P.*, 3, 320 (1932).

† We are not here considering those parallel to the surface of the mica.

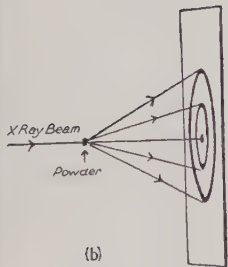
*Incident Rays*



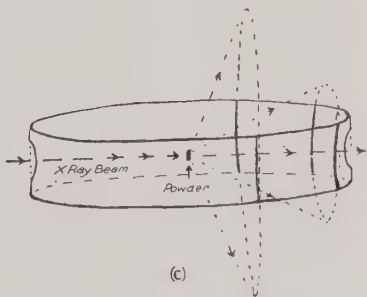
(a)

(a) Focusing property of a bent crystal  
(Reflecting planes assumed normal to the surface)

$BPB'$  = bent crystal  
 $C$  = its centre of curvature  
 $PIC$  = circle of focus



(b)



(c)

(b) and (c) Powder photographs

(b) Shows how rings are formed when powder photographs are taken with a flat plate.

(c) Demonstrates how more or less curved lines are obtained when the diffraction pattern is received on a cylindrical film.

FIG. 14

cylinder axis. All, of course, make the same angle with the radii of the cylinder (see Fig. 14(a)). Any given wavelength is, by Bragg's law, reflected at the same angle from all these planes and therefore makes a constant angle with all the corresponding radii of the cylinder. In this way, rays of the same wave-length, incident at the appropriate angle, are brought to an approximate focus no matter where they may strike the surface of the crystal. The spectrum may be shown to fall on a circle whose radius of curvature is half that of the cylinder and touching the crystal at its centre. In the ordinary spectrometer the sharpness of the spectra is governed by the width of the slit, which, therefore, is narrow and limits their intensity. Here we need no slit at all, and times of exposure may be cut down from hours to minutes.

POWDER METHOD. Whilst in this chapter we have tried to show how the diffraction of X-rays by crystals is used to investigate the X-ray spectra, yet it has been apparent that the converse treatment is possible—that with radiation of known  $\lambda$ , information may be obtained about unknown crystal structures. This is one of the greatest contributions of X-rays to science, but we must content ourselves with referring the reader to the standard works on the subject.\* However, it is appropriate to mention the powder diffraction method, which has been of much importance in crystallographic research. It differs from the methods so far described. In these, single crystals have been used. However, many substances are not easy to obtain as good single crystals. In these cases the substance is often finely powdered and made up into a rod-shaped pellet with the aid of some adhesive material. The pellet thus contains a large number of crystals orientated at random, and, if a narrow monochromatic beam be allowed to fall on it, then, no matter what set of crystal planes we consider, there is always a number of crystals

\* E.g. *The Crystalline State*, by W. L. Bragg (Bell).

n which these planes are correctly aligned to give Bragg reflection. Thus, if  $\theta$  is the glancing angle corresponding to the value of  $d$  for a particular set of planes, the reflected radiation will make an angle of  $2\theta$  with the incident beam, and, since the crystals are orientated at random about the beam as axis, the reflected rays form a cone about it of semi-angle  $2\theta$  (Fig. 14 (b) and (c)). Other sets of planes, with other values of  $d$ , give cones of different semi-angles. It is usual to place the pellet on the axis of a cylindrical chamber lined with photographic film. When developed, the film shows black lines, which represent the intersection of the cones by the cylinder. The positions of the lines give the values of  $\theta$ , and these yield the values of  $d$ .

UNIT OF WAVE-LENGTH. Results from the ruled grating spectrometer \* are usually expressed in terms of the Angstrom unit, which is the unit employed in optical spectroscopy and which is defined as  $10^{-8}$  cm. The X-ray wave-lengths are, however, roughly 1,000 times smaller than those of the visible spectrum, so a smaller unit, the X-unit (X.U.) is more frequently employed. This was chosen to be  $10^{-11}$  cm. Determinations by the crystal spectrometer depend on the value allotted to the lattice constant of the crystal, and this is known to far less accuracy than that with which the spectrometer measurements † can be made and with which it is desirable to express the results. An assumed value of 3029.04 X.U. for the constant of calcite ‡ was adopted as a standard value by Siegbahn and his school, and wave-length tables are usually based on this definition. In this way the unit of wave-length is based, not on the centimetre, but on the lattice constant. The X-unit, defined by the above value, is now known to differ from  $10^{-11}$  cm. by about 2 in 1,000.

\* To be discussed in Chapter V.

† Often to 1 in  $10^5$ .

‡ At  $18^\circ$  C. and for first-order spectra.

### CHAPTER III

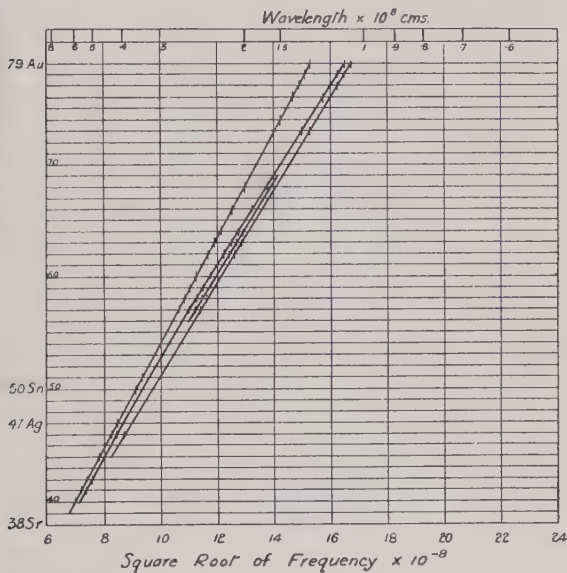
## X-RAY SPECTRA

## EMISSION SPECTRA

MOSELEY'S LAW. In the first spectrum as illustrated in Fig. 9, it was seen that the L series of palladium was made up of three distinct components which were separated by about  $1^\circ$ , i.e. the L radiation was not truly homogeneous, but was a group of radiations. A systematic search into the characteristic radiations of some thirty-eight elements was undertaken by Moseley \* in 1913. He found that both the K and L series could be separated in this way into a system of lines in all cases. In general the K series consisted each of two lines ; the longer wave-length, and more intense line was called the  $K_\alpha$ , the other the  $K_\beta$  line. In the same way the L radiation from each element was found to be made up of three lines which were called  $L_\alpha$ ,  $L_\beta$ ,  $L_\gamma$ , in order of decreasing wave-length and intensity. The spectra of the various elements were of the same general character, but varied in wave-length in a very regular manner. Moseley found that the regularity was most pronounced if he plotted the square root of the frequency of corresponding components against the *atomic number* of the source, rather than the atomic weight (where the atomic number may be regarded as the number of free positive charges in the nucleus). Moseley's work emphasized the importance of atomic number ( $Z$ ) and may be said to have established its real significance and use in physics. Fig. 15 shows a typical diagram giving Moseley's results, in which it will be seen that the linear relation between (frequency) $^{\frac{1}{2}}$  and  $Z$  is very definite ; in fact, he

\* *Phil. Mag.*, 26, 1024 (1913) and 27, 703 (1914).

was able to predict in a few cases that new elements were to be expected in places where a departure from this regularity was noticed in a preliminary plot. One of these elements has since been isolated by Bohr and called hafnium ( $Z = 72$ ). Confirmation was also to be had from his results that the atomic number should be in the reverse



Relation between the Atomic Number of the source and the square root of the frequency of the radiation

FIG. 15

order from the atomic weight in certain pairs of elements whose chemical properties also demanded this reversal (e.g. cobalt and nickel, and tellurium and iodine). Incidentally these results provided a comparatively rapid means for the analysis of substances which otherwise require a lengthy and involved chemical process.

From the point of view of spectroscopy the important feature of Moseley's work was the fact that the frequency,  $\nu$ , of the radiation in the corresponding components of both the K and L groups was simply related to the atomic number in a way which is expressed in the following equation :

$$\nu = A(Z - \sigma)^2$$

where  $A$  and  $\sigma$  are constants for each set of lines. This result, which is known as Moseley's Law, was shown by him to be consistent with Bohr's theory.

Since X-ray spectroscopy plays a large part in the elucidation of atomic structure, it will be necessary to give at this point some consideration to atomic theory.

**BOHR'S THEORY AND LATER MODIFICATIONS.** The so-called Rutherford-Bohr atom consists of a nucleus of positive charge  $Ze$  (where  $Z$  is an integer and is the atomic number) surrounded by  $Z$  electrons, each of negative charge  $e$ , which move about it in orbits (stationary orbits). They are held in these orbits by the electrostatic nuclear attraction. Not all orbits are permitted : the possible ones are determined by postulates which are set out later in this section. Further, it is assumed that the electron may revolve in an orbit without radiating. This is in conflict with classical mechanics, according to which an accelerated electron must radiate—and an electron moving in a circle or ellipse is always accelerating to the centre or to a focus as the case may be. Such radiation would, however, lead to results very different from those observed.

The innermost permitted orbit is called the *K* orbit ; the next the *L* orbit ; and so on. Later, we shall show that electrons in the inner orbits must have less energy than those in outer ones. When the atom absorbs energy from radiation or from the impact of a fast moving electron (as in the X-ray tube) the energy may cause the ejection of an inner electron despite the attraction of the nucleus.

This may occur if the energy available is greater than the negative nett energy of the electron in the nuclear field. The ejected electron leaves a vacancy in an inner orbit, and this is filled by an electron falling in from an outer orbit of higher energy. In its inter-orbital jump this electron thus loses energy \* and this appears as X-radiation. The orbit into which the electron falls determines the type of radiation—a transition to a *K* orbit gives K radiation, &c. The initial orbit—e.g. the *L*, *M*, or *N* orbit—decides the component of the radiation. In short, a characteristic X-radiation is supposed to be caused by the jump of an electron from one orbit to another nearer the nucleus, the frequency of the radiation being governed by the pair of orbits concerned.

If an electron moves in a circular orbit of radius *a*, it is assumed :

(1) That the electrostatic attraction of the nucleus (of charge *Ze*) balances the centrifugal force  $\frac{mv^2}{a}$ ; or

$$\frac{Ze^2}{a^2} = \frac{mv^2}{a} \quad . \quad . \quad . \quad (1)$$

(2) That the possible orbits are those in which the angular momentum is an integral multiple of  $h/2\pi$ , where *h* is Planck's constant, or

$$mva = \frac{nh}{2\pi} \text{ where } n \text{ is a whole number (the quantum number)} \quad . \quad . \quad . \quad (2)$$

(3) That when an electron jumps from an orbit of radius *a*<sub>1</sub>, of energy *W*<sub>1</sub>, to another of radius *a*<sub>2</sub> and energy *W*<sub>2</sub>, the frequency *v* of the radiation emitted is given by

$$hv = W_1 - W_2 \quad . \quad . \quad . \quad (3)$$

\* Actually it is better to consider the whole atom as losing the energy.

The term  $W$  is the total energy of the electron, i.e.\*  
 $\frac{mv^2}{2} - \frac{Ze^2}{a}$ .

Hence, substituting the values of  $a$  and  $v$  from (1) and (2),

$$W = -\frac{2\pi^2 e^4 Z^2 m}{n^2 h^2} \quad . \quad . \quad . \quad (4)$$

In the case of an atom other than hydrogen the expression for the attraction as given in (1) must be modified because the remaining  $Z - 1$  electrons exert a repulsion on the one considered. Electrons in outer orbits should have little effect; electrons in the same orbit should diminish the nuclear attraction, but by an amount difficult to estimate; and the electrons in orbits still closer to the nucleus should reduce the effective nuclear charge by an amount equal to their own charge. We must, in fact, replace the nuclear charge  $Ze$  by  $(Z - b)e$  where  $b$  is the 'screening constant', due to the electronic repulsion.

Thus  $W = -\frac{2\pi^2 e^4 m(Z - b)^2}{n^2 h^2} \quad . \quad . \quad . \quad (5)$

The value of  $b$  will naturally be different for the different orbits.

According to (3), the frequency of the radiation resulting from an electron transition is

$$\begin{aligned} \nu &= \frac{2\pi^2 e^4 m}{h^3} \left[ \left( \frac{Z - b_2}{n_2} \right)^2 - \left( \frac{Z - b_1}{n_1} \right)^2 \right] \\ &= \frac{2\pi^2 e^4 m (Z - b_2)^2}{h^3} \left[ \frac{1}{n_2^2} - \frac{1}{n_1^2} \left( \frac{Z - b_1}{Z - b_2} \right)^2 \right] \end{aligned}$$

and if  $b_1$  and  $b_2$  are small compared with  $Z$  and since  $\frac{1}{n_1^2}$  is much smaller than  $\frac{1}{n_2^2}$

\* Since the P.E. is  $\int_{\infty}^a Ze \cdot \frac{e}{r^2} \cdot dr = -\frac{Ze^2}{a}$ .

$$\nu = \frac{2\pi^2 e^4 m}{h^3} (Z - b_2)^2 \left[ \frac{1}{n_2^2} - \frac{1}{n_1^2} \right] \text{ (approximately)}$$

$$= R(Z - b_2)^2 \left[ \frac{1}{n_2^2} - \frac{1}{n_1^2} \right] \quad . \quad . \quad . \quad . \quad . \quad (6)$$

where  $R$  is Rydberg's constant (the constant for the optical spectra of hydrogen, for which  $Z = 1$ , and for which, as there is only one electron,  $b = 0$ ).

Considering, therefore, the radiation emitted when an electron drops from an  $L$  orbit ( $n_1 = 2$ ) to a  $K$  orbit ( $n_2 = 1$ ), we get  $\nu = \frac{3R}{4}(Z - b_K)^2$ . Moseley's experimental formula  $\nu = A(Z - \sigma)^2$  is identical with this if  $A = 3R/4$  and  $\sigma = b_K$ . Moseley's determinations of the  $K_\alpha$  lines gave triumphant confirmation of the former identification, and indicated the probable truth of the latter. Further confirmation came from his  $L_\alpha$  measurements, for which  $A$  was found to be equal to  $R(1/2^2 - 1/3^2)$ , representing a transition from an  $M$  orbit ( $n_1 = 3$ ) to an  $L$  orbit ( $n_2 = 2$ ).

It is customary to speak of the electrons for which  $n = 1, 2, 3, \&c.$ , as residing in the  $K, L, M, \&c.$ , 'shells'. It is clear that the energies of the electrons in the various shells are more fundamental in the specification of atomic structure than are the radiations arising from the transitions. To remove a  $K$  electron from the atom a certain amount of energy, given by equation (5), (with positive sign and  $n = 1$ ) is needed. This energy is characteristic of the particular element, and is called its  $K$  energy level. Similarly there are  $L, M, N, \&c.$ , levels. They represent the amount by which the energy of an atom ionised in the  $K, L$  or  $N$  shell exceeds the energy of the normal atom. The levels are usefully depicted in a diagram such as Fig. 16(a). The energies, and (since energy =  $h\nu$ ), the frequencies of the various X-ray lines are given by the differences of these levels. For example  $h\nu_{K_\alpha} = K - L$ , for the  $K_\alpha$  radiation is the result of a change from a  $K$ -ionized

to an  $L$ -ionized atom. A glance at the diagram shows that  $h\nu_{K\beta} = h\nu_{L\alpha} + h\nu_{K\alpha}$ . Measurement of the frequencies of these radiations demonstrates the truth of this relation and hence provides a check of the system of obtaining frequencies from the differences of terms such as the energy levels. However, a comparison of the diagram with the spectra shown in Figs. 18 and 19 (page 51 and

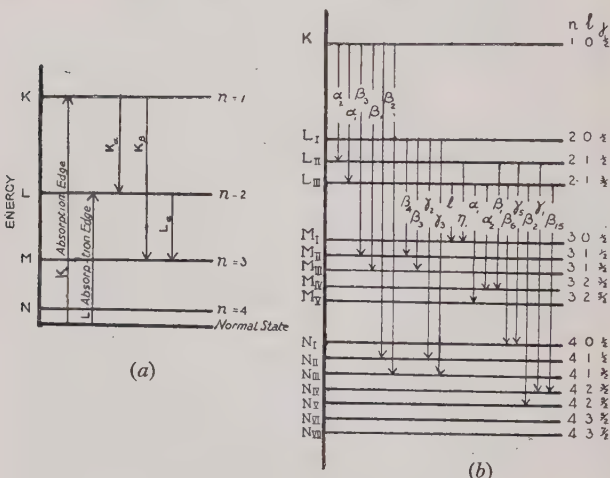


FIG. 16 (Not to scale)

$l$  may change by  $\pm 1$ , and  $j$  by  $\pm 1$  or  $0$   
( $M-N$ ) transitions and  $O$  and  $P$  levels are omitted

page 52) makes it plain that the simple theory given is not adequate to explain all the spectral lines obtained by the X-ray spectroscopists. The  $K_\alpha$  line, for example, was early shown to be double. The Sommerfeld-Wilson theory provided an explanation of some of the surplus radiations. Thus, while in equation (2) the quantum number  $n$  was entirely devoted to specifying angular momentum, this new modification split the quantum

number into two parts, one governing the angular momentum and the other controlling a radial motion, which is, of course, absent in a circular path. This modification therefore envisaged, not only circular, but also elliptical orbits of different shapes and, as a result, of slightly different energies. Still the theory predicted too few spectral lines. However, the necessary increase in the complexity of the theoretical picture was provided later by taking account of the spin angular momentum of the electron itself.

With the coming of the wave-mechanics, the clear picture of electron orbits has disappeared. It has been replaced by a cloud-like picture, in which the density of the cloud represents the probability of an electron being at the place considered. The form of the cloud can be worked out with an accuracy depending on the number of electrons involved. A  $K$  electron may be at any distance whatever from the nucleus, but, as we shall show later (page 76), its most probable distance is that prescribed by the Bohr theory. The new theory once more predicts discrete energy levels, which are again given by equation (5). It would have been untenable had it not done so. Further, in addition to the total quantum number  $n$  of that equation, a quantum number  $l$  occurs in the solution of the Schrödinger wave equation which governs the angular momentum. For a total quantum number  $n$ ,  $l$  may have any value from 0 to  $(n - 1)$ . The electron spin momentum corresponds to a quantum number of  $1/2$ . The two angular momenta compound in such a way that their resultant is given by a quantum number of  $(l + 1/2)$  or  $(l - 1/2)$ .\* This resultant quantum number is called  $j$ . Thus, in a heavy atom there are the following levels :

\* The value of an energy level is the excess energy of an atom ionized in the shell concerned over the energy of the normal atom. We are thus dealing with the energy and therefore with the quantum numbers of a shell lacking one electron. This

$K$  levels.  $n = 1, l = 0$  (zero angular momentum),  $j = 1/2$  (entirely due to electron spin).

$$\begin{cases} L_I \text{ levels. } n = 2, l = 0, j = 1/2 \\ L_{II} \quad " \quad " \quad l = 1, j = 1 - 1/2 = 1/2 \\ L_{III} \quad " \quad " \quad l = 1, j = 1 + 1/2 = 3/2 \end{cases}$$

$M$  levels. ( $n = 3$ ).  $M_I$  ( $l = 0, j = 1/2$ ),  $M_{II}$  ( $1, 1/2$ ),  $M_{III}$  ( $1, 3/2$ ),  $M_{IV}$  ( $2, 3/2$ ),  $M_V$  ( $2, 5/2$ ).

An atom normally contains a number of electrons sufficient to neutralize the positive charge on the nucleus. These electrons naturally tend to congregate in the states of lowest energy. We might, perhaps, expect to find them all in the  $K$  shell. This is not the case. On both experimental and theoretical grounds it is established that the  $K$  shell can contain only 2 electrons, the  $L$  shell 8, the  $M$  shell 18, and so on. As regards the subdivisions of the shells,  $L_I$  can hold 2,  $L_{II}$  can hold 2 and  $L_{III}$  4 electrons. The governing rule is that the number of electrons that can exist in any sub-group is  $(2j + 1)$ . For example, the  $M_{II}$  sub-shell ( $n = 3, l = 1, j = 1 - 1/2 = 1/2$ ) has 2 electrons; thus, of the 79 electrons in the gold atom, 2 dwell in the  $K$  shell, others fill the  $L, M, N$  and  $O$  shells, and one is left over to go into the deepest  $P$  level. This last electron is the valence electron.

It is interesting to note that, whilst the wave-mechanics allots a quite complicated probability cloud to a single electron in some of these states, yet, when all the electrons

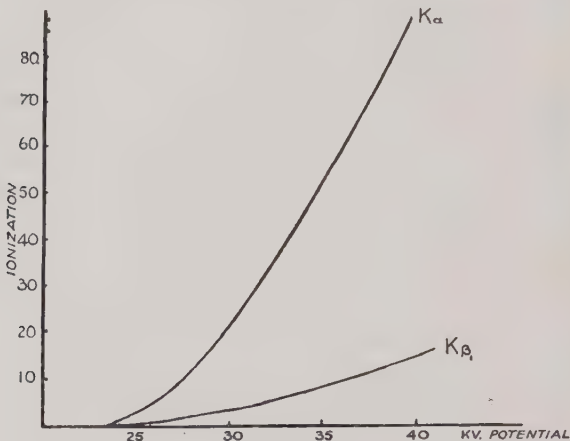
entails consideration of the total momenta of a number of electrons and would appear to be a fairly difficult proposition. Actually it is rather simple in the present case. This is because the total angular momentum and the total spin are zero for a complete shell, and therefore the momenta of a single one of the electrons are equal and opposite to those of the residue of the shell. Consequently, we may represent the singly ionized shell by quantum numbers  $l$  and  $1/2$  corresponding to a single electron. The X-ray spectra justify this, and have characteristics similar to those of the optical spectra of atoms with single valence electrons (e.g. Na, K, &c.).

n the shell are present, the result is complete spherical symmetry. Also, just as on the Bohr theory the *K* electrons were closer to the nucleus than the *L*, and the *L* closer than the *M*, so the various probability clouds concentrate in this order round the nucleus.

Consequent upon the filling of all the deeper levels, it is not possible to raise a *K* electron into the *L* shell. There is no room for it. To remove an electron from the *K* shell, it is in fact necessary to take it right out of the atom, or, what is almost the same thing, to take it to the first unoccupied level. An immediately observable consequence of this should be that, if an element is bombarded by faster and faster electrons until, ultimately, they are able to knock a *K* electron out of the atom, then, and only then, will the  $K_{\alpha}$  radiation appear. At the same moment the other *K* radiations will be emitted, for transitions will be possible from the *M*, *N*, and *O* shells to the vacant place in the *K* shell. There is good evidence of this. Thus, Fig. 17 indicates the intensities of the  $K_{\alpha}$  and  $K_{\beta_1}$  lines of rhodium when that element is bombarded by electrons propelled by various voltages. Both radiations appear simultaneously at 23,300 volts. The hardest radiation in the rhodium *K* spectrum is  $K_{\beta_2}(K - N_{II, III})$  with a wave-length of 534 X.U. By the relation  $eV = h\nu = hc/\lambda$ , where *V* is the equivalent voltage and *c* the velocity of light, this wave-length corresponds to 23,100 volts. Hence the first condition for the excitation of these  $K_{\alpha}$  and  $K_{\beta_1}$  radiations is that a *K* electron should be ejected somewhat beyond the *N<sub>II, III</sub>* level, which, in the case considered, can only be at a small energy depth in the atom.

A complete energy level diagram is shown in Fig. 16 (*b*), the sub-levels and their quantum numbers being given. It will be noticed that radiations do not arise from every pairing of levels. This is a manifestation of the Selection Principle, familiar in optical spectroscopy. The only

transitions allowed are those in which  $l$  changes by  $\pm 1$  and  $j$  changes by 0 or  $\pm 1$ . The other forbidden radiations sometimes occur, but they are never strong. Because of the scale of the drawing, the diagram does not show any X-ray lines due to transitions between sub-levels of the same shell. Such lines were not observed till recently, for the small energy difference involved entails a small frequency and a long wave-length. The diffraction grat-



(Curves from Webster, *Phys. Rev.*, 7, 605 (1916))

FIG. 17

ing methods, opening up the exploration of the soft X-ray region, have led to the discovery of this type of X-ray spectral line.

The appearance of the  $K$  spectra of the elements As (33), Se (34), Br (35), Rb (37) and Sr (38) may be seen in Fig. 18, which is a drawing of photographs given by Siegbahn. Moseley's  $\alpha$  line and shorter wave-length  $\beta$  line are both seen to be double. The component with

dex 1 in a line group is the line of greatest intensity, that with the index 2 is the next in intensity, and so on. The line is about twice as strong as  $\alpha_2$ , and, in the case of silicon, for example, their wave-lengths are 1173.43 and 77.40 X.U. respectively. The figure demonstrates how the wave-lengths of the lines diminish with increasing atomic number. Reference to Fig. 16 (b) will show the transitions to which the various spectral lines correspond.

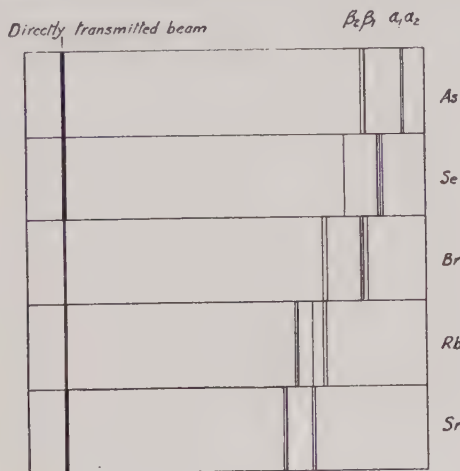


FIG. 18

With few exceptions the  $K$  spectra of all the elements have been examined, from uranium (92) down to lithium (3), from a wave-length of a little more than 100 X.U. to one of rather more than 200,000 X.U. Below lithium there are only the elements He and H, and as neither of these has, in the normal state, any electron outside the  $K$  shell, the spectra of these elements are optical spectra and cannot be termed X-rays.

In Fig. 19 we give a tracing of a photograph by Friman

of the L series of a few of the heavier elements. The diminution of wave-length with increase of atomic number is again apparent, and the spectra are seen to be more complex than in Fig. 18. The  $\alpha$ ,  $\beta$  and  $\gamma$  groups are in order of decreasing wave-length, and the intensities of the component lines again decrease with increasing index number. In the case of tungsten, the L spectrum covers the range from 1,675·0 X.U. for  $L_l$  to 1,025·8 X.U. for  $L_{\gamma_1}$ . The intensities of the two tungsten  $L_\alpha$  lines are in the ratio of about 10 : 1. The lightest element with elec-

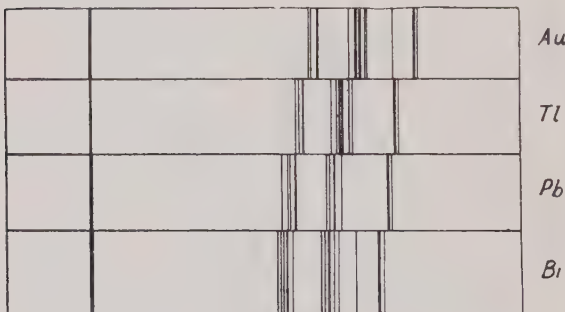


FIG. 19

trons in the M shell and therefore the lightest capable of giving L spectra is sodium (11).

The M and even the N series have received much systematic attention, whilst an O series line has been observed and measured for thorium.

The very soft X-ray spectroscopy, usually carried out by diffraction grating methods, has, like that of the ordinary X-rays, profited greatly by the contributions of Siegbahn and his co-workers at Uppsala.

X-RAY SATELLITES. The ordinary X-ray lines which correspond to the energy level diagram of Fig. 16 (b) are

often called diagram lines. Improved spectroscopic technique has shown that these are frequently accompanied by 'satellites' or 'non-diagram' lines. They are usually close to the diagram lines on the short wave-length side and are weak. For instance, on the short-wave side if  $K_{\alpha}$  is a group of five satellites (the  $K_{\alpha_{3,4}}$  group) whose intensity relative to  $K_{\alpha}$  diminishes with increasing atomic number. There is still evidence of the group at  $Z = 45$  (rhodium).

As Wentzel originally suggested, the satellites appear to be the result of transitions in multiple ionized atoms. Let us consider the case of  $K_{\alpha}$ . This diagram line is the result of a transition from a  $K$  ionized atom to an  $L_{II}$  or  $L_{III}$  ionized atom—( $K - L_{II, III}$ ). The satellite group is due to a transition from  $KL$  to  $LL$ , i.e. from an atom with a 'hole' in the  $K$  shell and a hole in the  $L$  shell to the state with two holes in the  $L$  shell. However, to produce such an effect it is first necessary to produce the  $KL$  ionization. In the case cited, the two electrons are simultaneously ejected by a single bombarding electron. In certain cases, however, the more important mechanism by which the second ionization is performed is the internal photoelectric process known as the Auger effect. This is discussed in Chapter VI.

WIDTH OF X-RAY LINES. Modern technique, and in particular the use of the two-crystal spectrometer, has shown that X-ray lines have measurable widths. The width is measured between the two points at which the intensity is half that of the line peak. Its magnitude in X.U. increases with decreasing atomic number, and depends also on the particular line considered. For gold ( $Z = 79$ ) the  $K_{\alpha_1}$  width is 0.15 X.U. (equivalent to 57.5 electron-volts), and that of  $L_I$  3.40 X.U. (19.8 e.-v.). For titanium ( $Z = 22$ )  $K_{\alpha_1}$  it is 1.22 X.U. (2.00 e.-v.).

A finite width is not foreign to classical ideas. Thus, consider an electron making free simple harmonic oscillations.

tions. It will only do this if it does not radiate. If the accelerations of the electron cause it to radiate, then the loss of energy means a damping of the vibration, whose simple sine form is thereby distorted. Fourier procedure shows that the motion may be expressed as the resultant of a vast number of vibrations of slightly different frequencies. The radiations must conform to these frequencies, and, as a result, are not monochromatic, but consist of a narrow band of wave-lengths. The predicted distribution of intensity in the band is, in general, correct, but the width is wrong. This classical theory gives it as 0·12 X.U. for all X-ray lines: the actual width of Au  $L_l$  is about thirty times greater than this, and is by no means exceptional.

On the quantum theory, an X-radiation is regarded as the result of the transition of an atom from one state to another of lower energy. We shall therefore focus our attention on these states. Consider a number of atoms in a given excited state. Owing to transitions to states of lower energy, the number remaining in the state will diminish with increasing time. Just as, on the classical theory, the rate of decay of the vibration gave the frequency spread, so here the greater the rate of decay of the state the greater the energy spread of that state. The distribution expressions in the two cases are practically identical. The predicted energy (or frequency) width of the X-ray line is the sum of the widths of the initial and final states. The widths obtained, although no longer constant, are still in general too small, but this difficulty has now been cleared up by taking into account the accelerated decay caused by the Auger effect.\*

This work is of obvious importance, and, in the X-ray field, is not subject to the masking effects experienced in the optical region (e.g. Doppler broadening).

CHEMICAL AND PHYSICAL EFFECTS. The chemical or

\* For Auger effect, see Chapter VI, page 118.

Physical state of an element has been supposed to have no effect on its X-ray spectra. This is usually but not invariably true. For example, the width of the  $K_{\alpha_1}$  ( $K - L_{III}$ ) line of Mn has been shown to increase by nearly 25 per cent. in an alloy containing an equal number of Ni atoms. Evidently the neighbouring atoms in a solid can affect the spectra. Shifts of lines and the appearance of new ones have also been reported. Naturally the effects are, however, most marked in those lines which involve the transition of one of the outermost or valency electrons because

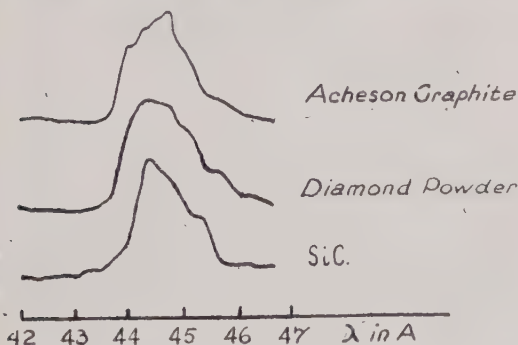


FIG. 20

Carbon  $Kd$  [ $K$ -(valence)]. Representing Photometer Curves by Siegbahn and Magnusson (Zeits. f. Physik, 96, 10 (1935))

these are most affected by the electric fields of adjacent atoms. Thus, in the much studied  $K_{\alpha}$  radiation of carbon [ $K$ -(valence)], the effect of allotropic and chemical form is clearly shown (Fig. 20). Roughly speaking, photometer curves such as those of the figure indicate the intensity distribution—the ‘shape’—of the X-ray line, and, since in this case the  $K$  level should be fairly narrow, give an idea of the energy distribution of the valence electrons. As another example, contrast the photometer curves of the [ $L_{II, III}$ -(valence)] line of Al metal with that of  $Al_2O_3$

in Fig. 21. The former curve is characteristic of the free (valence) electrons in a metal. They are evidently spread out into a wide band of energies (13 electron-volts) and the sharp cut-off at the short-wave edge of the line denotes a sharp upper limit to their energy. The line width agrees admirably with the Fermi-Sommerfeld theory of electron behaviour in conductors. This theory predicts a sharp energy limit and, for Al, an energy spread of 12 e.v. This is in marked contrast to the classical Maxwellian distribution, which, at room temperatures, predicts

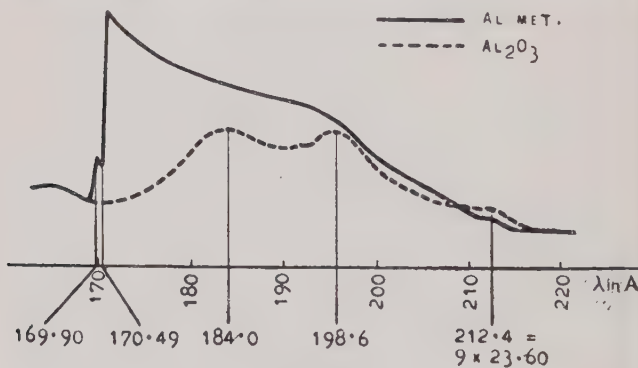


FIG. 21

(Siegmann and Magnusson, *Nature*, 132, 895 (1933))

free electron energies of the order of 0.1 e.v. Soft X-ray spectroscopic work on a number of such bands has given, in fact, excellent support to modern ideas of the electronic structure of solids.

**THE GENERAL X-RAY SPECTRUM.** Reference has already been made to the general or continuous X-radiation (page 13), to the intensity distribution in its spectrum (Fig. 22) and to the sharp termination of the spectrum on the short-wave side at a wave-length governed by the voltage on the X-ray tube. The relation between the

wave-length,  $\lambda_{min.}$ , of this limit and the exciting voltage,  $V$ , is  $V\lambda_{min.} = \text{const.} = \frac{hc}{e}$ , where  $c$  is the velocity of light.

This is known as the Duane-Hunt law. The quantum theory provides a ready explanation for it. Thus, if the

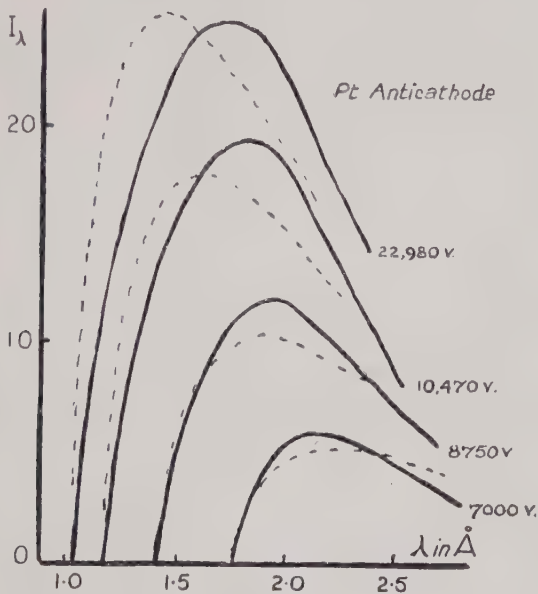


FIG. 22

Representation of some of the intensity distribution curves given by Kulenkampff (*Ann. d. Physik*, **69**, 578 (1922)).

The curves in broken lines are fully corrected: the full-line curves only corrected for absorption in the anticathode.

X-radiation is emitted in the form of quanta (of energy  $h\nu$ ), the greatest energy that a quantum can acquire at the expense of the kinetic energy of a bombarding electron is its whole energy,  $eV$ . When, on the other hand, the radiation process does not consume all the energy of the

electron, then the quantum energy  $h\nu$ , and hence the frequency, is less. The maximum frequency  $\nu_{max}$ . is clearly given by the relation :

$$h\nu_{max} = \frac{1}{2}mv^2 = eV.$$

Since  $\nu = c/\lambda$  we get  $V\lambda_{min.} = \frac{hc}{e} = \text{const.}$ , which is the Duane-Hunt law. This furnishes a very direct method of determining the ratio  $h/e$  and hence  $h$ , and, furthermore, a method of great accuracy.

The product  $V\lambda_{min.}$  may be determined by measuring the value of  $\lambda_{min.}$  for a given exciting voltage from curves such as those of Fig. 22. More usual, however, is the method of isochromats. Here, setting the spectrometer to reflect a certain wave-length (which may be done readily with the aid of a characteristic X-radiation of known wave-length) the intensity of the general spectrum at the value of  $\lambda$  is measured for various tube voltages. For small voltages,  $\lambda_{min.}$  is greater than the wave-length,  $\lambda_{spect.}$ , for which the spectrometer is set. As the voltage is increased, the general radiation advances towards shorter wave-lengths, and when, and only when,  $\lambda_{min.}$  has diminished to the value of  $\lambda_{spect.}$ , does ionization begin to occur in the spectrometer. With further voltage increase, the peak of the intensity distribution curve of Fig. 22, moving to smaller wave-lengths, approaches  $\lambda_{spect.}$  and the ionization mounts rapidly. Some isochromats—plots of ionization against voltage—are shown in Fig. 23. Since, at the voltage at which ionization first appears,  $\lambda_{min.} = \lambda_{spect.}$ , the feet of the isochromats provide the information for the produce  $V\lambda_{min.}$ , and hence for  $hc/e$ . If a spectrometer of very high resolution is used and the foot of the isochromat determined with great care, if the proper corrections are applied to the measured voltage on the X-ray tube, and if the vacuum in the tube is good, then a very accurate value of  $h/e$  may be obtained ( $c$  being known with sufficient

accuracy). Ohlin's experiments (see Birge \*) yield a value which accords well with that obtained by other means.

The intensity distribution curves of Fig. 22 are the result of a very painstaking work, and some of the difficulties which have been overcome deserve mention. Firstly, the X-rays, emanating in general from appreciable

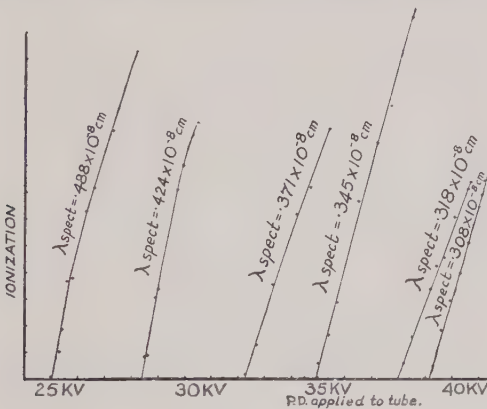


FIG. 23

Isochromats by Duane and Hunt (*Phys. Rev.*, 6, 166 (1915))

depths beneath the surface of the anticathode, and therefore having to pass through anticathode material on their way to the measuring apparatus, suffer some absorption, different parts of the spectrum being absorbed by different amounts. Absorption also occurs in the window of the X-ray tube and in the air between tube and ionization chamber. Again, some of the radiation passes right through the ionization chamber and escapes measurement, the loss being more pronounced for the harder parts of the spectrum. A further point is the variation with wave-

\* *Reports on Progress in Physics*, 8, 90 (1941).

length of the reflecting power of the crystal. Each of these effects is, if not satisfactorily dealt with, capable of distorting the form of the measured distribution curve.

A considerable simplification of the distribution curves ensues if intensity is plotted against frequency instead of wave-length. Thus, the energy radiated between  $\lambda$  and  $\lambda + d\lambda$  is proportional to  $I_\lambda d\lambda$ . The same quantity may

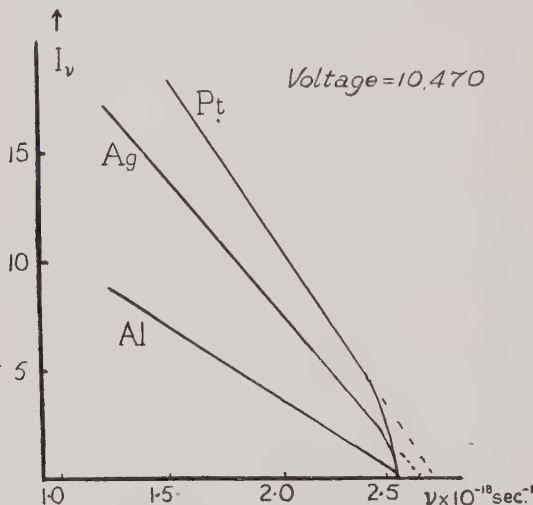


FIG. 24 (a)

Representation of some of Kulenkampff's (*Ann. d. Physik*, **69**, 586 (1922)) curves.

The scale of ordinates is different for each.

The experimental points have been omitted.

be written  $-I_v dv$ . But  $\lambda = c/v$ , and  $d\lambda = -cdv/v^2$ , so that  $I_v = I_\lambda c/v^2$ . In a plot of  $I_v$  against  $v$  the factor  $1/v^2$  greatly changes the form of the curve. The result, shown in Fig. 24 (a), is straight lines, with an increase of slope near the high-frequency limit.

Owing to the loss of velocity suffered by the electrons penetrating into the anticathode, the X-rays in the curves

so far given are produced by electrons with a wide range of velocities. Obviously, it is desirable to know the nature of the radiation produced by electrons of a definite known velocity. Hence, as in the experiments on polarization, recourse is had to anticathodes so thin that few of the electrons suffer appreciable energy loss.  $I_\nu - \nu$  curves obtained in this way are shown in Fig. 24 (b). They have

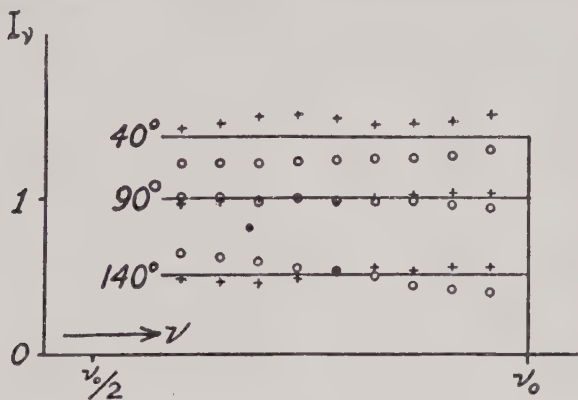


FIG. 24 (b)

(Nicholas, Bureau of Standards, Inst. of Research, 2, 837 (1929))

a very simple form, the intensity being constant up to the frequency limit, where it suddenly drops to zero. The thick anticathode results of Fig. 24 (a) must clearly be regarded as built up of a succession of thin anticathode curves, corresponding to successively diminishing velocities.

As Fig. 24 (b) shows, the form of the distribution curves is much the same over a wide range of angles,  $\psi$ , between direction of observation and cathode-ray beam. However, when  $\psi$  is small, and also as it approaches  $180^\circ$ , there is a greater proportion of soft radiation. The continuous radiation is hardest when  $\psi$  is about  $67^\circ$ .\*

\* Kulenkampff, *Ann. der Physik*, 87, 597 (1928).

On the theory of the general spectrum we cannot make more than a few remarks. It is clear that something more than the simple theory of Chapter I is required. A more detailed examination is necessary; the collisions of the cathode-ray electrons with the anticathode atoms must be considered. From the classical point of view it is expected that the radiation arises as a result of the accelerations of the bombarding electrons in the strong fields near the atomic nuclei. Calculations have been made on this basis, but, to explain the termination of the radiation at the high frequency limit, it is also necessary to invoke the quantum theory, which, as we have seen, gives the limit correctly. It is interesting to find that, if this is done, the calculations are in satisfactory accord with experiment. They correctly predict the distribution curves of Fig. 24 (*b*); they correctly give the total energy in the spectrum as proportional to the atomic number of the anticathode material and to the square of the tube voltage; and they give the right order of magnitude for this energy. More recently the problems of the continuous spectrum have been successfully attacked from the point of view of the wave-mechanics.

### ABSORPTION

The principles involved in the measurement of absorption coefficients have been discussed in Chapter I, but in the experiment described there, the X-ray beam was admittedly inhomogeneous. Nowadays, monochromatic radiation is readily obtained. The X-ray spectrometer provides the means. The absorbing medium may be conveniently placed between the slits *A* and *B*, which confine the beam on its way to the spectrometer crystal (Fig. 8, page 24), and the measurements may be made much as in Chapter I. This time, however, they are made at the definite wave-length prescribed by the setting of the spectrometer. A practical difficulty arises. When the absorp-

tion is large, the absorbing sheet must be thin ; and when the sheet is thin it is apt to be of uneven thickness. This trouble may be overcome by keeping the sheet in motion across the beam. Thus, the effective thickness is now, not that at any particular point on the sheet, but is the mean thickness over an appreciable area. This thickness may be ascertained by weighing.

For the measured absorption two processes are responsible. In the first of these the energy is consumed in the ejection of photo-electrons ; in the second the X-rays are scattered out of the beam by the electrons of the absorbing substance. (This process has been mentioned on page 12 and will be discussed at greater length in Chapter IV). The mass absorption coefficient may thus be divided into

two terms, so that  $\frac{\mu}{\rho} = \frac{\tau}{\rho} + \frac{\sigma}{\rho}$ , where  $\tau$  is the true (photo-electric) absorption coefficient and  $\sigma$  the scattering coefficient.\* It is not easy to separate them, and it is not always necessary to do so.

Since the scattered radiation emerges from the absorber in all directions, some will pass on with the transmitted beam. If, however, the beam is limited in width by narrow slits, the proportion of scattered radiation emerging from them will be negligible and the 'absorption' by scattering will be fully effective. Such is the case with the X-ray spectrometer.

The dependence of absorption on wave-length is of paramount importance. The general form of the variation is shown in Fig. 25. The absorption rises with increasing wave-length, but at the points labelled  $K$ ,  $L_I$ ,  $L_{II}$ ,  $L_{III}$  it drops suddenly, only to resume its previous general rise. At  $K$  the wave-length is just shorter than the shortest  $K$  emission line, and at  $L_I$ ,  $L_{II}$ , and  $L_{III}$  just shorter than that of the shortest line due to electrons falling into the  $L_I$ ,  $L_{II}$ ,  $L_{III}$  shells, respectively. In fact, according to the

\* This coefficient is discussed in Chapter IV.

relation  $eV = h\nu$ , the discontinuities in the curve (called absorption edges) correspond to the excitation voltages of the emission spectra. The interpretation of the curve becomes clear. There is a general increase in absorption with wave-length, broken by the edges. At the  $K$  edge the quanta are no longer of sufficient energy to remove the  $K$  electrons, and, with the ceasing of this  $K$  photoelectric process, the absorption suddenly drops. Further increase in wave-length brings increase in absorption until the point  $L_I$  is reached. Here  $h\nu$  becomes less than the ioniz-

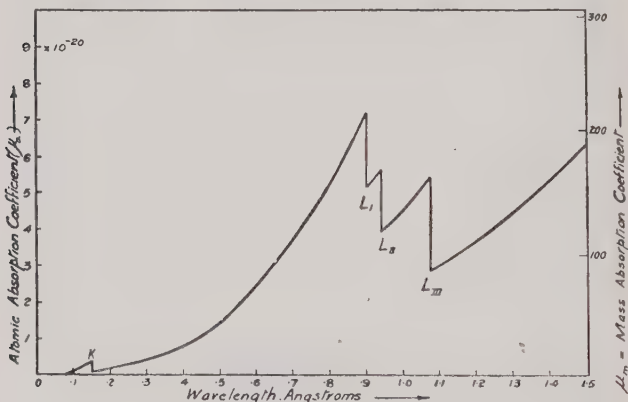


FIG. 25

ing energy of the  $L_I$  electrons, the  $L_I$  absorption process ceases and the absorption coefficient suddenly falls again. The other edges bear similar interpretations.

The theoretical importance of the edges is manifest. Their values of  $h\nu$  proclaim directly the minimum energy to remove an electron from the various atomic shells. In fact, they evaluate the energy levels, and they do it with an accuracy exceeding that of the excitation voltages. The energy levels in the tables of the standard treatises are based on such determinations. It is not necessary to

measure all the edges for an element. In many cases it would not be easy. As an example, the  $L_{III}$  level may be evaluated by means of the  $K$  edge and the  $K_{\alpha_1}$  emission line. Thus,  $h\nu_{K_{\alpha_1}} = (K - L_{III})$  and

$$h\nu_{K_{edge}} - h\nu_{K_{\alpha_1}} = K - (K - L_{III}) = L_{III}$$

Other levels may be found in similar fashion.

Fig. 26 is an energy-level diagram covering the whole range of elements. Not only does it show the energies of electrons in the various shells, but, in addition, it gives important information on the process of atom-building—of the manner in which, as we pass from atoms of lower to those of higher nuclear charge, electrons are added one by one to fill the various shells. In the figure the square roots of the energy levels \* are plotted against atomic numbers in the manner of the Moseley diagram. The  $K$  and  $L$  curves appear at first sight to be straight lines, as is to be anticipated from the Bohr theory (eq. (5), page 44). Closer inspection shows that this is not quite true, and the other curves show marked changes of slope. They are due to the slight increase of the screening constant  $b$  as the number of electrons in the atom increases. This effect is greater when electrons are being added one by one to 'inner' incomplete shells than when they are added as ordinary valence electrons, since, for the former, the increase in  $b$  is greater, so that the effective nuclear charge,  $Z - b$ , and consequently the energy levels, do not in such a case increase in magnitude so rapidly with  $Z$ . The slope of the curve is therefore diminished. The diagram shows quite clearly, for example, the effect of the filling of the  $N_{VI, VII}$  shell from  $Z = 58$  to  $Z = 71$ . (There are already, at  $Z = 58$ ,  $O$  and even  $P$  electrons present.)

\* Actually the ordinates are values of  $\sqrt{\frac{W}{R}}$ , where  $R$  is the Rydberg constant.

When examined with apparatus of sufficient resolving power, absorption edges are found to have finite width.

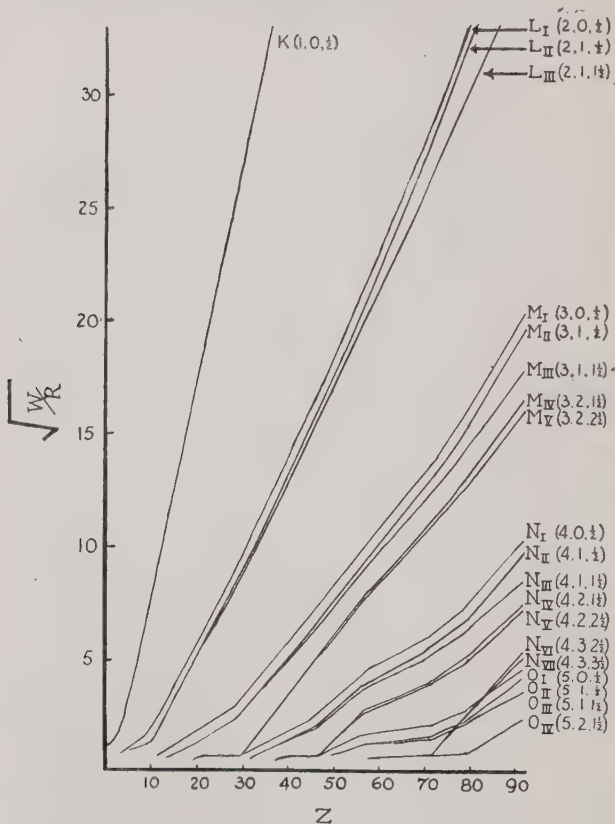


FIG. 26

Moseley diagram of the X-ray energy levels  
(Curves from Coster, *Physica*, 4, 418 (1937))

The edges are not quite the vertical falls in absorption indicated by Fig. 25, but are spread over a small range of

wave-length. The width of the *K* edge, expressed in energy units, has been found to vary as  $Z^4$  for the elements above  $Z = 33$  and to be constant for the lighter elements. *K* edges are wider than *L*. For example, for tungsten, the *K* width is 133 electron-volts (Richtmyer and Barnes) and  $L_{III}$  11.6 (Semat).

By assuming that the energy levels are evaluated by the absorption edges, we have had to be prepared for small errors, for we have become involved in the assumption that the edge occurs when the X-ray quantum is just sufficient to remove an electron out of the atomic field. In general this is untrue. The electron is not taken to a state of zero energy, but to a vacant level at the surface of the atom. (In a solid this level is probably more characteristic of the crystal lattice than of the atom.) Further, it is to be anticipated that this vacant level is not necessarily that of lowest energy, but the lowest for which the selection principle (see page 49) is satisfied. There is evidence for this in the fact that an energy level obtained directly from an absorption edge does not always quite agree with that obtained by the method of calculation given above and depending on the measurement of a different edge. The point here is that the two edges do not (owing to the selection principle) utilize the same vacant final level. When the absorber is not a solid but a monoatomic gas, the situation is simpler. In this case there exists at the surface of the atom the system of vacant levels which are responsible for optical absorption and emission spectra. From these spectra we know where the levels occur, and, incidentally, that they are very sharp indeed. Hence, as we pass from higher to lower X-ray frequencies, we should expect to find, first the continuous absorption due to electrons being removed from the atom, then absorption lines due to transitions to the vacant optical levels, after which the absorption of the particular electron shell should cease. This is found in practice. An

absorption curve for argon and its analysis are found in Fig. 27 (a).

A structure effect of a different kind is found for solids. (see Fig. 27 (b)). It consists of a series of small maxima

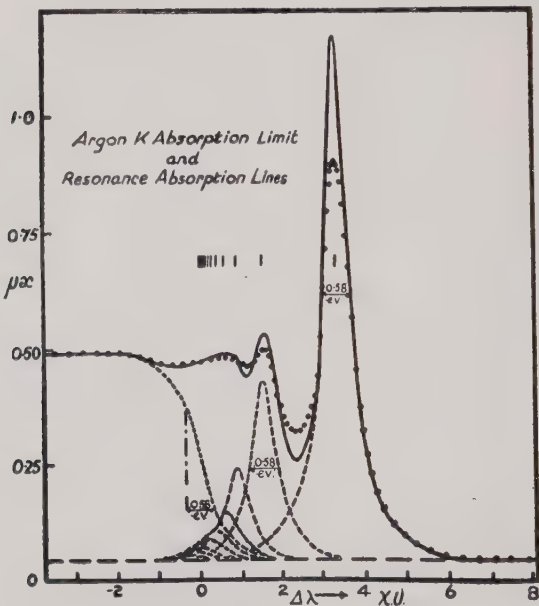


FIG. 27 (a)

(Parratt, *Phys. Rev.*, 56, 295 (1939))

The dots represent experimental values, the full line gives the corrected curve, and the broken line gives the analysis of the curve into absorption edge (on the left) and absorption lines.

and minima stretching in some cases over a range of several hundreds of electron-volts on the short-wave side of the absorption edge. This surprising phenomenon was explained by Kronig. It is due to the fact that an electron, moving through the crystal lattice of the solid, is not free

to have any velocity that it likes—that there are forbidden zones of energy. X-ray frequencies which would eject an electron with such energies are unable to do so, and local diminutions of absorption are the consequence. The forbidden zones may be regarded as resulting from the wave nature of the free electron. Its wave-length is inversely

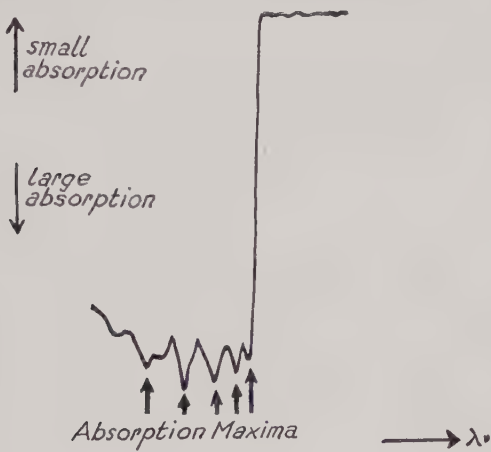


FIG. 27 (b)

*K* edge of copper

Photometer record \* of continuous spectrum after the radiation has passed through a copper screen. Smaller ordinates here represent larger absorption.

(Curve from Coster and Veldkamp, *Zeits. f. Physik*, **70**, 306 (1931)).

\* Measuring the blackening of the photographic plate, and, with appropriate procedure, permitting the calculation of relative X-ray intensities.

proportional to its velocity. For certain wave-lengths (and hence for certain velocities) it suffers Bragg reflection from the lattice and hence cannot penetrate the crystal. Thus it cannot escape from the atom and the absorption process is inoperative.

Many investigations of the effect of chemical combination have demonstrated shifts of the absorption edges,

sometimes amounting to more than 10 electron-volts. A shift of several volts may also be produced by a change of state from solid or liquid to vapour.

Between and beyond the absorption discontinuities  $\mu_{atomic}$  increases rapidly with increase of wave-length : it also increases very quickly with increase of atomic number. This is mainly due to the true photoelectric absorption, although the scattering coefficient also changes in the same sense. The true atomic absorption coefficient varies as  $\lambda^3$  over most of the X-ray region, but for wave-lengths appreciably greater than about 15 $\text{\AA}$  the variation seems to be less rapid and more nearly proportional to  $\lambda^{2.5}$ . Over a wide range  $\tau_{atomic}$  is proportional to  $Z^4$ , but there is evidence that the power is less than 4 for wave-lengths of the order of 100 $\text{\AA}$ . Since  $\tau$  becomes very large for heavy elements and for long wave-lengths, the scattering for these cases forms only a small proportion of the absorption, and  $\tau$  is nearly enough equal to  $\mu$ .

The chemical state of an element does not affect the value of  $\tau_{atomic}$  for ordinary hard X-rays, but for the very soft radiations this does not appear to be true. This is not surprising, for, whilst the hard X-ray absorption is mainly concerned with the removal of electrons from inner shells, the soft radiations can only be absorbed by electrons near the surface of the atom, where the fields of the adjacent atoms are appreciable.

## CHAPTER IV

### THE SCATTERING OF X-RAYS

THOMSON'S THEORY OF SCATTERING. The classical method of regarding the genesis of X-rays, as briefly mentioned on page 14, was one in which the radiation was imagined to be set up as a result of the retardation of the electron in the parent cathode stream. On these lines Sir J. J. Thomson made a theoretical estimate of the scattering to be expected when X-rays fall on matter. His method was to calculate for electrons in the scattering substance the acceleration produced by the electric vector in the incident primary X-ray beam. Then, assuming that the accelerated electron radiates according to the classical mechanics, he deduced the intensity of the scattered radiation in any direction inclined to that of incidence. His calculation gave the intensity of the scattered beam  $I_\phi$ , in a direction inclined at  $\phi$  to the primary beam as

$$I_\phi = \frac{Ine^4}{2m^2c^4r^2}(1 + \cos^2\phi) \quad . \quad . \quad . \quad (1)$$

where  $r$  is the distance from the scattering substance,  $n$  the number of electrons, and  $I$  the intensity of the incident beam.

If we integrate the expression over a complete sphere we obviously obtain  $I_s$ , the total energy scattered in all directions, viz. :

$$I_s = \int_0^\pi I_\phi 2\pi r \sin\phi \cdot r \cdot d\phi$$

$$I_s = \frac{8In\pi e^4}{3m^2c^4}$$

which is, of course, independent of  $r$  and gives as the value of the fraction of energy scattered,  $\sigma$ ,

$$\sigma = \frac{I_s}{I} = \frac{8}{3} \frac{\pi e^4}{m^2 c^4} \cdot n \quad . \quad . \quad . \quad (2)$$

In (2) let us consider  $n$  to be the number of electrons per cubic centimetre of the scattering material. Suppose now we have a sheet of thickness  $dx$ . The energy falling on 1 sq. cm. per second is  $I$  and the amount scattered and therefore removed from the beam is

$$- dI = I\sigma \cdot dx.$$

Consequently the intensity  $I$  of a beam emerging from a sheet of finite thickness  $x$  is, by integration,

$$I = I_0 e^{-\sigma x} \quad . \quad . \quad . \quad (3)$$

where  $I_0$  is the incident intensity. Thus  $\sigma$  may be considered as an absorption coefficient due to scattering. In practice, however, it is more customary to speak of the mass scattering coefficient  $\sigma/\rho$  (where  $\rho$  is the density of the scattering substance).

Reverting to (2), it is seen that, if  $\sigma$  is determined experimentally, then, since  $e$ ,  $m$  and  $c$  are known,  $n$ , the number of electrons per cubic centimetre can be calculated, and, from this, the number of electrons per atom. The honour of making this fundamental determination belongs to Barkla. Since at the present time this number is known from other considerations, we may look on the result, when experimentally verified, as showing that the scattering is produced by all the electrons in the atom acting independently.\* The correct value is, however, obtained only for light elements and for X-rays of medium wavelength. This is capable of explanation. Thus, if the  $Z$  electrons in the atom are close together compared with the wave-length of the radiation, the scattering from all the electrons will be in phase and the resultant amplitude

\* For that assumption is made in equation (1).

$Z$  times that from a single electron. The total intensity will therefore not be increased  $Z$  times by the  $Z$  electrons, as would be the case if the radiations were independent, but  $Z^2$  times since intensity is proportional to amplitude squared. Hence, for heavy elements, where there is a great concentration of electrons near the nucleus, the scattering is abnormally large. The same is true for long wave-lengths. On the other hand, for wave-lengths less than  $0.1\text{\AA}$ , the observed scattering is always small, compared with the prediction of equation (2) which (taking no account of the above), makes  $\sigma$  independent of  $\lambda$ . Thus, for  $\gamma$ -rays,  $\sigma/\rho$  falls from its normal value of  $0.2$  to the order of  $0.05$ . Whilst this represents a real departure from classical prediction, it is adequately explained by the quantum theory, and is associated with the recoil of the scattering electron in the Compton scattering which is discussed later in this chapter.

ANGULAR DISTRIBUTION OF SCATTERED X-RAYS. The extent to which (1) is correct in expressing the angular distribution is shown in Fig. 28. Hewlett's curve was obtained from mesitylene— $C_3H_3(CH_3)_3$ —a liquid containing only atoms of low atomic weight. The radiation was monochromatic and of wave-length  $0.71\text{\AA}$ . It is seen that, whilst there is good agreement in the neighbourhood of  $90^\circ$ , there is an unmistakable disagreement below about  $50^\circ$ . In fact, as in the case of the earlier curve obtained by Barkla, the observed intensity is too great in the forward direction. To discover how far this discrepancy is due to the interference of the scattered radiation it is obviously desirable to consider the scattering from more simple substances.

SCATTERING BY GASES. In the case of the monatomic gases it is possible to investigate the angular distribution without any disturbing effects due to interatomic interference. Owing to the small number of electrons per cubic centimetre and the consequent low intensity of the

scattering, the experimental work is not easy, but, despite this, the distribution curves are well established. Fig. 29 shows the results obtained by Wollan for various gases. Once more we notice that the curves rise much too sharply at small angles to agree with the theoretical prediction of Fig. 28. Constructive interference within the atom supplies the reason. For example, in the direction of the

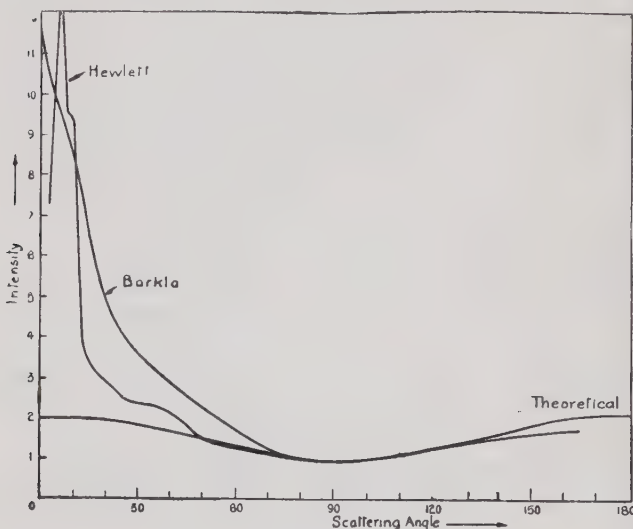


FIG. 28

direct beam ( $\phi = 0$ ), the X-rays scattered from all the electrons in the atom must be in phase, so that, as mentioned above, excess scattering is bound to arise. For larger angles the phase difference will increase and the resultant intensity diminish. Exact calculations of the interference effects have been undertaken by Raman and by Compton. Clearly something must be assumed about the relative positions of the electrons in the atom. Both

treatments assume spherical symmetry and an unknown radial probability distribution of the electrons about the nucleus. The resulting expression is the sum of two terms—one proportional to  $Z^2$  representing a summation

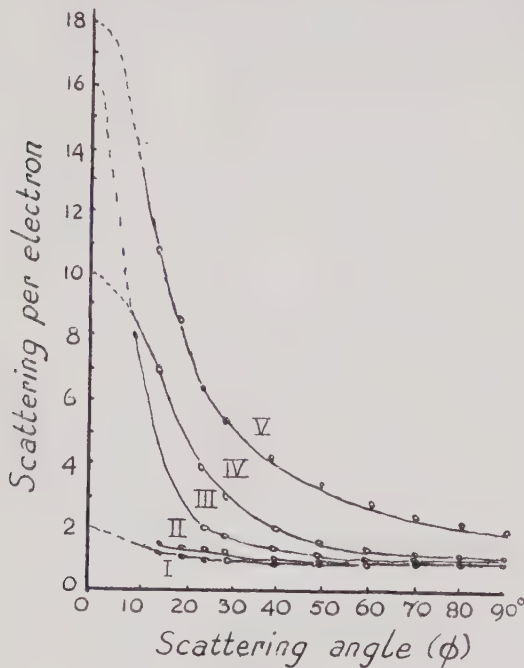


FIG. 29

$\lambda = 0.71 \text{ \AA}$ . Curve I hydrogen. Curve II helium. Curve III oxygen.  
Curve IV neon. Curve V argon  
(Wollan, *Phys. Rev.*, **37**, 862 (1931))

of amplitudes for the  $Z$  electrons, and one proportional to  $Z$  and representing therefore a summation of intensities. The former is called the coherent—or interfering—radiation, and the latter the incoherent. This last term

arises through the motion of the discrete electrons in the atom. A wave-mechanical calculation by Wentzel agrees with the classical formula of Raman and Compton, and serves finally to identify the  $Z$  term as the incoherent radiation which suffers a change of wave-length by the Compton effect (described later in the chapter).

To make a direct comparison between theory and experiment, a knowledge of the electron distribution in the atom is required. Such distributions have been worked out on the basis of the new quantum mechanics by Hartree. When these are inserted into the scattering formula, an excellent agreement is found with the experimental scattering curves. Perhaps even more interesting is the fact that, if the experimental data are used in combination with the scattering expression, it is possible to work out (as Compton has done) the probability distribution of electrons in the atom. This is virtually a picture of the atom. Such results are of considerable importance, for views on the behaviour of the electrons in the atom have changed in recent years and it is desirable to ascertain whether or not the modern view is correct. According to the Bohr theory the electrons were in definite orbits, which, in the case of helium, for example, were circles of equal radii. The wave-mechanics, however, tells us that the position of the electrons is less definite and can only be expressed by a continuous probability curve. In Fig. 30 the broken curve shows the theoretical radial distribution curve for He and the vertical line marked  $a$  indicates the radius of the normal Bohr orbit. The full-line curve, obtained by Wollan from his scattering experiments, amply justifies the new theory. Wollan's results for neon are also of great interest, for they show two peaks in the radial distribution curve, corresponding to the  $K$  electrons close to the nucleus and the  $L$  electrons farther out.

For polyatomic molecules the scattering problem becomes a stage more complex, for here must be con-

sidered the interference of the radiations from the several atoms within the molecule. Fortunately, the monatomic gas experiments have demonstrated the correctness of the theoretical treatment, which may therefore be used to work out the amplitude of the coherent scattering of each atom. If the structure of the molecule is known, these amplitudes can be compounded. For example, in the

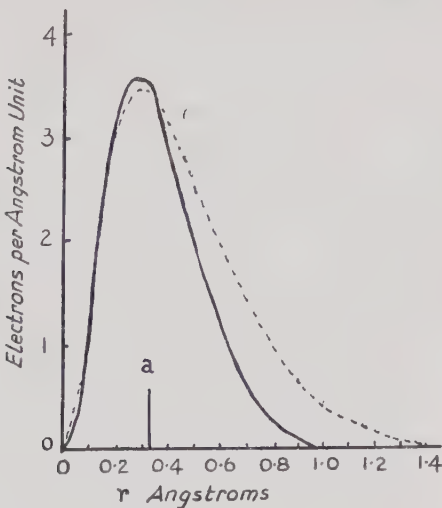


FIG. 30

Radial electron distribution (helium)  
(Wollan, *Phys. Rev.*, **38**, 15 (1931))

case of a diatomic molecule it is merely a problem of two scattering centres a known fixed distance apart, but orientated at random. The incoherent scattering, since it does not interfere, is obtained by simple addition of the incoherent scattering from the several atoms. The calculations agree with the experimental results as well as can be expected. Since the inter-atomic distance is involved

in the calculations, this quantity may be determined by giving it the value that produces the best fit between the theoretical and experimental curves. For oxygen and nitrogen the values obtained are  $1\cdot22$  and  $1\cdot09\text{\AA}$  respectively.\* These figures agree well with  $1\cdot21$  and  $1\cdot10\text{\AA}$ , the corresponding values derived from the Raman spectra of these gases.

SCATTERING BY LIQUIDS AND AMORPHOUS SOLIDS. Debye and Scherrer in 1916 showed that diffraction patterns were obtainable from liquids. As in powder photographs (see Fig. 14 (b)), rings are exhibited, but they are few in number and are very diffuse. The intensity curves differ from those for gases in one very important respect, for whilst both monatomic and diatomic gases show increasing intensity as small angles of scattering are approached, for liquids the intensity remains small. Since individual atoms or molecules must scatter in much the same way in liquids as in gases, it appears that in liquids there must be another type of interference not hitherto encountered. This must be ascribed to the interference of the radiations from the separate molecules. For this to happen, the arrangement of the molecules in a liquid cannot be entirely random.<sup>†</sup> This intermolecular interference obviously provides a tool for the detailed study of the structure of liquids. The subject is receiving a good deal of attention, but we cannot do more here than indicate where further information may be obtained.<sup>‡</sup> Amorphous solids produce much the same sort of diffuse diffraction rings as do liquids, and for glasses and for carbon the X-ray study has been of especial value.

\* Compton and Allison, *X-Rays in Theory and Experiment*, p. 164.

† This is not very surprising, for the size and shape of the molecules must have some local influence on the distance apart and arrangement.

‡ See Randall, *The Diffraction of X-Rays by Amorphous Solids, Liquids and Gases* (Chapman & Hall).

It is interesting to find that when a substance (e.g. argon) changes from a liquid to a high-pressure vapour and then to its more rarefied form, the scattering pattern changes gradually from the 'liquid' to the 'gaseous' type. There is no sudden change.

INTENSITY OF SCATTERING FROM CRYSTALS. Already, in Chapter II we saw that the sharp intensity maxima given by crystals at definite reflection-angles indicated a regular periodic arrangement, and that by measuring these angles the spacing of the reflecting planes could be obtained and the structure of the crystal determined. More information is obtained by measuring the intensities of these reflections. On comparing the different order reflections from a given set of planes an interesting fact becomes apparent. The intensity dies off more rapidly with increasing order number than would be the case if the whole of the scattering \* took place in the reflecting planes. Once more we are reminded that the scattering centres are electrons, that these are not concentrated at the centre of the atom and that there will be mutual interference between their scattered radiations. The reflections, therefore, may be considered to take place not at planes through the atomic centres but at 'electronic sheets' of finite thickness, and the observed phenomena are the result of two interference effects; first, that within the thickness of the individual sheets and, secondly, that between the resultant radiations from these sheets. Already it has been shown that the path difference of radiations reflected from two parallel planes is  $2d \cdot \sin \theta$  and thus increases with the scattering angle  $\phi (= 2\theta)$ . Consequently the phase difference between the constituent electron layers *within* a sheet increases with increasing angle, and the

\* The reflection is, of course, the result of scattering, the reflection from a plane of scattering centres obeying the well-known laws because only in the direction prescribed by these laws are the scattered radiations all in phase.

resultant amplitude from a sheet is therefore diminished for the higher reflection orders, for which  $\theta$  is large.

It is, of course, possible to use the calculations of the modern atomic theory to estimate the electronic density at successive layers throughout a sheet, to work out the intensities of the reflections and to compare the result with experiment. In this way the Hartree theory has again received verification. Thanks, however, to one of the most ingenious ideas of modern physics, due to Sir Wm. Bragg, we are able to proceed more directly, and to determine the electron distribution throughout the lattice from the intensity measurements. Thus, the electron distribution along a line perpendicular to a particular set of planes is periodic and may be represented by a Fourier series equivalent to the representation of a sound wave by a fundamental note and overtones. It can be shown that the various orders of reflection from the set of planes are due each to a different term in the Fourier series, and the intensities of these reflections, therefore, give the magnitudes of the various Fourier terms. With the intra-planar electron distribution evaluated, it is an easy step to calculate the radial electron arrangement in the atoms, and thus again, as in the experiments on gases, to obtain a picture of the atom. The phenomena of X-ray scattering have therefore been of considerable value in giving a direct check on modern conceptions of atomic structure. To the crystallographers also, the Fourier analysis procedure (in a more advanced form) is of importance in the determination of complex structures.

THE COMPTON EFFECT. In 1923, A. H. Compton, in a striking investigation, demonstrated that, when X-rays are scattered, some of the radiation suffers a change in wavelength. His explanation of the phenomenon is based on the quantum theory. Before proceeding to the problem it is necessary to remind the reader of one or two of the tools which may be used. Firstly, there is the quantum

concept that when there is an interchange of energy between matter and radiation it always takes place in integral multiples of a unit or quantum of magnitude  $h\nu$ , where  $h$  is Planck's universal constant: there is no gradual interchange. Secondly, the principle of relativity leads one to associate with the energy of the quantum,  $h\nu$ , a momentum,  $h\nu/c$ , where  $c$  is the velocity of the radiation. Thirdly, the application of the principle of relativity shows that if  $m$  is the mass of an electron at rest, it has a mass equal to  $m/\sqrt{1 - \beta^2}$  (where  $\beta$  is  $v/c$ ) when moving with a velocity  $v$ . The same principle shows that the kinetic energy of the electron is

$$mc^2(1/\sqrt{1 - \beta^2} - 1).$$

It may be seen that when  $v$  is small, this expression reduces to  $\frac{1}{2}mv^2$ , and the expression for the mass becomes equal to  $m$ .

Compton visualized the quantum  $h\nu$  as a concrete centre of energy, in a way reminiscent of the corpuscular theory of light, and considered what would happen when such a quantum (or 'photon') came into collision with a stationary free electron. In the case of the emission of photo-electrons we assume that the whole of the energy of the quantum is given to the electron (as is seen on page 115), but in the case of the free electron of the present problem it was assumed that the ordinary laws of impact of elastic spheres would hold.

In Fig. 31 a quantum of energy in a beam of frequency  $\nu$  incident in the direction  $IO$ , meets a stationary electron at  $O$ . The result is that the electron moves off in a direction  $OP$  with a velocity  $v$  and the residual quantum, reduced to some smaller value  $h\nu'$ , moves in the direction  $OS$ .

Referring to the figure we see that the *momentum* of the electron is in a direction inclined at  $\theta$  to the incident direction, and is  $mv/\sqrt{1 - \beta^2}$ ;  $\frac{h\nu'}{c}$ , the new momentum

of the scattered quantum, is in a direction inclined at  $\phi$  to the incident direction.

We may express the conservation of energy in the form of an equation as

$$hv = hv' + mc^2 \left( \frac{1}{\sqrt{1 - \beta^2}} - 1 \right) . . . . (1)$$

Then, expressing the momentum in the line of incidence

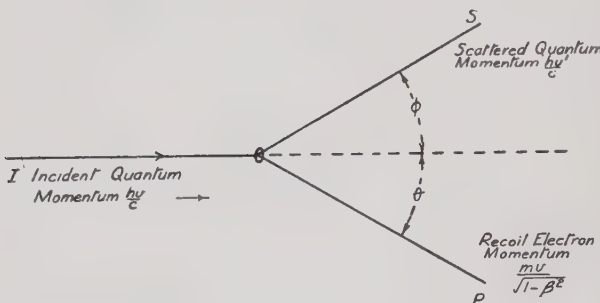


FIG. 31

The collision of an incident quantum  $h\nu$  and a free electron, resulting in the recoil of the electron and the scattering of the residual quantum  $h\nu'$ .

and at right angles to this direction two more equations are obtained :

$$\frac{h\nu}{c} = \frac{h\nu'}{c} \cdot \cos \phi + \frac{mv}{\sqrt{1 - \beta^2}} \cdot \cos \theta . . . . (2)$$

$$O = \frac{h\nu'}{c} \cdot \sin \phi + \frac{mv}{\sqrt{1 - \beta^2}} \cdot \sin \theta . . . . (3)$$

Solving these three equations we obtain Compton's result, for the wave-length of the scattered radiation  $\lambda'$ , corresponding to the frequency  $\nu'$

$$\lambda' = \lambda + \frac{h}{mc} (1 - \cos \phi)$$

i.e. the change in wave-length to be expected on this theory is

$$\lambda' - \lambda = \frac{h}{mc} (1 - \cos \phi) . . . . . (4)$$

It will be noted that the predicted change of wave-length has the following properties :

- (1) It is independent of the wave-length of the incident beam ;
- (2) it is independent of the nature of the scattering substance ;
- (3) it varies with the angle of scattering.

These results offer a direct challenge to experiment, and the work of Compton and his collaborators made a worthy counterpart to the theoretical investigation just summarized.

Molybdenum  $K\alpha$  rays were directed on to a carbon scatterer and the rays scattered in a given direction with respect to that of incidence were limited by lead slits which acted as the slits of a Bragg spectrometer, which in turn served to measure the wavelength of the scattered rays. By moving the X-ray tube round to direct the beam

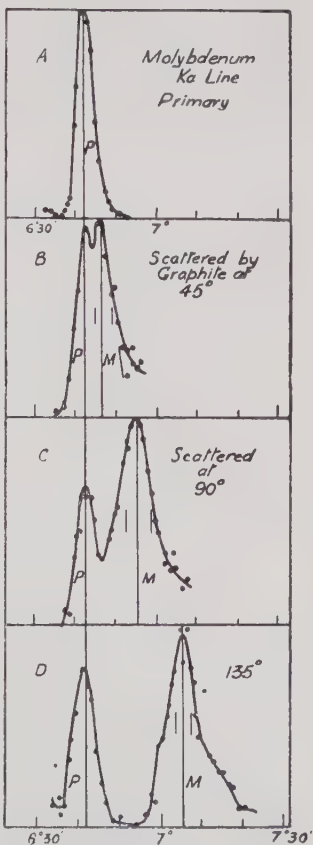


FIG. 32

through the slits it was possible to obtain the plot of the incident beam; also by moving the tube the angle of scattering could be set at any value. Fig. 32 shows the result of these investigations. The top figure gives the plot of the incident beam about the position of the  $K\alpha$  line and the other figures show the effect on this line of scattering at different angles. It is to be seen that the change of wave-length is unquestionable; the modified line is present, together with an unchanged line in each case.

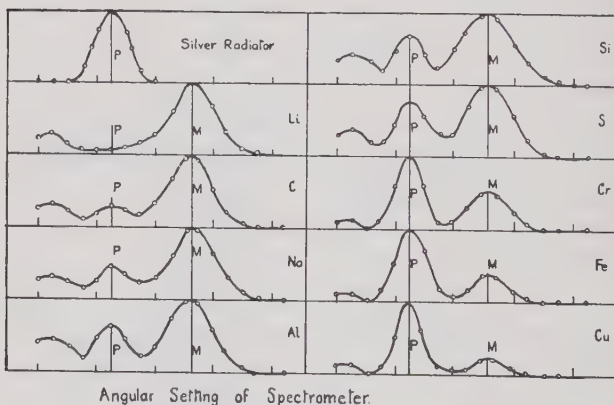


FIG. 33

It will be noted that the change in the position of the modified line increases with increase of the angle of scattering as anticipated.

Fig. 33 shows the result of a second set of observations (Woo) designed to test the second point mentioned above. It is seen that when a given angle of scattering is taken ( $120^\circ$ ) and different scatterers are used, that the change in wave-length is the same, but the relative amount of modified scattered ray changes; the higher the atomic number of the scatterer the higher the fraction of the

unmodified ray; with lithium the whole of the radiation is modified, with silver there is no modified ray.

With regard to the first property of the change in wave-length mentioned above, namely that it is independent of the wave-length of the incident beam, it would appear that this change should occur in the visible region. Experiments which were made by Ross, on the scattering of mercury light by paraffin, made it clear that no such change takes place. On the other hand, experiments with  $\gamma$  rays show that all the scattered rays in this case are changed in wave-length.

Again using a fixed wave-length on different scatterers the amount of modified radiation in Woo's experiments was seen to decrease as the atomic weight of the scatterer increased. Now, it was seen that the result of equation (4) was obtained by assuming that the quantum encountered a *free* electron, but it is clear that, if the electron is bound, and unable to move, it will not take any energy from the incident quantum, which proceeds without loss, i.e. the radiation is unchanged. This occurs either when the incident quantum is small, as in the case of visible light, or, for an incident quantum of higher value when the binding of the electron is great, but does not occur for the relatively large quantum associated with the  $\gamma$  ray. We should therefore expect from this theory the type of result which is found in the experiments.

The one final point about the theory which is to be mentioned is concerned with the electron which encounters the incident quantum, shown in Fig. 31 as recoiling at an angle  $\theta$ . This so-called *recoil electron* had already been observed in the cloud condensation experiments of Wilson and Bothe, and the theory at once gave a satisfying explanation of the short tracks as is shown on page 119.

To account for the *intensity* of the scattered beam which we have seen is not explicable in terms of classical mechanics under all conditions of wave-length and atomic

weight, various theories have been advanced, notably by Debye, Jauncey, Woo, Compton and Breit. The quantum theories of Compton and Breit appear equally well to fit the observed results. But a recent solution in terms of the new quantum theory by Dirac is identical with Breit's result, and at the same time Dirac finds that equation (4) may be developed directly by this new method of attack. This equation has also been deduced without the assumption of Compton by the methods of wave-mechanics by Schrödinger.

There is another, and very interesting, phenomenon associated with the Compton effect. The modified line

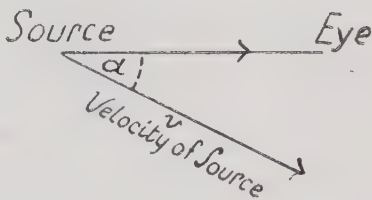


FIG. 34 (a)

is always wider than the unmodified. Its width and its form are dependent on the scattering substance. Since (4) makes no provision for this, it is apparent that some complicating factor has escaped consideration. In fact, the simplifying assumption has been made that the scattering electron is initially at rest, and it remains to discover whether allowance for its motion will account for the experimental facts. It is well known that, if a source of radiation is moving towards an observer, the Doppler effect occurs—the wave-length of the radiation received is diminished. If the source recedes, the wave-length is increased. Thus, in the case of Fig. 34 (a),  $\frac{\delta\lambda}{\lambda} = \frac{-v}{c} \cos \alpha$ . When light is reflected by a mirror, the image formed by

the mirror becomes the effective source. If now the mirror is moving, the image must move, and a Doppler effect be produced even though the true source be at rest. In the present problem the X-rays come to the observer, not directly, but by way of the scattering electron. We shall consider the latter as a moving mirror and find the Doppler effect due to the image. The situation is shown in Fig. 34(b). Owing to the velocity,  $v$ , of the electron,

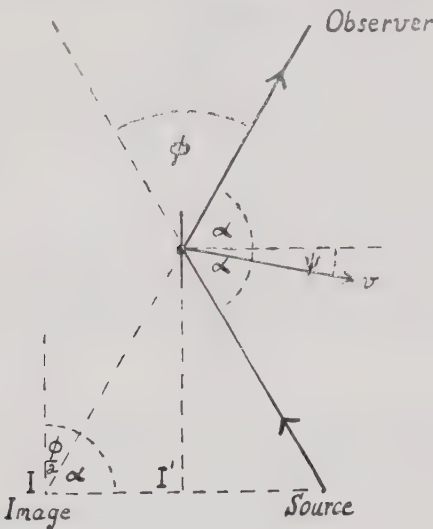


FIG. 34 (b)

the image is moving in direction  $II'$  with velocity  $2v \cdot \cos \psi$ . It therefore approaches the observer with velocity  $2v \cdot \cos \psi \cdot \sin \frac{\phi}{2}$ .

$$\text{Hence, } \frac{\delta\lambda}{\lambda} = -\frac{2v}{c} \cos \psi \sin \frac{\phi}{2} \quad . \quad . \quad . \quad (5)$$

Thus, since the electron may be going in any direction,

## CHAPTER V

### OPTICAL PHENOMENA

As we have seen, the hypothesis that X-rays are transverse electromagnetic waves, similar to visible light but of shorter wave-length, has received powerful support from the phenomena of polarization and of crystal diffraction, and an outline has been given of the success which attends it in accounting for the scattering by gases and liquids. These effects tend to be complicated, and it is particularly satisfactory that it is now possible to reproduce for X-rays the phenomena of refraction, reflection, interference and diffraction by methods similar to those of optics.

REFRACTION. To demonstrate the refraction of a radiation, the most straightforward procedure is to pass it through a prism and to show that the incident beam has been deviated. Such an experiment was tried for X-rays by a number of distinguished workers, none of whom found a deflection. The X-ray refractive index of the prism materials was evidently very close to unity. More recently, however, with improved technique, not only has deviation been observed and measured, but X-ray prism spectra have been obtained. Adequate deviation is attained by using a prism of large angle (say  $90^\circ$ ), and by placing it either so that the beam almost grazes the prism surface at incidence or so that the beam nearly grazes at emergence (see Fig. 36). With either arrangement the deviation is much greater than that of the symmetrical minimum deviation setting which one employs in the optical spectroscope. The deviation is greater the greater the wave-length. The reader will notice in Fig. 36 that the beam, on leaving the prism, is bent, not away from, but towards the normal to the surface. This must indicate

that the refractive index of the prism is less than unity. It is a phenomenon seldom encountered with visible light but invariably with X-rays.

It is entirely in accord with the electron theory of refraction. This theory supposes the refracting medium to contain electrons which have their own natural frequencies of vibration and which, when an electromagnetic wave passes through, are set into forced vibration by its periodic electric field. The theory yields for the refractive index the value :

$$\mu = 1 + \frac{e^2}{2\pi m} \sum_s \frac{n_s}{(\nu_s^2 - \nu^2)} . . . . . (1)$$

provided that the second term on the right-hand side is small compared with unity. In the expression,  $e$  and  $m$  are respectively the charge and mass of the electron,  $\nu_s$  is a natural frequency,  $n_s$  the number of electrons per unit volume having this frequency and  $\nu$  is the frequency of the radiation. For visible light  $\nu$  is less than  $\nu_s$  for most of the electrons, but for X-rays with frequencies some thousands of times greater than those of the visible spectrum,  $\nu$  is much greater than  $\nu_s$ , the fractional term is negative and hence  $\mu$  is less than unity. Since the denominator is large, the fractional term is small and  $\mu$  is therefore only very slightly different from 1. This is precisely what experiment tells us. Since  $\nu \gg \nu_s$ , we may write the equation in the form :  $\mu = 1 - \frac{e^2 n}{2\pi m \nu^2}$ , where  $n$  is the total number of electrons per unit volume. Alternatively, if  $\lambda$  is the wave-length of the radiation,

$$1 - \mu = \frac{e^2 n \lambda^2}{2\pi m c^2} . . . . . (2)$$

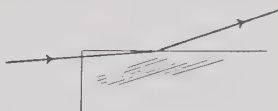


FIG. 36

Refraction of X-rays at the surface of a right-angled prism (exaggerated)

## CHAPTER V

### OPTICAL PHENOMENA

As we have seen, the hypothesis that X-rays are transverse electromagnetic waves, similar to visible light but of shorter wave-length, has received powerful support from the phenomena of polarization and of crystal diffraction, and an outline has been given of the success which attends it in accounting for the scattering by gases and liquids. These effects tend to be complicated, and it is particularly satisfactory that it is now possible to reproduce for X-rays the phenomena of refraction, reflection, interference and diffraction by methods similar to those of optics.

**REFRACTION.** To demonstrate the refraction of a radiation, the most straightforward procedure is to pass it through a prism and to show that the incident beam has been deviated. Such an experiment was tried for X-rays by a number of distinguished workers, none of whom found a deflection. The X-ray refractive index of the prism materials was evidently very close to unity. More recently, however, with improved technique, not only has deviation been observed and measured, but X-ray prism spectra have been obtained. Adequate deviation is attained by using a prism of large angle (say  $90^\circ$ ), and by placing it either so that the beam almost grazes the prism surface at incidence or so that the beam nearly grazes at emergence (see Fig. 36). With either arrangement the deviation is much greater than that of the symmetrical minimum deviation setting which one employs in the optical spectroscope. The deviation is greater the greater the wave-length. The reader will notice in Fig. 36 that the beam, on leaving the prism, is bent, not away from, but towards the normal to the surface. This must indicate

that the refractive index of the prism is less than unity. It is a phenomenon seldom encountered with visible light but invariably with X-rays. It is entirely in accord with the electron theory of refraction. This theory supposes the refracting medium to contain electrons which have their own natural frequencies of vibration and which, when an electromagnetic wave passes through, are set into forced vibration by its periodic electric field. The theory yields for the refractive index the value :

$$\mu = 1 + \frac{e^2}{2\pi m} \sum_s \frac{n_s}{(\nu_s^2 - \nu^2)} . . . . . \quad (1)$$

provided that the second term on the right-hand side is small compared with unity. In the expression,  $e$  and  $m$  are respectively the charge and mass of the electron,  $\nu_s$  is a natural frequency,  $n_s$  the number of electrons per unit volume having this frequency and  $\nu$  is the frequency of the radiation. For visible light  $\nu$  is less than  $\nu_s$  for most of the electrons, but for X-rays with frequencies some thousands of times greater than those of the visible spectrum,  $\nu$  is much greater than  $\nu_s$ , the fractional term is negative and hence  $\mu$  is less than unity. Since the denominator is large, the fractional term is small and  $\mu$  is therefore only very slightly different from 1. This is precisely what experiment tells us. Since  $\nu \gg \nu_s$ , we may write the equation in the form :  $\mu = 1 - \frac{e^2 n}{2\pi m \nu^2}$ , where  $n$  is the total number of electrons per unit volume. Alternatively, if  $\lambda$  is the wave-length of the radiation,

$$1 - \mu = \frac{e^2 n \lambda^2}{2\pi m c^2} . . . . . \quad (2)$$



FIG. 36

Refraction of X-rays at the surface of a right-angled prism (exaggerated)

Evidently  $\frac{1 - \mu}{\lambda^2}$  should be constant for a given prism, and the measurements of Larsson show that this is indeed the case. Hence, the electron theory and the conception of the electromagnetic wave appear to be successful for X-rays as for light. A sterner test is available. Thus, in equation (2), the quantity  $en$ , the total electronic charge per unit volume, may be determined with great accuracy with the aid of electrolytic measurements. Hence if the value of  $\mu$  for X-rays of known wave-length be found from a prism experiment, then the fundamental ratio  $e/m$  may be evaluated.\* Using a  $90^\circ$  prism of diamond and radiation of wave-length  $1.39220\text{\AA}$ , Bearden † found  $\mu$  to be  $(9224.4 \pm 1.0) \times 10^{-9}$  less than unity, and, using the refraction expression in a rather more precise form than that given here, found for  $e/m$  the value  $(1.7601 \pm 0.0003) \times 10^7$  e.m.u.-gm. $^{-1}$ . A weighted mean of this quantity by various methods gives  $(1.7591 \pm 0.0002) \times 10^7$  e.m.u.-gm. $^{-1}$ .‡ This is surely a triumph for the theory.

As early as 1914 Darwin had pointed out that for X-rays the refractive indices of materials should differ slightly from unity, and that, as a consequence, the reflection maxima from crystals should be slightly displaced. Different orders of reflection should be affected by different amounts. Later, experiment showed that very small deviations from the equation  $n\lambda = 2d \sin \theta$  do, in fact, exist, and that their magnitudes are in conformity with the theoretical predictions of refractive index. The amended Bragg formula is :

$$n\lambda = 2d \sin \theta \left[ 1 - \frac{(1 - \mu)}{\sin^2 \theta} \right].$$

\* The value of  $c$ , the velocity of light, is known with great accuracy.

† *Phys. Rev.*, **54**, 698 (1938).

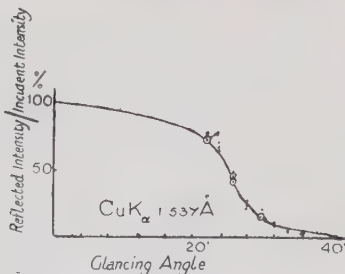
‡ See Dunnington, *Rev. Mod. Phys.*, **11**, 65 (1939). Birge also (1941) gives the value  $(1.7592 \pm 0.0005) \times 10^7$ .

In the ordinary X-ray region this affects wave-length evaluations by roughly 1 in  $10^4$ .

**REFLECTION.** When a beam of X-rays falls on a mirror there is usually no appreciable reflection. The beam either penetrates it or is absorbed on its way through. However, as we shall show, in certain circumstances nearly all the radiation may be reflected. This is possible as a result of the refractive indices of materials being less than 1. Thus, when X-rays pass from a vacuum (or from air) into any material, with the usual law  $\sin i / \sin r = \mu$ , this peculiarity of  $\mu$  entails that  $\sin r$  is greater than  $\sin i$ , and the beam is bent away from the normal to the surface. When  $i$  is made sufficiently large—when the incident beam makes only a small angle with the surface— $r$  becomes  $90^\circ$ , and for any further increase in  $i$  refraction ceases and the beam is entirely reflected. Total reflection should set in at an angle of incidence  $i_c$  such that  $\sin i_c / \sin 90^\circ = \mu$ . At this critical angle of incidence, the reflected intensity should jump from a very small value almost to that of the incident beam. A. H. Compton pointed out that this counterpart of the total internal reflection phenomenon of ordinary optics should occur, and he proceeded to demonstrate it by experiment, to measure the critical angle  $i_c$  and hence to find  $\mu$ . The rise in intensity at the critical angle is, however, somewhat indefinite and becomes even more so for the softer radiations. This again is entirely in accord with the classical theory, which predicts a more gradual rise in intensity when the absorption coefficient of the mirror is high for the radiation concerned. The excellent agreement between theory and experiment is shown by the curves of Fig. 37.

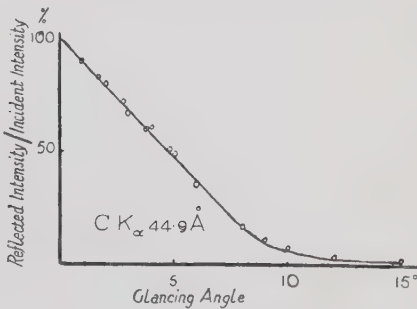
**INTERFERENCE.** One of the many experiments which demonstrate the interference of visible light is that of 'Haidinger's fringes', in which, under suitable conditions, alternations of brightness and darkness are shown in the light reflected from a parallel-sided thick transparent

(a) Fairly hard radiation. Rise at critical angle fairly sharp



The curve, representing theory, and the points, representing experiment, from Nähring, *Phys. Zeits.*, **31**, 800 (1930). The point marked with a flag is a fitting point.

(b) Soft radiation. (High Absorption.) No sharp effect at critical angle. Flint glass



The curve representing theory (with arbitrary critical angle and absorption coefficient) and points representing experiment, from Valouch, *J. de Physique et le Rad.*, **1**, 261 (1930).

Chosen critical angle =  $7^{\circ} 45'$

FIG. 37

sheet. The interference occurs between the waves reflected at the front surface of the sheet and those which penetrate this surface but are reflected at the back face

and subsequently re-emerge from the front (see Fig. 38). Making a simple geometrical calculation, we find that the path difference between the rays reflected in this way from the front and back faces amounts to  $2\mu t \cdot \sin \phi$ . It thus depends on  $\phi$ —which is, of course, governed by the angle  $\theta$ , which the incident beam makes with the sheet. When  $\theta$  is such that  $2\mu t \sin \phi$  is equal to a whole number  $n$  of wave-lengths, then the two sets of reflected waves are in phase and add together, but when  $2\mu t \sin \phi$  is equal to  $(n + 1/2)$  wave-lengths, then the waves are in opposition and tend to annul one another. Actually this is not quite true, for the light which is reflected from the front suffers

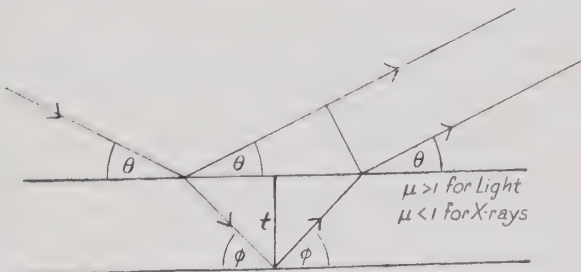


FIG. 38

a phase-change equivalent to a change of path of  $\lambda/2$ . As a result of these considerations we arrive at the conclusion that there should be destructive interference for  $2\mu t \sin \phi = n\lambda$  and enhanced intensity for  $2\mu t \sin \phi = (n + 1/2)\lambda$ . Evidently, if by some means we vary  $\theta$ , then, provided the thickness  $t$  of the sheet be sufficient, we produce a succession of bright and dark alternations of the reflected beam.

This effect, so familiar in optics, has now been observed for X-rays by Kiessig. The X-ray wave-lengths are much smaller than those of visible light, and so also are the thicknesses of the sheets employed in the X-ray experi-

ment. In fact, films of nickel of the order of  $10^{-5}$  cm. thick were used. To get adequate reflection, the incidence was in the neighbourhood of the critical angle for the front face. When  $\theta$  was varied by rotation of the film, clear maxima and minima of intensity were obtained. Thus we are provided with our simplest evidence of the interference of X-rays. Incidentally, as Kiessig shows in his paper, the measurements of the angles at which the maxima or minima occur permit the calculation both of the refractive index of the film for X-rays and also of its thickness. For the latter purpose the procedure may, in the future, become of considerable practical importance.

The interference of X-rays has also been demonstrated in Lloyd's Mirror experiments by Linnik and by Kelstrom, who has performed a whole series of beautiful interference and diffraction experiments.

**DIFFRACTION.** Although demonstrations of diffraction by a slit, of diffraction past a straight edge, and of diffraction by a straight wire have all been successfully performed for X-rays, limitations of space preclude their discussion in the present monograph. We shall instead devote some considerable attention to the use of the diffraction grating. Far more than demonstrations of the wave-nature of X-rays, experiments with gratings have been of the greatest value in X-ray investigation, first, because they have made it possible to make absolute measurements of wave-lengths and hence to test the rather indirect determinations of crystal spectroscopy, and, secondly, because they permit the investigation of the hitherto almost inaccessible region of the spectrum between the ordinary X-rays and the ultra-violet.

**THE USE OF RULED GRATINGS.** The grating consists of a plane (or concave spherical) metal or glass surface on which parallel equidistant lines are ruled with a diamond. An account of its use in ordinary spectroscopy will be

found in any textbook on physical optics. The distance between the successive rulings of a grating is usually of the order of  $10^{-4}$  cm. and the wave-length of ordinary light is of the same order. That of X-rays is, however, ten thousand times smaller. It would therefore appear that such a grating would be too coarse—that its dispersion would be too small for accurate measurements of wave-length to be possible. This difficulty is, however, overcome by allowing the X-ray beam to strike the grating at almost grazing incidence. Taking the distance between

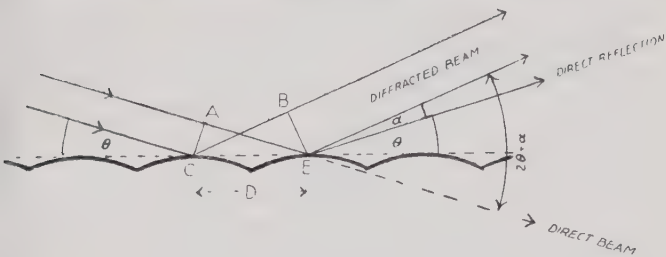


FIG. 39

the rulings to be  $D$  and the other quantities as indicated in Fig. 39, the ordinary grating formula \* may be written :  $n\lambda = AE - CB$

$$\text{or } n\lambda = D\{\cos \theta - \cos(\theta + \alpha)\},$$

and if the angles are small

$$n\lambda = D \left\{ 1 - \frac{\theta^2}{2} - \left( 1 - \frac{(\theta + \alpha)^2}{2} \right) \right\} = D \left\{ \frac{2\alpha\theta + \alpha^2}{2} \right\} = \frac{D\alpha}{2}(\alpha + 2\theta)$$

(neglecting powers of the angles higher than the second).

\* Expressing the angle  $(\theta + \alpha)$  at which the radiation diffracted from the successive rulings of the grating will reinforce and so produce the spectral line of the wave-length  $\lambda$ .

Now assume that the incident beam is tangential to the grating—that  $\theta = 0$ . Then

$$n\lambda = \frac{D\alpha^2}{2} \text{ and the dispersion is given by } \frac{d\alpha}{d\lambda} = \sqrt{\frac{n}{2\lambda D}}.$$

For normal incidence, the dispersion for short wavelengths is readily shown to be  $\frac{n}{D}$ .

Hence, by using tangential incidence the dispersion is increased in the ratio  $\sqrt{\frac{D}{2n\lambda}}$ . If  $D = 10^{-4}$  cm.,  $n = 1$ , and  $\lambda = 10^{-8}$  cm. this dispersion ratio is 71. Evidently the grazing incidence arrangement yields a very considerable increase in dispersion. Nevertheless, the dispersion in ruled grating spectrometers is always inferior to that in the crystal instruments.

A second difficulty might arise since normally very little radiation would be reflected from the grating, and, for soft X-rays, even the incident intensity is very weak. However, by using grazing incidence, the total reflection phenomenon is invoked and adequate intensity is thrown into the diffracted spectrum. The first spectra to be recorded in this way were obtained by Compton and Doan.

The problem of focusing arises. It is out of the question to use lenses. Their X-ray refractive index is too near unity for them to produce appreciable focusing, and the softer X-rays would not penetrate them. The grating is therefore left to do its own focusing. The salient point here is that a small amount of error of focus does not matter. The situation is demonstrated in Fig. 40 in which  $GOG'$  represents a *plane* grating and  $S$  the slit. If a collimating lens system could have been used, the rays would have been represented by such parallel lines as  $AG$ ,  $SF$  and  $BH$  and wave fronts by  $AB$  and  $GH$ . Without collimation, radiation to the edge of the grating travels a distance  $SG$  instead of  $AG$ , or an excess of path of

$SG(1 - \cos \phi)$ , whilst the path of the ray to the centre of the grating is unchanged. Again, paths from the grating edges to the diffracted image are similarly too great. However, applying Rayleigh's criterion, the width of the image should not be appreciably increased nor the resolution diminished provided the total excess path of each of the extreme rays does not exceed  $\lambda/4$ . It may be seen from the figure that the path excess may be made small by using grazing incidence and by reducing the width of the grating. A simple calculation on the basis of the figure will show that the grating width should be restricted to the order of a millimetre. But the ordinary theory

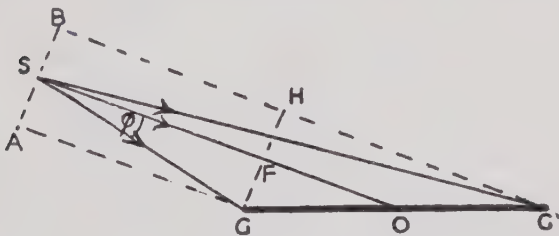


FIG. 40  
(Width of grating exaggerated)

of the diffraction grating shows that the sharpness of the images increases with the number of rulings employed, or, better, that the resolving power is ideally equal to  $Nn$ , where  $N$  is the number of rulings and  $n$  the order of the spectrum. From this point of view, the grating should be as wide (and hence have as many rulings) as possible. In short, even a plane grating may be said to be self-focusing, but the resolving power is limited to that corresponding to an optimum width, which is, unfortunately, small.

Much work has been done with plane gratings, but more recently the concave grating has come into X-ray use

because of its superior focusing property. In the standard textbooks on optics or spectroscopy it is shown that if a concave grating of radius of curvature  $R$  is mounted tangentially on a circle of diameter  $R$ , then, if the slit is on the circle, all the spectra will be in focus on the periphery. A photographic plate, bent so that its surface coincides with the circle, will receive focused spectra. For X-ray work we need grazing incidence, and this leads to a rather unorthodox arrangement. It is shown in Fig. 41. Even

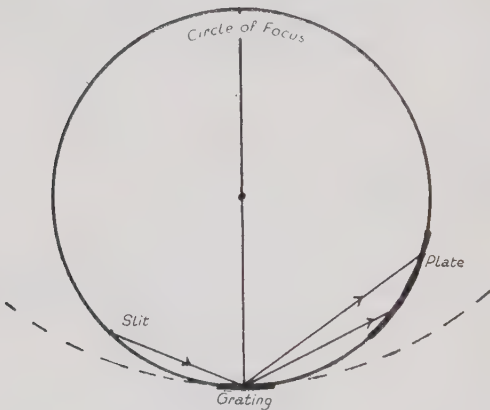


FIG. 41

with this disposition, the focus is not perfect if the grating is too large, but the best width is now of the order of a centimetre—roughly ten times that of the plane grating, so the intensity is increased, and, more important, the number of rulings and consequently the resolving power.

If the spacing of the grating rulings (the grating constant) is determined, then the measurement of the angles of incidence and diffraction permits the calculation of X-ray wave-lengths in absolute measure. The grating constant may be found in several ways. It may be

measured directly by means of a travelling microscope : it may be found optically by measuring the angles of incidence and diffraction for a known visible spectral line ; or its measurement may be rendered unnecessary by obtaining, on one and the same photographic plate, high orders of the X-ray spectra under examination and extreme ultra-violet lines of known wave-length. The latter yield a wave-length scale for the plate from which the X-ray wave-lengths may be calculated. Any of these methods gives X-ray wave-lengths directly in centimetres.

When these absolute values were compared with those from the crystal measurements, a discrepancy was apparent. This difference has been confirmed as the accuracy of grating experiments has increased. Grating wave-lengths exceed those given by the crystal by 0.203 per cent. It is pretty certain that the error is in the crystal values, and that the responsibility lies with the lattice constant from which the wave-lengths are calculated. It will be remembered that this constant depended on a knowledge of Avogadro's number  $N$ , the number of atoms per gram-atom. This number is obtained from electrolysis, for, if  $e$ , the electronic charge, is the charge carried by a monovalent ion, then the charge corresponding to the deposition of one gram-equivalent is  $Ne$ . Hence knowledge of  $e$  yields knowledge of  $N$ . If  $e$  is wrong,  $N$  is wrong, the lattice constant is wrong and the X-ray wave-length is wrong. With the other quantities in the calculation relatively secure, doubts were cast on the hitherto irreproachable value of  $e$  ( $4.768 \times 10^{-10}$  e.s.u.). It had been found by the oil-drop method and depended on the viscosity of air. New experiments seem to show that the viscosity value which had been used was in error by more than  $1/2$  per cent. Combining the new values with the original and also new oil-drop experiments, a value of  $4.8036 \times 10^{-10}$  e.s.u. is obtained for  $e$ .\* The

\* A later determination gives the value  $4.802 \times 10^{-10}$  e.s.u.

X-ray value of  $e$ —that required to bring concord between crystal and grating X-ray wave-length measurements—is  $4.8025 \times 10^{-10}$  e.s.u. Hence not only has the error in  $e$  been brought to light, but there is now apparently a satisfactory fit between X-ray and oil-drop determinations. It must be said, however, that the state of the values of the fundamental atomic constants and of the combinations in which they occur in practice still leaves something to be desired.

Before the advent of ruled grating spectroscopy, the exploration of the soft X-ray region beyond about  $25\text{\AA}$  was largely carried out indirectly. Crystal spectroscopy was hampered by the fact that all the ordinary crystals had lattice constants less than  $10\text{\AA}$ , whilst, since for a diffraction maximum  $n\lambda = 2d \cdot \sin \theta$ ,  $\lambda$  cannot be greater than  $2d$ . However, it is possible to go further into the soft X-ray region if one of the long chain fatty acids is employed. Thus stearic acid gives a value of  $79\text{\AA}$  for  $2d$ , and it is possible to find substances with even higher values. This extension of the use of crystals is of great value owing to the high dispersion obtained. On the other hand, if they are used too far into the soft region there is some doubt about the resulting wave-lengths since the refractive indices are unknown. Few experiments have been carried beyond about  $30\text{\AA}$ .

There is no such limit to the use of the grating. It is at its best in long-wave measurements, and wave-lengths of several hundred Angstroms are commonly measured with it. Since the absorption of X-rays roughly follows a  $\lambda^3$  law, the soft X-rays are absorbed heavily even by air. Hence a soft X-ray spectrograph has to be enclosed in a vacuum chamber and, as the radiation would not penetrate any wall, the X-ray tube must be in direct connection with this chamber. The spectra are usually recorded on special photographic plates in which the absorption of the radiation by the gelatin is overcome, and having thin glass

in order that they may be bent to the radius of the circle of focus (the Rowland circle). Hot cathode X-ray tubes are used, with bombarding potentials of several thousands of volts. A concave grating vacuum spectrograph is shown in Fig. 42.

The wave-lengths of the soft X-ray spectra are usually obtained by throwing on to the same plate the known spectrum of a vacuum spark. This spark is produced

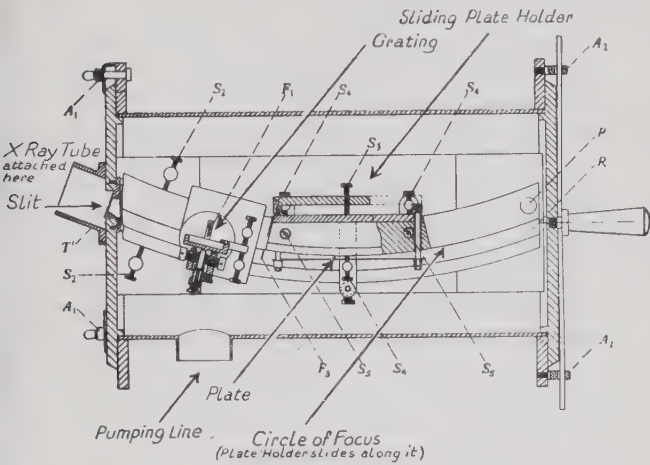


FIG. 42

(Chalklin, F. C., Watts and Hillson, *Phys. Soc. Proc.*, **50**, 926 (1938))  
(Lettering refers to text of paper)

between two electrodes placed close together *in vacuo* and with a condenser connected across them. A current is fed into the condenser and the voltage across the spark gap consequently rises. Eventually, when the electric field has increased to nearly a million volts per centimetre, an electron discharge takes place. Heat is generated, volatilization occurs at the surfaces of the electrodes and

a momentary but very heavy current is delivered by the condenser. So great is this current that the vaporized atoms suffer multiple ionization. With its number of electrons reduced in this way, the effective nuclear charge of a vaporized atom is increased and its optical spectrum moves from the visible into the far ultra-violet or soft X-ray region. The wave-lengths of many such spectra are known by comparison in high orders with standard optical lines.

The grating spectrograph has been used with success in the examination both of emission and of absorption spectra, the results linking with and adding to the knowledge of atomic energy levels obtained by crystal spectroscopy. Dealing with long wave-length radiations, it is concerned with the small energy levels—those corresponding to the outer electronic shells. Of particular interest are the X-ray lines in which the valence electrons are involved. The valence energy levels, shown by optical spectra to be so narrow and definite for substances in the gaseous phase, become broadened when the atoms are crowded together in solids. The extent of this broadening and the form of the resulting band are informative on electronic conditions in the solid state. They may be calculated from the width and shape of the X-ray lines, but only by the soft X-ray grating technique can they be determined with accuracy. Thus, since  $h\nu = \frac{hc}{\lambda} = eV$ , or  $\lambda = \frac{hc}{eV}$ , we have

$$d\lambda = -\frac{hcdV}{eV^2}.$$
 Hence if a broadened energy level causes an X-ray line to have a width of  $dV$  electron-volts, then the wave-length width of the line is much greater for a soft radiation of small  $V$  than for an ordinary hard X-ray line. The width and form of the soft line are therefore more readily determined. For this reason it is better to examine a surface level by means of a soft line and the grating method than to use a hard line and the crystal

technique despite the fact that the crystal resolution is better than that of the grating. Incidentally the natural widths of the deep levels would be rather a nuisance if too hard rays were used.

## CHAPTER VI

### PHOTOELECTRONS AND IONIZATION

IN the early days of X-rays, the electron emission which takes place from substances when they are irradiated by X-rays was referred to as the 'corpuscular secondary radiation'. The effect was first recorded by Perrin. Later it was shown that when metals were exposed to X-rays in a vacuum they acquired a positive charge due to the loss of negative electricity and that, if a sufficiently large opposing electrostatic field were applied, the loss could be entirely arrested. Finally, the magnetic deflection of the negative particles enabled an estimate to be made of their mass and charge and identified them as electrons. The process was shown to be identical in character with the photoelectric emission in the visible region. Indeed, it is now called the photoelectric effect of X-rays, and it is this process and some of the properties of the photoelectrons with which we shall concern ourselves in this chapter.

ABSORPTION AND RANGE. The study of the photoelectric action of X-rays is pursued by means of experiments performed *in vacuo*, for even the quickest-moving electron is readily absorbed in air which is thereby ionized. This makes the measurement of charge, &c., quite unreliable without the complete evacuation of the containing vessel. Sir J. J. Thomson assumed that the photoelectrons lose energy in encounters with other electrons in matter, and consequently pass on with a reduced velocity. On these lines he was able to deduce the relation between the original velocity ( $v$ ) and the final

velocity ( $v_x$ ) after passing through  $x$  cm. of a medium, to be of the form

$$v^4 - v_x^4 = kx \quad . \quad . \quad . \quad (1)$$

where  $k$  is a constant.

If an electron is directed into a gas, it produces along its path ionization which becomes zero at a point which depends on the gas pressure and the original velocity of the electron. When the ionization ceases the velocity has been reduced to a negligible fraction of its initial value. If we measure the length of the path from the starting point to the point where it ceases to ionize (where it ceases to have the properties by which it is recognized) we obtain what is called the *range*,  $r$ , of the particle, which by equation (1) is seen to be given by

$$v^4 = kr \quad . \quad . \quad . \quad (2)$$

In the case of an electron ejected from a solid the velocity of emergence depends on the point of origin within the solid. The final velocity of emergence will obviously depend upon the initial velocity, the value of the appropriate  $k$  in the solid, and the length of the path in the solid, as shown in (1). If we employ a very thin film of the substance as source, e.g. gold leaf, we may eliminate this depth effect to a large extent and so provide a means of studying the range of photoelectrons in gases. Whiddington verified expressions (1) and (2) by experiment, and determined the values of  $k$  for various elements. From a study of the total range of the photoelectrons he was able to determine their velocity of ejection. He had previously shown by experiment that the 'K radiation' was emitted by the anticathode when bombarded by electrons whose minimum velocity must exceed  $10^8 \times$  (Atomic weight of the anticathode), and was able to combine the two experiments and give the following important conclusion:—The maximum velocity of ejection of a photo-electron produced by X-rays of a given wave-length is

equal to the least possible velocity of the cathode ray originally responsible for that X-ray. This may be expressed in the form

$$\frac{1}{2}mv^2 \rightleftharpoons h\nu.$$

Without certain refinements this means, reading left to right, that there is an equivalence between the 'cathode ray' and the X-ray quantum it produces ; reading right to left it means that the energy of the photoelectron is equivalent to that of the quantum which has ejected it.

**EXPERIMENTAL METHODS.** The experimental methods which have been used to investigate the photoelectric effects of X-rays are :

- (1) Ionization method.
- (2) Stopping potential method.
- (3) Stopping magnetic field method.
- (4) Magnetic spectrum method.
- (5) Cloud condensation method.

In the **Ionization method** a very thin film of the material to be used as source of electrons is suspended near the back of an ionization chamber opposite a thin aluminium window which is suitably strengthened to enable the pressure within to be varied over a wide range. The total ionization at each pressure is measured and plotted against the corresponding pressure as shown in Fig. 43 (a). Now at a given pressure the total ionization produced in the gas is made up of two parts : (a) the ionization produced 'directly' in the gas ; \* this is proportional to the pressure of the gas, and (b) the dense ionization produced in a layer near the film by the photoelectrons which it emits. It is clear that if the incident beam is constant the ionization due to the second cause ( $I_c$ ) is independent of the pressure so long as all the photoelectrons are absorbed in the gas (that is neglecting the slight change in the absorption of the X-ray beam before it reaches the

\* See page 7.

film). Therefore the observed ionization  $I$  is given by

$$I = I_c + aP,$$

where  $a$  is a constant, and  $aP$  is the ionization produced in the gas 'directly'.

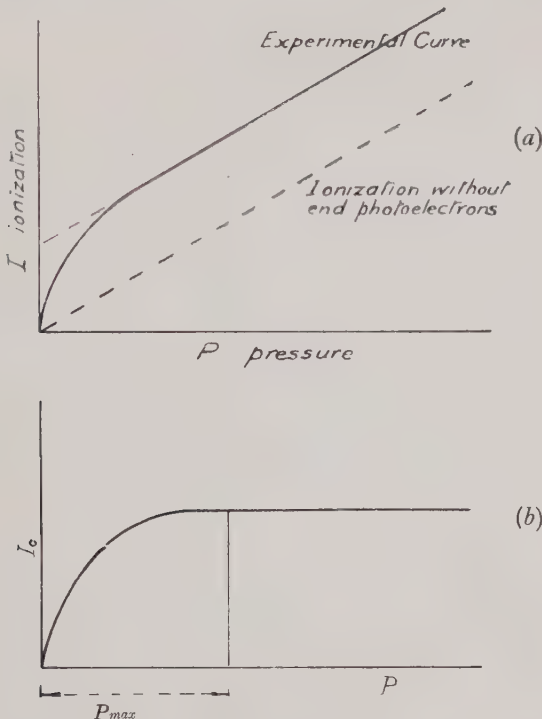


FIG. 43

In the figure the broken line, parallel to the straight part of the experimental curve, and passing through the origin represents  $aP$ . The difference between the ordinates of the broken and the full line curves gives  $I_c$ , which may be plotted as in Fig. 43(b). From this curve is obtained the

minimum pressure at which all the electrons are absorbed, or, in other words, the pressure corresponding to maximum ionization, shown in the figure as  $P_{max}$ . If  $t$  is the X-ray path in the chamber from the window to the film, and the temperature in degrees C. is  $\theta$ , then the range of the electron at 0° C. and 76 cm. pressure is :

$$t \cdot \frac{P_{max} \cdot 273}{76 \cdot (273 + \theta)}.$$

This method was used in many of the important earlier researches.

We shall not discuss the stopping potential and stopping magnetic field methods here, but shall pass on to discuss the magnetic spectrum procedure.

The **magnetic spectrum method** of measuring the velocities of photoelectrons depends on the fact that a charge  $e$ , moving at right angles to a uniform magnetic field of strength  $H$ , is subjected to a force at right angles to the field and to the direction of motion. This force, whose magnitude is easily shown to be  $Hev$ , tends to deflect the moving charge, but the deflection is limited by the centrifugal force  $\frac{mv^2}{r}$ . Hence the curvature of the

path is given by the equation  $Hev = \frac{mv^2}{r}$ . Evidently, if  $H$  and  $v$  are constant,  $r$  is constant and the path is a circle.

In the apparatus shown in Fig. 44, the source of electrons is beneath a slit in a horizontal platform, on the upper surface of which is a photographic plate. The whole, for obvious reasons, is placed in a light-tight box, and suitable lead blocks prevent the direct action of the X-rays on the plate. When a transverse magnetic field is applied, the photoelectrons which are ejected from the source by the action of a beam of X-rays are bent into circular arcs. Some, passing through the slit, are bent round and strike the plate in the manner indicated. Each group of electrons with one velocity forms a circle of one

radius and meets the plate in a line parallel to the slit. If the effective source is narrow, so also is the line on the plate, even if the slit is wide. From the measured position of the line and the known dimensions of the apparatus, the radius of curvature,  $r$ , of the path may be calculated and  $v$  may be obtained from the formula given above.

Thus  $v = \frac{Her}{m}$ . Of course, for high-speed electrons, where  $v$  is an appreciable fraction of the velocity of light, the value of  $m$  must be taken as  $\frac{m_0}{\sqrt{1 - \beta^2}}$ , where  $\beta = v/c$  and  $m_0$  is the rest mass of the electron. This applies to the

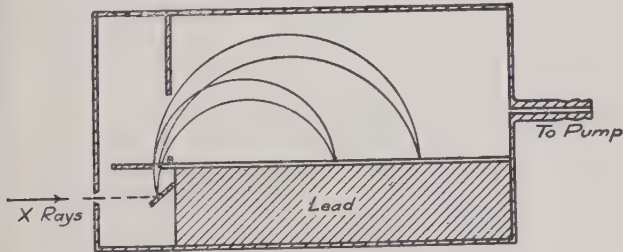


FIG. 44

Apparatus used in the production of the Magnetic Spectrum of a source of electrons.

photoelectrons ejected by very short wave-length X-rays or by  $\gamma$ -rays. For a heterogeneous source there are as many line images on the plate as there are velocities from the source, and the lines constitute the *magnetic spectrum*.

The **cloud condensation method** is one which gives direct evidence of the behaviour of electrons in the production of ionization, and indeed, by photographing the instantaneous position of individual ions it provides a very powerful means for the investigation of the action of all ionizing agents. For example, the first published pictures by C. T. R. Wilson confirmed in a striking way the theory that in the case of ionization in gases, the whole

effect was due to the secondary action of the electrons which the X-rays liberate from the gas molecules. The apparatus took the form shown in outline in the diagram (Fig. 45). *AB* is a glass vessel in the lower half of which is a plunger, *P*, standing over water. Through the tube *T* connexion is made to an evacuated reservoir, not shown in the figure. When the piston *H* is moved to the left the pressure difference causes a sudden depression of *P* and consequent expansion, and cooling of the gas in *AB*. When no precautions have been taken, a mist is formed in this process by the condensation of the cooled water vapour on dust particles in the air. The drops of water surrounding the dust particles form a cloud which slowly falls to the bottom of the vessel. When the process has been repeated a few times the space becomes dust free, and thereafter a sudden expansion and cooling of the air results in the supersaturation of the air, without the formation of mist in the space, as no centres of condensation remain. It had been found previously that if X-rays are passed through such a dust-free space which is cooled in the way described, water drops form on the ions produced.

Wilson arranged the apparatus as shown so that in a dust-free atmosphere a movement of the piston to the left causes the following sequence of events: (1) By sudden expansion, supersaturation of the space was produced when the piston *H* passed the tube *T*. (2) The thin thread between the weights *C* and *D* broke when the piston was stopped. (3) *D* passed between the spark gap 11 and caused the charged condensers *F*, *F*<sup>1</sup> to discharge through the X-ray tube, and so pass a beam of X-rays through *AB*. (4) After a short interval of time, which could be adjusted by altering the distance between the two spark gaps, *D* discharged, in a similar way, a pair of large condensers *K*, *K*<sup>1</sup>, by reducing the gap 22. This caused a spark to pass in the gap *S*, and so provided a strong flash of illumination on the water drops condensed

on the ions, which were photographed by a camera placed at right angles to the figure opposite *AB*.\*

The photographs showed that all the ionization takes place along definite irregular tracks, which are in fact lines of gas molecules ionized by the electrons which the X-rays have ejected from the molecules of gas. The tracks, in other words, show the paths of the electrons.

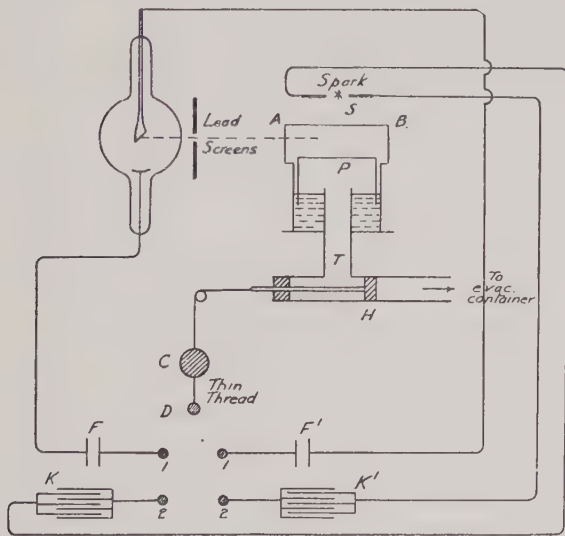


FIG. 45

Later, the sequence of events described above was incorporated in an apparatus with improvement in detail of design, and a technique has been developed whereby, using a stereoscopic pair of photographs, the depth effects may be appreciated and the lengths of tracks may be estimated. For example, a short image on a single plate

\* A more usual arrangement is obtained if the camera and spark positions are interchanged.

may be interpreted either as a short track or else as a long track seen end on: with a stereoscopic pair these may be distinguished. Another method consists in taking simultaneously two pictures at right angles to each other. This also enables an estimate of length and direction of the tracks to be made.

EXPERIMENTAL RESULTS. The first noteworthy result obtained by the magnetic deflection method, by Innes (1907,) showed that the velocity of the photoelectron was independent of the intensity of the X-ray beam used to eject it. This was found by altering the distance between the source of X-rays and the metal from which the electrons were obtained. It was shown that the intensity of the beam merely controlled the number of electrons given out. On the other hand, Beattie and Whiddington showed that the velocity was determined by the 'penetration' of the X-rays; the more penetrating the beam (i.e. the shorter the wave-length) the greater the value of  $v$ .

The classical electro-magnetic theory could offer no explanation for these results. According to that theory the ejection of the electron was brought about by the acceleration of the corpuscle by the electric vector of the wave. Thus, in complete disagreement with experiment, it suggested that the greater the intensity of the radiation and hence the greater the magnitude of its electric vector, the greater should be the kinetic energy of the expelled electron. On the other hand, the quantum theory, as in the case of the photoelectric effect of visible light, fits the facts in a striking manner. As we have seen, this theory demands that, when there is interchange of energy between radiation and matter, it shall take place in integral multiples of a quantum  $h\nu$ . Now if the quantum is all expended on the emitted electron, it is apparent that the kinetic energy of the electron is ordained by the frequency of the radiation (and by the parent substance), but not at all by the intensity. The intensity, however, will govern the

number of quanta and hence the number of photoelectrons ejected. Hence there is agreement with the experimental facts so far given. Again, according to this theory, each ejected electron must extract from the beam a quantum of energy. In other words, the true absorption of the X-rays in matter should be proportional to the number of photoelectrons emitted. It is interesting to recall the results of an experiment by H. Moore, who found by means of ionization measurements that the number of photoelectrons in a gas was proportional to the fourth power of the atomic weight of the gaseous atom. Remembering that the true absorption is proportional to the fourth power of the atomic number (and therefore approximately to the fourth power of the atomic weight), we conclude that there is indeed proportionality between true absorption and the number of photoelectrons.

Now, considering an individual electron, we see that the energy  $h\nu$  which it absorbs is used in two ways: (a)  $W_0$  in dragging it to the surface of the atom, and (b)  $\frac{mv^2}{2}$  in imparting to it kinetic energy. Hence we have the well-known Einstein equation,

$$h\nu = W_0 + \frac{mv^2}{2} \quad . \quad . \quad . \quad (3)$$

an expression which O. W. Richardson and K. T. Compton had verified in the visible and ultra-violet range.\* For X-rays it is clear that the value of  $W_0$  should depend on the level within the atom from which the electron is ejected, so that for a given substance  $W_0$  should have a number of values,  $W_K$ ,  $W_L$ , &c. Experiments by Simons, who used thin films and an ionization method, indicated that this was the case, and the complete proof was provided by M. de Broglie in experiments with the magnetic

\*  $W_0$  having a slightly different significance.

spectrum apparatus. Fig. 46 shows, in diagrammatic form, the type of result obtained when silver was irradiated by the K-rays of tungsten.\* It shows clearly that the velocities have more than one value; in fact, the interpretation of the photographs by de Broglie showed that not only were there present velocities given by

$$\frac{1}{2}mv^2 = h\nu - W_K(\text{Ag}), \quad \frac{1}{2}mv^2 = h\nu - W_L(\text{Ag}),$$

where  $\nu$  is the frequency of the tungsten radiation, but velocities due to the differences between *four* K lines of tungsten and the K level of silver. In fact, the resolution

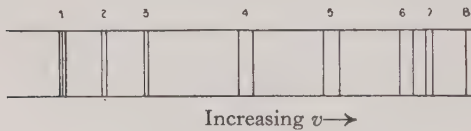


FIG. 46.

Magnetic spectrum produced by the irradiation of silver by Tungsten K radiations.

Group of lines corresponding to a velocity obtained from equation (4), assigned to the following differences of energy.

- (1)  $a_1$  and  $a_2$  of Ag and the three L levels of Ag } Auger
- (2)  $a_1$  and  $a_2$  of " " " M level " } effect
- (3)  $\beta$  of " " L levels " } (see page 118).
- (4) and (5)  $a_1 a_2 \beta_1 \beta_2$  of W and K level "
- (6)  $a_1$  and  $a_2$  of W L levels "
- (7)  $a_1$  and  $a_2$  of W " M level "

of the  $K_{\alpha_1}$  and  $K_{\alpha_2}$  lines of tungsten in this form of spectrum was more complete than in the direct spectroscopic analysis.

The values of the energies,  $W$ , obtained in these experiments were in good agreement with those given by other methods.

When dealing with the case of the faster electrons the

\* Owing to the loss of energy which some of the electrons suffer before reaching the surface of the photoelectric source, the lines on the plates actually spread out on the side of small velocities. The effect is diminished by using a thin source.

form of equation used employed the relativity expression for the kinetic energy of the electron, e.g.:

$$mc^2 \left( \frac{1}{\sqrt{1 - \beta^2}} - 1 \right) = h\nu - W_K(\text{Ag}) . \quad (4)$$

The method has since been used extensively by Robinson for the accurate determination of the energy in the different levels of many atoms. It is also of interest to note that the method provides one of the few means of making a reliable estimate of the wave-length of  $\gamma$ -rays, by the application of (4) to the results obtained with substances whose energy levels have been completely determined by X-ray methods.

Turning our attention now to the results obtained by the ingenious method of C. T. R. Wilson, we find a considerable amount of direct information about the photo-electron, the recoil electron and the process of ionization.

As we have mentioned, the course of an X-ray beam through the expansion chamber is marked by a series of irregular tracks, each of which denotes the path of an electron ejected from a molecule of the gas. There are two distinct classes of track—long ones and short ones. The longer ones, representing electrons with greater energy, will be considered first. They are the result of the photoelectric effect, in which the whole energy of the incident quantum is devoted to detaching the electron from the molecule and endowing it with kinetic energy. The initial directions of the tracks are of interest, for they show the direction in which the photoelectrons are emitted. On the basis of the classical theory it might be expected that all the electrons would be ejected in the direction of the electric vector of the radiation, i.e. at right angles to the beam. This is in conflict with experiment. It is true that in some cases there is no photoelectric emission in the directly forward or backward directions, but this is not always so, and there is emission in all other directions.

In addition, the angular distribution of the photoelectrons is not symmetrical about the electric vector. More electrons have a forward than a backward component of velocity. This asymmetry increases with the frequency of the incident radiation. A forward component of velocity would be accounted for by simple quantum theory if the incident quantum were to bequeath to the photo-electron its forward momentum  $\frac{h\nu}{c}$ . The electron would then emerge ahead of the electric vector and by an angle which would increase with increase of frequency of the radiation. Such a process would, however, imply emission at a definite angle: it would not give the angular distribution which is actually observed. The explanation of the phenomenon evidently presents difficulties: it is another of the problems which have been cleared up recently by the wave mechanics. Incidentally, we should mention that, when plane polarized X-rays are used, the direction of emission is not limited to the plane containing the electric vector and the direction of the beam. More electrons are emitted in this plane than in any other, but emission may occur in any other plane through the beam except possibly that at right angles to the vector.

Wilson chamber experiments brought to light the *Auger effect*. Auger noticed that, at the beginning of photo-electron tracks, there was often a dense blob of ions. This was not readily explicable, for ionization is heaviest when an electron is moving its slowest and therefore should be most marked at the end and not at the start of the track. One of the gases used by Auger in his expansion chamber was argon. To increase the lengths of the photoelectron tracks from the argon atoms, he diluted this fairly heavy gas with 95 per cent of hydrogen. The dense blob of ions was now revealed as a second track starting in the same place as the first. Sometimes a third and fourth track were observed. There is little doubt that the two

or more electrons come from one and the same atom, and that the process by which they are produced is typified by the following example: First an X-ray quantum ejects (say) a *K* electron from the atom. This produces the first track. The vacancy in the *K* shell is filled by an electron from (say) the *L* shell and energy is liberated. This energy may, instead of being radiated away, be used to eject another (say) *L* electron and so produce a second track. If this explanation is indeed correct, it follows that the lengths of these Auger tracks must be independent of the frequency of the incident X-rays. Thus, in the example quoted, the kinetic energy of the Auger electron, and hence the length of its track, should be governed solely by the energy freed in the (*K*—*L*) transition and the energy required to remove another *L* electron from the atom. Experiment confirms this.

Next we consider the short tracks, which were called by Wilson 'fish tracks'. Their cause was a matter of some speculation, but they are now known to be associated with the recoil electrons which were postulated in Compton's quantum theory of scattering.

From the equations of page 82 it is possible to deduce for the kinetic energy of the recoil electron the following expression in terms of  $\theta$ , the angle of recoil,

$$\text{Kin. En.} = h\nu - \frac{2hv}{mc^2} \cos^2 \theta$$

$$\left( 1 + \frac{hv}{mc^2} \right)^2 - \left( \frac{hv}{mc^2} \cos \theta \right)^2,$$

from which it appears that the energy of recoil of the electron is zero in a direction at right angles to the incident beam, and that the maximum kinetic energy is to be expected in the direction of the beam. For all angles the value of the energy of recoil is less than  $hv$ . Those short tracks which are in the direction of the beam are in fact found to be longer than the rest, and the lengths indicate

that the magnitude of the kinetic energy expression is correct. The photographs also seem to confirm that the tracks are all in the forward direction. Further support of the view that the 'fish tracks' are due to the recoil electrons is obtained from a count of the relative numbers of such tracks and of the long ones due to the photoelectrons. It has been shown that the number of photoelectrons is proportional to the true absorption of the radiation. In the same way it is to be supposed that the number of 'fish tracks' is proportional to the number of scattered quanta. Hence it would seem that the ratio of the numbers of the two kinds of track should be the same as the ratio of the scattering coefficient  $\sigma$  to the true absorption coefficient  $\tau$ . However, not all the scattered radiation should produce recoil electrons. Only that radiation which suffers a change of wave-length should do so. If allowance is made for this, then it is found that the ratio of the numbers of the two sorts of track is in satisfactory accord with  $\frac{\sigma}{\tau}$ .

It is often possible to observe the track which is produced when the scattered quantum, having travelled some distance from the scattering molecule, ejects a photoelectron from another molecule. This allows the angle of scattering,  $\phi$ , to be measured, for the position of the scattering molecule will be marked by the beginning of a 'fish track' and the quantum must have gone along the straight line from this point to the starting-place of the photoelectron track.  $\phi$  is evidently the angle between this line and the direction of the beam. But  $\phi$  can be calculated from the recoil angle,  $\theta$ , by means of the equations of the Compton effect (page 82). The observed and the calculated values agree satisfactorily. It is seen, therefore, that the cloud condensation experiments add considerable support to the Compton theory of scattering. It remained, however, to show that the recoil electron was emitted

at the same time as the reduced quantum. It was indeed suggested that the effect might be statistical in character. This point was cleared up by an ingenious experiment performed by Bothe and Geiger, who used a  $\beta$ -ray counter-method.\* A counter is illustrated on the left of Fig. 47. When a single electron enters at  $A$  there is set up in the space a sufficient ionization current (by collision) to produce a recordable charge on the string electrometer. With a suitably chosen potential across the counter, the ionization current is only momentary, and the accumulated charge on the electrometer leaking away through the high

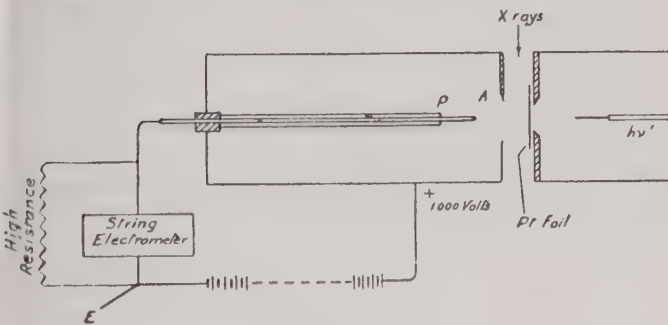


FIG. 47

resistance, leaves the apparatus ready to record the coming of the next electron. In the Bothe-Geiger experiment, two counters were arranged with their openings facing each other. One of the openings was free, but the other was covered with thin platinum foil. A narrow beam of X-rays was passed in the direction shown in the figure and was scattered by hydrogen gas. The recoil electron could enter the counter on the left (recoil counter), but was prevented by the foil from going into that on the right (quantum counter). The scattered quantum could, how-

\* Bothe and Geiger, *Zeits. f. Physik*, 32, 639 (1925).

ever, pass through, and if it produced a photoelectron from the inner side of the foil, could be recorded by the counter. The times of arrival of the electrons and quanta were compared by photographing the movements of the strings of the electrometers on the same strip of film, on which was superimposed a time scale which measured  $1/1,000$  second and in the later experiments allowed an estimate of time to  $1/10,000$  second. Since many of the scattered quanta do not produce the photoelectron necessary to start ionization in the counter, more recoil electrons than quanta were recorded. It might be thought that for every response of the quantum counter a recoil electron should be registered in the other. There are reasons which preclude this. However, Bothe and Geiger observed many simultaneous discharges and estimated that the probability of so many occurring by chance was only one in 400,000. We may, therefore, conclude that the recoil electron is produced at the same time as the scattered quantum, and may regard the Compton theory of scattering as resting on a firm foundation.

## BIBLIOGRAPHY

THE following books are recommended for more detailed reading :

*X-rays in Theory and Experiment*, Compton and Allison (Macmillan & Co.), replacing *X-rays and Electrons*, by Compton  
*X-rays and Crystal Structure*, W. H. and W. L. Bragg (G. Bell & Sons)

*The Crystalline State*, W. L. Bragg (G. Bell & Sons)

*X-ray Crystallography*, R. W. James (Methuen & Co., Ltd.)

*X-rays*, de Broglie (Methuen & Co., Ltd.)

*The Spectroscopy of X-rays*, Seigbahn (Oxford University Press)  
or the original *Spectroskopie der Roentgenstrahlen*, Seigbahn (Springer)

*The Diffraction of X-rays by Amorphous Solids, Liquids and Gases*,  
Randall (Chapman & Hall)

Early experimental work dealt with in—

*Roentgen Rays*, collected papers published by the American Book Co.

*X-rays*, Kaye (Longmans, Green)

References to original papers used in the text of this monograph :

*Chap. I* :

Clay, *Proc. Phys. Soc.*, **46**, 703 (1934)

Kuhlenkampff, *Phys. Zeit.*, **30**, 513 (1929)

Worsnop, *Science Progress*, **90** (1928)

*Chap. II* :

Cauchois, *J. de Phys.*, **3**, 320 (1932)

*Chap. III* :

Chalklin, *Phil. Mag.*, **16**, 363 (1933)

Richtmeyer, *Rev. Mod. Phys.*, **9**, 391 (1937)

Hirsch, *Rev. Mod. Phys.*, **14**, 45 (1942)

Parratt, *Phys. Rev.*, **44**, 695 (1933)

Landshoff, *Phys. Rev.*, **55**, 631 (1939)

*Chap. IV* :

Birge, *Rep. on Prog. in Phys.*, **8**, 90 (1941)

*Chap. V* :

Bearden, *Phy. Rev.*, **54**, 698 (1938)

Dunnington, *Rev. Mod. Phys.*, **11**, 65 (1939)

de Broglie, *J. de Phys.*, **2**, 265 (1921)

Watson and Akker, *Proc. Roy. Soc.*, **126**, 138 (1929)

Auger, *J. de Phys.*, **6**, 205 (1925)

Bothe and Geiger, *Z. f. Phys.*, **32**, 639 (1925)



# INDEX

Absorption, 62  
— coefficient of, 9  
— — atomic, 11  
— — mass, 11  
— edge, 63  
Angstrom unit, 39  
Auger effect, 118

Barkla, 12, 15, 72  
Birge, 92  
Bohr's theory, 42  
Bothe and Geiger, 121  
Bragg, W. L., 20  
Bragg's Law, 23  
— — deviation from, 92

Cauchois, Mlle, 36  
Change of wave-length on scattering, 83  
Characteristic radiation, 12  
Chemical effect, 54  
Cloud condensation method, 111  
Compton, A. H., 74, 93  
— and Allison, 14  
— and Doan, 98  
— and Raman, 75  
Compton effect, 80  
— reflection of X-rays, 93  
Compton, K. T., 115  
Counter, ray, 121  
Critical absorption frequency, 62  
Crystal structure, 26  
Cube centred crystal, 30  
Cubic crystal, 27

Darwin, 92

de Broglie, 27, 115  
Deviation from Bragg's Law, 92  
Diffraction, 17, 96  
— grating, 96  
Drude-Lorentz dispersion formula, 91  
Duane and Hunt, 57  
du Monde, 89

Efficiency of X-ray production, 13  
Electron, recoil, 82  
Electronic radiation, 12  
Emission spectra, 40  
Excitation of characteristic radiation, 47

Face centred cube, 30  
Fish tracks, 119  
Focal spot, 4, 6  
Frequency, critical absorption, 64  
Friedrich and Knipping, 18  
Friman, 51

Gas tube, 2  
General radiation spectrum, 56  
— — — total intensity, 57  
Grating, diffraction, 96  
— concave, 103

Hard X-rays, 2  
Hafnium, 47  
Heating of anticathode, 5  
Homogeneous radiation, 12  
Hot-filament tube, 5  
Hunt, 57

- Ion tube, 2
- Ionization method, 8
- Indices of crystals, 28
- Interference, 93
- J phenomenon and series, 13
- K radiation, 12
- L radiation, 12
- Lattice constant, 21
- Laue, 18
- Linear absorption coefficient, 9
- Magnetic spectrum, 110
- Mass absorption coefficient, 11
- Moore, H., 115
- Moseley, 45
- Moseley's Law, 40
- Photoelectric effect, 106
- Photographic method, 6
- Physical effects, 54
- Planck, 43
- Polarization, 14
- Powder method, 38
- Recoil electrons, 82
- Reflection at crystals, 21
  - at gratings, 96
- Refraction by prisms, 90
- Richardson, O. W., 115
- Ross, 12, 85
- Rydberg's constant, 45
- Satellites, 52
- Scattering :
  - angular distribution, 73
  - classical theory of, 71
  - Compton theory of, 81
  - liquids, by, 78
- Secondary radiations, 12
- Seigbahn, 35, 39, 55
- Soft X-rays, 2
- Space lattice, 19
- Spectra, emission, 40
- Spectrometer, 23, 34
  - double crystal, 35
  - bent crystal, 36
  - vacuum, 103
- Sputtering, 4
- Thomson, J. J., 106
  - theory of scattering, 71
  - determination of  $v$  for electrons, 106
- Total intensity of general radiation, 56
- Vacuum spectrometer, 103
- Walter and Pohl, 17
- Wave-length, unit of, 39
  - determination of, 28
  - of soft X-rays, 103
- Whiddington, 107
- White radiation, 56
- Width of spectral lines, 53
- Wilson, C. T. R., 112
- Woo, 84
- X-unit, 39









**FINE STRUCTURE IN LINE SPECTRA  
AND NUCLEAR SPIN**  
By S. TOLANSKY, B.Sc., Ph.D., A.Inst.P.,  
D.I.C. (3s. 6d. net)

**INFRA-RED AND RAMAN SPECTRA**  
By G. B. B. M. SUTHERLAND, M.A., Ph.D.  
(3s. 6d. net)

**THERMIONIC EMISSION**  
By T. J. JONES, M.Sc. (3s. 6d. net)

**ELECTRON DIFFRACTION**  
By R. BEECHING, A.R.C.S. (3s. 6d. net)

**MAGNETISM**  
By EDMUND C. STONER, Ph.D. *New  
Edition, entirely Revised.* (3s. 6d. net)

**THE EARTH'S MAGNETISM**  
By S. CHAPMAN, M.A., D.Sc. (4s. net)

**MERCURY ARCS**  
By F. J. TEAGO, D.Sc., and J. F. GILL,  
M.Sc. (3s. 6d. net)

**MOLECULAR BEAMS**  
By R. G. J. FRASER, Ph.D. (3s. net)

**ALTERNATING CURRENT  
MEASUREMENTS**  
By DAVID OWEN, B.A., D.Sc. (5s. net)

**COSMOLOGICAL THEORY**  
By G. C. McVITTIE, M.A. (3s. net)

**DIPOLE MOMENTS**  
By R. J. W. LE FÈVRE, D.Sc., Ph.D.  
(4s. net)

**FLUORESCENCE AND PHOSPHORES-  
CENCE**  
By E. HIRSCHLAFF, Ph.D. (4s. net)

**AN INTRODUCTION TO VECTOR  
ANALYSIS**  
By B. HAGUE, D.Sc. *Second Edition.*  
(4s. 6d. net)

**THE CYCLOTRON**  
By W. B. MANN. *Third Edition.*  
(4s. net)

**THE SPECIAL THEORY OF RELA-  
TIVITY**  
By HERBERT DINGLE. (3s. 6d. net)

**WAVE GUIDES**  
By H. R. L. LAMONT, M.A., Ph.D.  
*Second Edition.* (4s. net)

**WAVE FILTERS**  
By L. C. JACKSON, M.Sc., D.Sc. *Second  
Edition.* (4s. 6d. net)

**HIGH FREQUENCY TRANSMISSION  
LINES**  
By WILLIS JACKSON. (6s. net)

# *Monographs on Physical Subjects*

ATOMIC SPECTRA. By R. C. JOHNSON, D.Sc. (5s. net)

WAVE MECHANICS. By H. T. FLINT, D.Sc., Ph.D. *Third Edition.* (4s. 6d. net)

THE PHYSICAL PRINCIPLES OF WIRELESS. By J. A. RATCLIFFE, M.A. *Seventh Edition.* (4s. 6d. net)

THE CONDUCTION OF ELECTRICITY THROUGH GASES. By K. G. EMELEUS, M.A., Ph.D. *Second Edition.* (3s. net)

X-RAY CRYSTALLOGRAPHY. By R. W. JAMES, M.A., B.Sc. *Third Edition.* (4s. net)

THE COMMUTATOR MOTOR. By F. J. TEAGO, D.Sc. (3s. net)

APPLICATIONS OF INTERFEROMETRY. By W. EWART WILLIAMS, M.Sc. *Second Edition, Revised.* (4s. net)

THERMIONIC VACUUM TUBES. By E. V. APPLETON, M.A., D.Sc., F.R.S. *Fourth Edition.* (4s. 6d. net)

PHOTOCHEMISTRY. By D. W. G. STYLE, B.Sc., Ph.D. (3s. net)

THERMODYNAMICS. By A. W. PORTER, D.Sc., F.R.S. *Second Edition.* (4s. 6d. net)

WIRELESS RECEIVERS. By C. W. OATLEY, M.A., D.Sc. *Fourth Edition.* (4s. net)

ATMOSPHERIC ELECTRICITY. By B. F. J. SCHONLAND, O.B.E., M.A., Ph.D. (3s. net)

THE METHOD OF DIMENSIONS. By A. W. PORTER, D.Sc. *Third Edition.* (4s. net)

COLLISION PROCESSES IN GASES. By F. L. ARNOT, B.Sc., Ph.D. (Camb.). (4s. 6d. net)

PHYSICAL CONSTANTS. Selected for Students by W. H. J. CHILDS, B.Sc., Ph.D. *Fourth Edition.* (4s. 6d. net)

ELECTROMAGNETIC WAVES. By F. W. G. WHITING. *Third Edition.* (4s. 6d. net)

THE GENERAL PRINCIPLES OF QUANTUM THEORY. By G. TEMPLE, Ph.D., D.Sc. *Third Edition.* (4s. net)

THE KINETIC THEORY OF GASES: Some Modern Aspects. By Professor MARTIN KNUDSEN. *Second Edition.* (3s. 6d. net)

LOW TEMPERATURE PHYSICS. By L. C. JACKSON, Ph.D. (3s. 6d. net)

HIGH VOLTAGE PHYSICS. By L. JACOB, M.Sc., A.R.C.S. (3s. 6d. net)

RELATIVITY PHYSICS. By W. H. McCREA, Ph.D. (4s. 6d. net)

X-RAYS. By B. L. WORSNOP, B.Sc., Ph.D., and F. C. CHAI, D.Sc. *Second Edition.* (5s. net)

*Continued on back flap*

KQ-081-658

